Loss of chromatic sensitivity in patients with age-related maculopathy - correlation with structural changes in the retina

Mrs Roopa Vemala

Doctor of Philosophy

Applied Vision Research Centre
School of Health Sciences

City, University of London
January 2018

Table of Contents

CONTENTS

CONTENTS

CONTENTS

CONTENTS

TABLE OF FIGURES:

TABLE OF FIGURES

TABLE OF FIGURES

TABLE OF FIGURES

List of Tables

LIST OF TABLES

Acknowlegements:

I am grateful to my supervisors Professor John Barbur for his constant support, patience and belief in me over the years and Miss Sobha Sivaprasad for providing a ground for performing the study and for her input and expertise into the research.

This work could not have been possible without the support from City University, through my three years doctoral studentship, for which I will always be thankful.

I am also grateful to the Medical Retina Department of Kings College Hospital, my host organisation where this study was performed.

I am grateful to all the participants, who took great interest and passionately performed the test to the best of their abilities to help research into the condition affecting them.

I am truly indebted to my family for letting me take up this mammoth task and being a silent onlooker as I stumbled through it especially my husband Raj and my Parents.

My son Reyansh who was born during the course of the study. My older son Samarth for providing a constant distraction and making me feel a great sense of accomplishment at the completion of the project, I hope I can make up for the lost time for them.

Declaration:

I grant powers of discretion to the university Librarian to allow the thesis to be copied in whole or in part without further reference to me. This permission covers only single copies made for study purposes, subject to normal conditions of acknowledgment.

Symbols and Abbreviations:

ARM: *Age-related Maculopathy*

AMD: *Age-Related Macular Degeneration*

BlinD: *Basal Linear deposit*

BlamD: *Basal laminar deposit*

CAD: *Colour Assessment and Diagnosis test*

CMT: *Central Macular Thickness*

CNV: *Choroidal neovascularisation*

CD: *Cuticular Drusen*

CV: *Colour Vision*

CS: *Contrast Sensitivity*

cSLO: *Confocal Scanning Laser Ophthalmoscope*

DA: *Dark Adaptation*

EC: *Esterified Cholesterol.*

EOD: *Early Onset Drusen*

FAF: *Fundus Autofluorescence*

FAM : *Fundus Autofluorescence in Age-related macular degeneration*

FAZ: *Foveal Avascular Zone*

GA: *Geographic Atrophy*

ICL: *Inner collagenous layer*

ICGA: *Indocyanine Green Angiogram*

IT: *Ishihara Test*

L cones: *Long Wavelength Sensitive Cones*

LCD: *Large Colloid drusen*

M cones: *Middle or Medium Wavelength Sensitive Cones*

MP: *Macular pigment*

ML-DH: *Malattia leventinese-Doyne honeycomb retinal dystrophy*

mfERG: *Multifocal Electectroretinography*

NA: *Normal Aging*

OCT: *Ocular CoherenceTopography*

OCL: *Outer Collagenous Layer*

PST: *Photostress Test*

RPE: *Retinal Pigment Epithelium*

RPD: *Reticular Drusen*

RG: *Red Green*

SDOCT: *Spectral domain OCT*

SD: *Standard Deviation*

S cones: *Short Wavelength Sensitive Cones*

SDD: *Subretinal Drusenoid Debris*

SF: *Spatial Frequency*

SW gratings: *Sine Wave gratings*

SWAP: *Short Wave Automated Perimetry*

SNU: *Standard Normal Units*

TCS: *Temporal contrast sensitivity*

TDOCT: *Time Domain OCT*

UC: *Unesterified Cholesterol*

UHROCT: *Ultra-high resolution OCT*

VF: *Visual Field*

VA: *Visual Acuity*

VEGF: *Vascular Endothelial Growth Factor*

WARMGS: *Wisconsin Age-Related Maculopathy Grading Scheme*

YB: *Yellow Blue*

Abstract:

Purpose: To assess colour vision in Age-related macular degeneration (AMD) while relating chromatic sensitivity to the severity of AMD and AMD morphologies such as drusen and reticular pseudodrusen. To evaluate if chromatic functional loss precedes structural changes in initial stages of AMD, and if it can be a valuable risk stratification tool for advanced AMD.

Methods:

Chromatic sensitivity was tested using the Colour Assessment and Diagnosis (CAD) test developed by City, University of London and correlated to the structural changes from fundus photography and spectral domain OCT. All patients were asymptomatic with a visual acuity of 6/12 or better. CAD thresholds were compared to clinical classification in all AMD eyes (Ferris et al., 2013); Soft drusen and Reticular drusen (RPD); Central macular thickness (CMT); Fundus autofluorescence (FAF) pattern (Einbock et al., 2005; Wong et al., 2014) and Soft drusen characteristics (Bird et al., 1995). Cases of conversion to 'Wet' AMD were identified through a repeat clinical assessment after the first 12 months. Chromatic sensitivity in early onset drusen (EOD) included comparing their colour thresholds to AMD eyes. Student t-test were used for correlation and $P<0.05$ was considered significant.

Results

All eyes with AMD had chromatic sensitivity loss in either one of RG / YB or both ($p<0.0001$) in comparison to the age-matched normative data set.

The eyes involved exhibited a range of colour thresholds measured on CAD system (CAD thresholds) affecting both the colour mechanisms but YB losses were at a higher magnitude than RG losses ($p<0.001$). There was no correlation to the AMD severity grades in clinical classification because of large inter-subject variability within each group. Intermediate AMD was the largest group.

Mean chromatic sensitivity increased from normal aging (NA) to soft drusen to reticular drusen, NA< soft drusen< RPD ($R^2=0.9$). Even though EOD (n=10) had the same morphological appearance of drusen as ARM, lower and better CAD thresholds were recorded.

Reticular drusen revealed the highest mean CAD thresholds for RG (~ 19 units) and for YB (~14 units), followed by soft drusen group (~ 7 units for both RG/YB). Comparison of CAD thresholds in soft drusen and RPD groups with all other groups (Normative, NA, EOD) was statistically significant ($p<0.0001$).

Forty nine eyes with soft drusen were stratified for drusen morphology, number, size, the area covered and the main location of the drusen on the ETDRS grid.

Drusen size was the only characteristic feature found to be significantly associated with both RG / YB chromatic sensitivity loss. Grade 5 eyes were statistically different compared to the rest of the grades ($p<0.0003$ RG and $p<0.02$ YB).

Autofluorescence was performed in 76 eyes and the results assigned to the 8 FAF patterns from FAM study (Einbock et al., 2005). The patchy pattern of FAF had the highest CAD thresholds and this was in agreement with the FAM group as being the high-risk pattern.

CMT was measured in 88 eyes, 3 eyes were noted to have early GA and they showed very severe loss of RG and YB thresholds. The p value correlating the CAD thresholds of eyes with CMT<200 and >200 μm was statistically significant with P<0.01 for RG and <0.002 for YB.

Review of baseline CAD thresholds in cases converted to wet AMD at the end of 12 months, revealed six eyes had converted to wet AMD. The baseline CAD thresholds of these eyes were not conclusive of being predictive of the impending change to wet AMD.

Conclusions:

The visual acuity and hence the integrity of cone photoreceptors remains relatively unaffected in early and intermediate stages of AMD. The processing of cone signals in the retina can however be heavily disrupted with subsequent loss of both YB and RG chromatic sensitivity in the eyes. The greatest losses relate to eyes with reticular pseudodrusen. Chromatic sensitivity change was indicative in early macular thinning but failed to herald the onset of wet AMD in our study sample.

Introduction:

Early signs of age related macular degeneration (AMD), characterised by drusen and pigmentary changes in the macula, have a global prevalence of 8.01% in people aged 50 years or older, whereas the prevalence of the sight threatening late AMD which includes geographic atrophy (GA) and choroidal neovascularisation (CNV) is 0.37 (Wong et al., 2014). Early AMD is characterised by the presence of medium sized drusen (≥ 63<125 μm) without pigmentary abnormalities while eyes with large drusen or with pigmentary abnormalities associated with at least medium drusen are termed as intermediate AMD by Beckman's classification. Five -year risks of progressing to late AMD are 50% for the highest intermediate AMD risk group (Ferris et al., 2013). However, it is acknowledged that classification based on colour photographs or biomicroscopy alone ignores changes relevant to the disorder such as RPE dysfunction, loss of photoreceptor function, or the development of reticular pseudodrusen.

The main ocular structures involved in AMD are photoreceptors, RPE, Bruch's membrane, and choriocapillaries. There is a progressive decline in RPE and photoreceptors which results in GA (Bird, 2010). Such evolution to GA is currently thought to be a default end pathway for AMD; whereas wet AMD is the reactive outcome that targets a subset of AMD patients with a particular genetic predisposition as this can occur at any stage of the default pathway (Neelam et al., 2009) .

AMD intervention should therefore be targeted at the earliest stage of the disease to prevent development of GA and the potential for CNV. Wet AMD or CNV also require a diagnostic tool which can identify AMD changes from as early as the preclinical stage of the disease. Significant histological changes occurred long before the clinical manifestation of drusen and

pigmentary changes are observable (Sarks et al., 1988). Although structural changes can be accessed through OCT and autofluorescence, these methods do not quantify the degenerative transition accurately, diffused deposits through Bruch's membrane cannot be differentiated by imaging techniques and histological changes (Curcio et al., 2013).

Hence functional assessment should have a high potential to detect / monitor AMD as it can in conjunction with the imaging modalities, provide a powerful tool for quantitative tracking of early stage AMD.

There is a lack of functional markers for disease progression and endpoint, as visual acuity may not be affected until later in the disease (Wu et al., 2014). People with intermediate AMD experience functional deficits such as delayed dark adaptation and focal deficits in retinal sensitivity, recent studies have correlated the decreased function to structural markers on spectral domain optical coherence tomography (SDOCT) (Wu et al., 2014; Vujosevic et al., 2016). With the advent of infrared reflectance, there is significant interest in reticular pseudodrusen (RPD). These deposits are internal to the retinal pigment epithelium and the presence of RPD is significantly associated with a decrease in scotopic thresholds suggesting rod dysfunction (Flamendorf et al., 2015). To date, cone dysfunction has not been evaluated using chromatic sensitivity in people with AMD, with or without RPD.

Normal colour vision is trichromatic and involves comparison of signals generated in short wavelength (S), middle wavelength (M) and long wavelength (L) sensitive cones. The RG (Red Green) channels utilizes L and M while YB (Yellow Blue) utilizes M, L and S cones (Konstantakopoulou, 2012). L and M cones peak at the fovea but the S cones which constitute only 8-10% of the photoreceptors peak at the foveal slope (Kolb, 1991). When assessing YB chromatic sensitivity using the CAD test the L and M cone signals remain unchanged with 'yellow' and 'blue' hues being signalled entirely by changes in the signals

for the S -cone (Rodriguez-Carmona, 2012) .Young, normal trichromats requires only 0.4% L and 0.8% M-cone contrast changes to detect RG colour differences (at threshold) while 7% S-cone contrast changes are needed in the case of YB colour differences.

The high sensitivity for detection of RG or YB colour signals and the large number of stages involved in chromatic processing makes colour assessment particularly suitable for detecting changes caused by the retinal disease. Impairment of colour vision (CV) is one of the earliest detectable changes in the visual process during the presence of a retinal disease.

A systematic review of 15 studies revealed loss of chromatic sensitivity with a tendency towards yellow-blue (YB) defect in retinal diseases (Neelam et al., 2009). Reports also show a correlation of changes in chromatic sensitivity with disease progression in AMD (O'Neill-Biba et al., 2010). It is suggested that colour saturation is affected earlier than hue discrimination (Neelam et al., 2009). The Colour Assessment and Diagnosis test (CAD) developed by City, University of London quantifies both saturation and thresholds and accurately detects early stages of AMD functional defects (O'Neill-Biba et al., 2010). The pilot study by O'Neill-Biba et al., showed significant but unequal loss of YB and RG sensitivity in 18 subjects of AMD with YB showing the greatest loss. They also found a correlation with the severity of AMD classification.

The above pilot study formed a basis for the present study to understand chromatic loss in a larger sample size as well to compare to various clinical criteria.

Aims of the study:

- To study chromatic sensitivity in AMD using the CAD system to quantify the RG and YB thresholds and to compare these thresholds against the upper limits established for healthy aging.
- To quantify the severity of colour vision loss in AMD and to correlate the RG and YB losses with the estimated progression of disease through AMD grading of the macula, based on examination of fundus photographs.
- To examine how the severity of RG and YB loss relates to drusen's spatial characteristics, and autofluorescence and spectral domain optical coherence tomography (OCT) imaging of the retina.
- To study the colour vision change in early onset drusen (EOD), as studying colour changes in drusen not related to AMD will help us to attribute the CAD changes beyond the structural changes of drusen.

The thesis is structured to understand in detail the anatomical, physiological and pathological factors involved in AMD. The dissertation also addresses the visual psychophysical tests in AMD and their role in detecting early changes of visual function in AMD. With this background the dissertation goes ahead to discuss the chromatic sensitivity in AMD with the aid of the results of the present study.

1. Anatomy and physiology of the eye with special relevance to AMD:

The Human Eye:

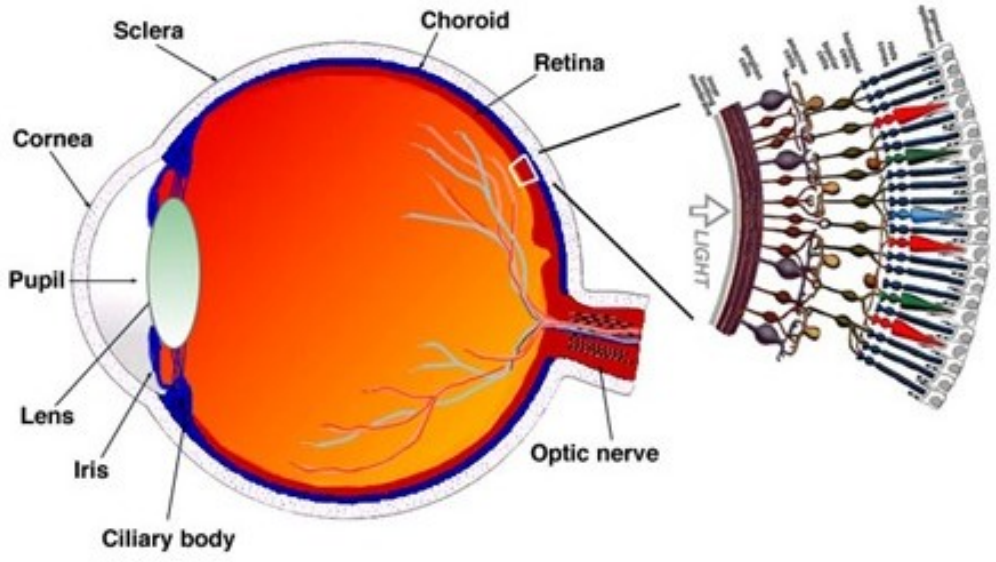

Figure 1.1: Drawing of a section through the human eye with a schematic enlargement of the retina (http://webvision.med.utah.edu).

The structures of the eye (Figure 1.1) concerned with the development of AMD have been described in the section below with due relevance to pathogenesis of the condition.

The choroid which is the vascular layer between the sclera and the retina lies behind the ciliary body. The choroid is the main oxygen and nutrient supplier to the outer retina and the Retinal Pigment Epithelium (RPE) through its choriocapillaris. The inner part of the choroid is called Bruch's membrane and plays a major part in Age-Related Macular Degeneration (AMD) and other chorioretinal diseases (Curcio et al., 2013).

.

1.1 Bruch's Membrane:

Bruch's membrane is a thin (2–4 μm), acellular, five-layered extracellular matrix located between the retina and choroid, Bruch's membrane lies between the metabolically active Retinal Pigment Epithelium (RPE) and a capillary bed (choriocapillaris) and thus, serves two major functions as the substratum of the RPE and a vessel wall (Marshall, 1998) . As a vessel wall of the choroid, Bruch's membrane's primary function is structural, as its structure is like vascular intima, with subendothelial extracellular matrix and an elastic layer corresponding to the internal elastic lamina. The abluminal surface of Bruch's differs from other vessel walls as it abuts a basal lamina, that of the RPE. The luminal surface faces a fenestrated vascular endothelium and Basal lamina, making Bruch's membrane structurally analogous to the renal glomerulus and providing a basis for commonality between retinal and kidney disease (Weiner et al., 2011). The importance of fluid and macromolecular transportation across the renal glomerulus is well known (Maddox and Brenner, 1977). Transportation is the second most important function of Bruch's membrane (Curcio et al., 2013).

Hogans five layered nomenclature for Bruch's membrane mentioned below is commonly used;

1. RPE basal Lamina (RPE-BL).
2. Inner Collagenous layer (ICL).
3. Elastic Layer (EL).
4. Outer Collagenous layer (OCL).

5. Choriocapillaris basal lamina (ChC-BL).

Aging is the largest risk factor for developing AMD (Smith, 2001) and Bruch's membrane undergoes significant age-related changes.

1.1.1a Lipid Accumulation in Bruch's membrane:

Debris deposition in ICL and OCL starts in the second decade in the macula and is delayed in the equatorial regions, a regional lag noted for individual components (Johnson et al., 2007). The most prominent changes in this regard are the accumulation of lipids. Clinical observations on fluid-filled RPE detachments in older adults led to Bird and Marshall's hypothesis that a lipophilic barrier in Bruch's membrane blocked a normal, outwardly directed fluid efflux from the RPE (Bird and Marshall, 1986) as opposed to leakage from CNV.

Lipoproteins can be assembled from several sources, including outer segments, remnant components from the photoreceptor nutrient supply system, and endogenous synthesis. According to this model (Curcio et al., 2011), plasma lipoproteins serve as vehicles for delivery of lipophilic nutrients, carotenoids (Loane et al., 2008), Vitamin E, and cholesterol to photoreceptors by RPE, which has functional receptors for low-density lipoproteins (LDL) and high-density lipoprotein (HDL) (Tserentsoodol et al., 2006). Nutrients are stripped from these lipoproteins by the RPE for delivery to the photoreceptors, and the remnants are repacked for secretion into the Bruch's membrane as a part of apo B-, containing lipoproteins where they begin to accumulate with time and become toxically modified to instigate inflammation in AMD.

Transportation across Bruch's membrane is increasingly hindered with age, due, at least partly, to the marked age-related accumulation of esterified cholesterol (EC) rich lipoproteins in this tissue impending pumping of fluid from RPE. Around 90% of the decline in the transport of some species from the choroid (Moore and Clover, 2001; Hussain et al., 2010) may include lipophilic essentials delivered by the lipoproteins.

This decline in transportation capabilities is thought to have functional consequences for the photoreceptors. A well-characterized change occurring through the lifespan of individuals with healthy macula is slowed dark adaptation attributed to impaired translocation of retinoids across the RPE-Bruch's interface (Jackson et al., 2002).

1.1.2 Relevance to Age- related macular degeneration:

During aging and AMD, characteristic extracellular lesions accumulate in tissue compartments anterior to the ICL, known as drusen and basal deposits (Sarks 1976, Booij et al., 2010). These lipid-containing aggregations ultimately impact RPE and photoreceptor health by impairing transport, causing inflammation and predisposing to CNV. Basal linear Deposit (BlinD) forms consequently to lipoprotein accumulation in Bruch's membrane and formation of lipid wall, likely to involve oxidation of individual lipid classes and local inflammation. Drusen could form by similar mechanisms, plus lipoprotein aggregation and other undefined processes that cause the distinctive dome-shaped of these lesions. Basal laminar deposits (BlamD) are formed parallel to lipid deposition in Bruch's and may indicate RPE stress (Curcio et al., 2013).

1.1.2a Drusen:

In a fundus view, drusen are yellow-white deposits 30-300 µm in diameter posterior to the RPE. On OCT they appear as variable hypo-reflective spaces in the same location (Khanifar et al., 2008). Histologically, drusen are focal, domed lesions between RPE basal lamina and the ICL of the Bruch's membrane in the same subretinal tissue compartment as the lipid wall and BlinD (Figure 1.2.1).

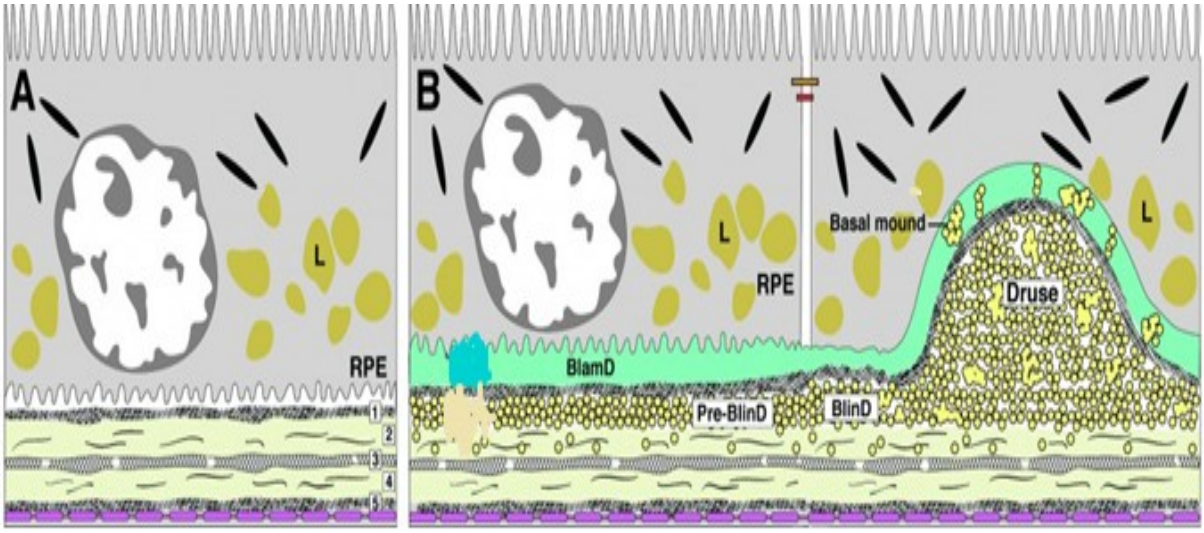

Figure 1.2.1: Aging and AMD macula showing RPE and Bruch's membrane.
Panel A -RPE and Bruch's membrane: 1. RPE basal lamina; 2. Inner collagenous layer; 3. Elastic layer; 4. Outer collagenous layer; 5. Choriocapillary endothelium basal lamina;Panel B: Changes in Aging and AMD leading to Drusen: Basal Laminar deposits (BlamD), Basal linear deposits (BlindD) and Druse are labeled. Reproduced from http; //Project Macula.cis.uab.edu adapted from Curcio-Ryan 2012.

Found in older adults (Klein et al., 1992), Drusen are more common in the peripheral retina than in the macula. Drusen are typically classified as "hard" and "soft" by the appearance of their borders. Soft drusen confer a high risk of advanced disease and are found only in the macula (Rudolf et al., 2008).

The RPE has been implicated as a source of many drusen components, via budding of membrane-bound packets of cytoplasm or secretion, but the components are not well characterised. Most prominent constituents are lipids identified as esterified cholesterol (EC) and unesterified cholesterol (UC), phosphatidylcholine, phospholipids and ceramides. Other components include vitronectin, TIMP-3, complement factor H, complement components C3 and C8, crystallins and Zinc (Curcio et al., 2013).

1.1.2b Basal Linear deposit (BlinD) and Basal Laminar deposit (BlamD):

BlinD is a thin (0.4-2µm) layer located in the same sub-RPE space as soft drusen. BlinD and soft drusen are alternate forms of the same pathology and can't be interchanged. Both the lesions are permissive for CNV.

BlamD forms small pockets between the RPE and the RPE-BL in many normal older eyes or a continuous layer as thick as 15µm in AMD eyes. Some authors consider a continuous layer of BlamD a histological definition of AMD (Yamada et al., 2006).

Ultrastructurally BlamD resembles a basement membrane with material containing laminin, fibronectin, and type VI collagen. Thick Blam D with advanced AMD risk contains lipid including EC and UC, also containing Vitronectin, MMP-7, TIMP-3, C3 and C5b-9 (Curcio et al., 2005). BlamD is a reliable marker of RPE stress (Marmorstein et al., 2007).

1.1.2c Reticular Drusen:

Located in subretinal space, subretinal drusenoid debris (SDD) was first described by Sarks (Sarks, 1976). They are similar to drusen in composition and are enriched in UC, apoE,

vitronectin and complement factor H (Figure 1.2.2). Like drusen they lack markers for photoreceptors, Muller cells, and RPE processes.

Clinically called Reticular drusen on fundus view and SDD on cross -sectional view, they are present in 60% of the eyes with geographic atrophy. SDD appears as focal deposits near the fovea and part of large sheets elsewhere in the macula (Spaide and Curcio, 2010).This coherent morphology suggests a specific formative process, possibly involving microglia resident in that compartment (Xu, 2008).

SDD are a candidate for a histological correlation of reticular pseudodrusen whereas basal linear deposits (BlindD) correlate to drusen. Curcio (2013) describes SDD as isolated or confluent drusenoid dollops punctuated by tufts of RPE apical processes and associated with photoreceptor perturbation. Histological studies in donor's eyes by Curcio et al (2013) found SDD and BlinD in 85.0% and 90.0% of non-neovascular AMD donor eyes respectively. SDD was thick (median 9.4μm) and more abundant in perifovea than fovea whereas BlinD was thin (median 2.1%) and more abundant in the fovea than the perifovea. SDD is preferentially localized to the perifovea where the rods are in high density and BlinD is thickest in the fovea, where there is a high density of cones thus suggesting that SDD and BlinD reflect differential aspects of rod and cone physiology, linking together macular photoreceptor topography and AMD pathology. This study showed that rods may play an important path physiological stimulus for the development of AMD due to the formation of SDD. A component of dry AMD, SDD is a recognised risk factor for the development of both geographic and choroidal neovascularisation.

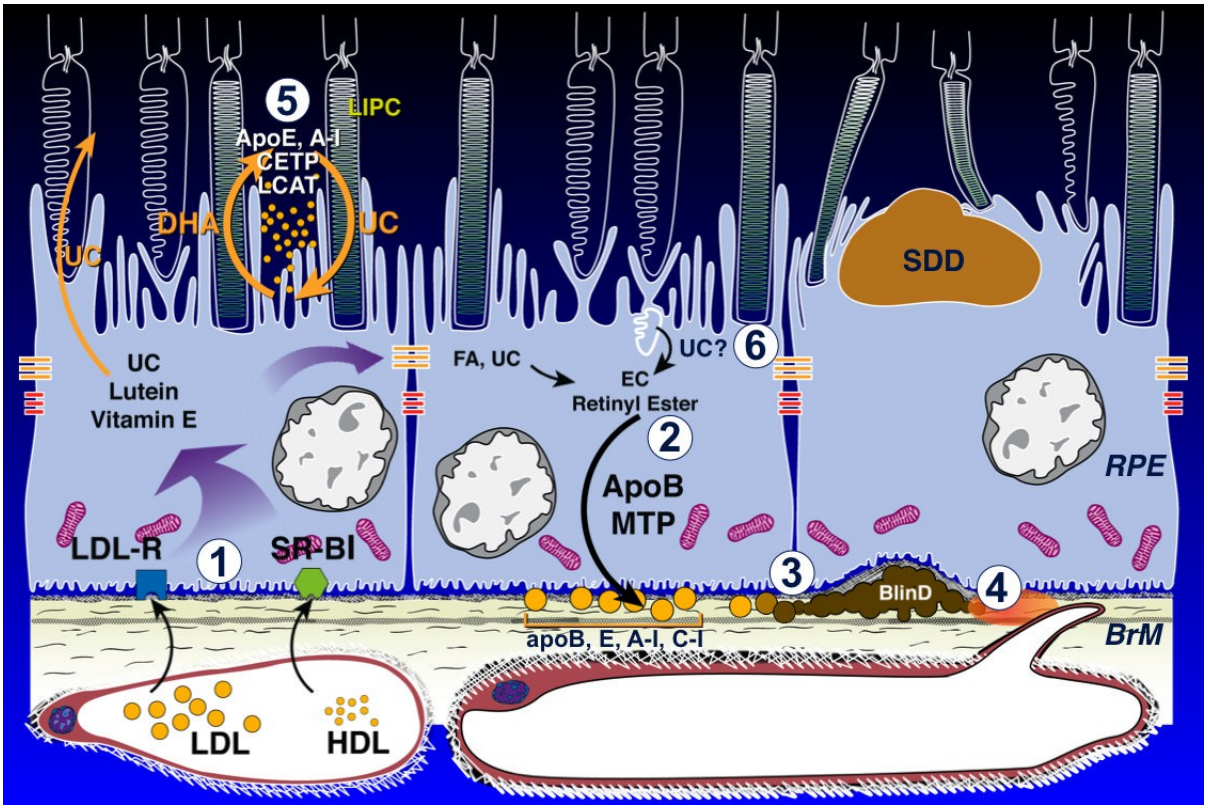

Figure 1.2.2: Biogenesis of Sub-RPE and Sub-Retinal AMD lesions: Model (Curcio etal.,2013), Panel left and center is a Aging Eye without AMD and right panel is a eye with AMD.

1) Plasma lipoproteins entering RPE. 2) ApoB, E lipoproteins secreted by RPE (gold circles) are assembled from multiple lipid sources.3) Lipoproteins accumulate throughout adulthood creating a lipid wall on BrM's inner surface.4) Lipoproteins fuse and form lipid pools and form UC-rich lipoproteins (Unesterified cholesterol) within BlindD/soft drusen.5) Disks in rod Outer segment lose UC and gain docosahexaenoate in transit from OS base to tip. 6) Cone OS maintain high UC content along with their length, this enters RPE via disk shedding, lysosomal uptake, and acid lipase activity.

Model of biogenesis of sub -RPE and sub retinal AMD lesions by Curcio et al (2013) (Figure 1.2.2) shows that plasma lipoproteins delivered by lipophilic nutrients enter RPE. ApoB, E Liporproteins secreted basolaterally by the RPE are assembled from multiple lipid sources and lipoproteins accumulate throughout adulthood creating a lipid wall on the bruch's membrane inner surface. Lipoproteins fuse and form lipid pools along with UC-rich lipoproteins within BlindD/soft drusen. Disks in rod outer segment lose UC and gain

docosahexaenoate (DHA) in transit from outer segment (OS) base to tip, OS derived DHA is stored as triglycerides in RPE after phogocytosis, return to OS. The HDL particles cycling between RPE and photoreceptors could handle both transfers and retention within inter photoreceptor matrix as UC containing SDD, especially under rod-rich perifovea.

Cone OS maintain high UC content along their length; this enters RPE via disk shedding, lysosomal uptake and acid lipase activity. UC is released for intercellular transfer, esterification and assembly into basolaterally- secreted lipoproteins especially under cone rich fovea.

Curcio described the histological appearance in 22 eyes of 20 Caucasian donors and SDD was found as either isolated or as confluent drusenoid moulds or dollops (Curcio et al., 2013). Photoreceptor structural changes were noted such as OS shortening, with inner segment deflection /absence and large SDD encroaching on photoreceptors were seen. Photoreceptor outer segments, mostly rods appear associated with microvilli bundles wrapping around SDD moulds to reach the RPE. Whether this implies that some RPE does not touch photoreceptors is not certain.

1.1.2d Thick basal laminar deposits in adult-onset autosomal dominant inherited disorders:

Three autosomal dominant inherited disorders with adult onset-Sorsby fundus dystrophy, Late-Onset Retinal Degeneration (LORD) and Malattia leventinese-Doyne honeycomb retinal dystrophy (ML-DH) share phenotypic similarities with AMD. The mutant genes encoding these conditions localise with BlamD, suggesting its key role in drusen formation. Sorsby and LORD are notable for thick BlamD and areas of retinal atrophy (Isashiki et al., 1999) involving macula and the periphery. ML-DH is notable for peripapillary deposits and

radially distributed drusen. The deposits of EC, UC, and apoB in BlamD may represent native lipoproteins in transit from RPE to the choriocapillaris rather than deposition/aggregations of plasma LDL as originally speculated (Curcio et al., 2013).

1.1.2e Response to retention hypothesis of AMD:

The parallels between the pathology of arterial intima of large arteries and that of Bruch's membrane are striking. Both feature cholesterol-rich lesions in subendothelial compartments within the systemic circulation involving the same biological molecules (Friedman, 2000). According to the response-to-retention hypothesis of atherosclerosis, plasma lipoproteins cross the vascular endothelium of large arteries, bind to extracellular matrix and initiate oxidative and non-oxidative processes leading to inflammation, macrophage recruitment and neovascularization, which eventually leads to diseases.

1.1.2f Neovascular AMD:

CNV involves VEGF stimulation of choriocapillaris endothelium, a compromise to Bruch's membrane and participation of macrophages (Grossniklaus and Green, 2004).Impaired transport across the Bruch's membrane in AMD, increasingly isolates the RPE from its metabolic source in the choriocapillaris and enhances the challenge of waste product disposal. VEGF released as stress signal initiates an angiogenic response by the endothelium. However, Bruch's membrane compromise is essential for CNV to proceed.

1.2 Choroid:

The choroid is the posterior part of the uvea, the middle tunic of the eye (Fig 1.3). It develops from different cell lines (mesenchyme) than the RPE and retina, which develop from the neural ectoderm. The choroid is comprised of blood vessels, melanocytes, fibroblasts, resident immune competent cells and supporting collagenous and elastic connective tissues.

As one of the most vascularized tissue in the body, its functions are supplying oxygen and nutrients to the outer retina, thermoregulation via heat dissipation, modulation of Intraocular pressure (IOP) via vasomotor control of blood flow and drainage of aqueous humor via the uveoscleral outflow (Nickla and Wallman, 2010).

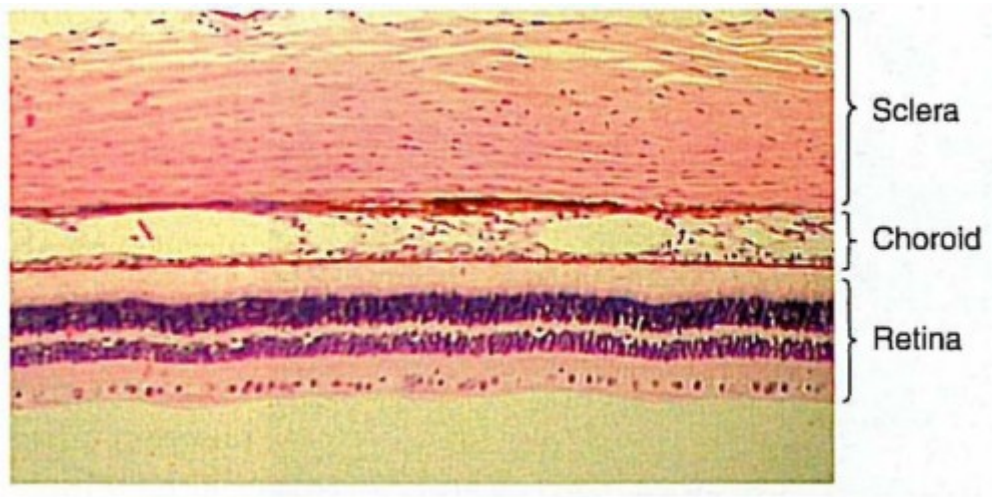

Figure 1.3: Photomicrograph of the three tunics at the back of the Primate eye. Retina, Choroid, and Sclera have been labelled. (Remington, 2005).

The choroid extends from the margins of the optic nerve to the pars plana, where it becomes the ciliary body. It is most commonly described as having 5 layers starting from the retinal side namely the Bruch's membrane, the choriocapillaris, the two vascular layers (Haller's and Sattler's) and the suprachoroid (Figure 1.4).

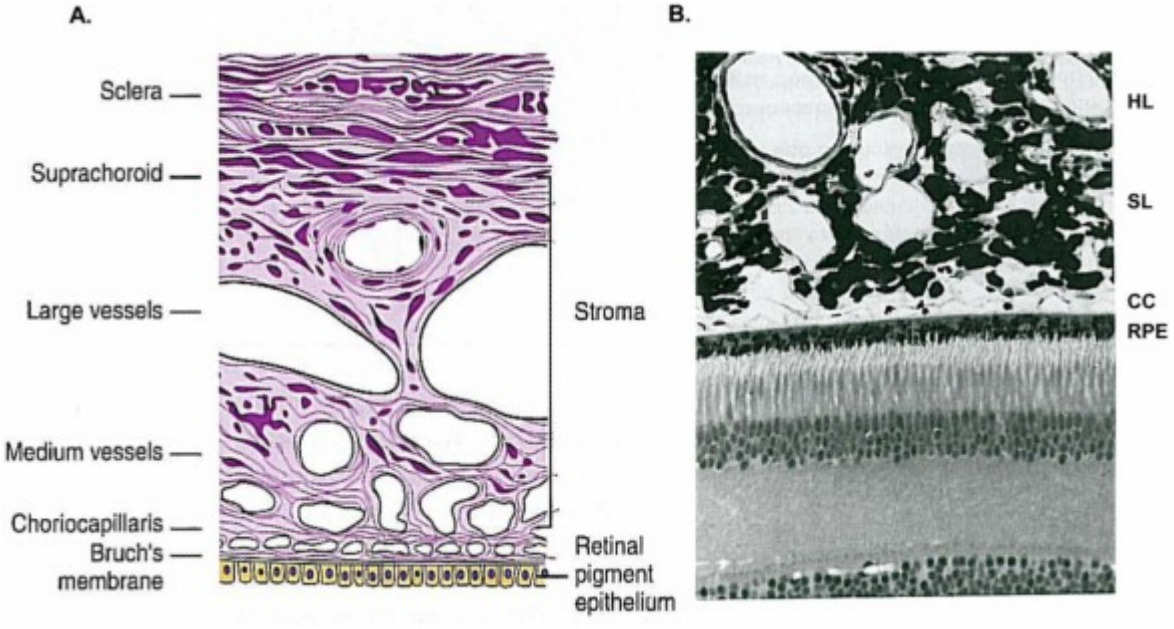

Figure 1.4: Histology of the choroid: A) Schematic diagram of the layers of the choroid. (LA, 2005)B) Semithin resin section of the outer retina and the choroid in the primate eye. RPE: retinal pigment epithelium; CC; choriocapillaris; Sattler's Layer; HL: Haller's layer (Forrester, 2002).

1.2.1 Choriocapillaris:

The choriocapillaris is a highly anastomosed network of capillaries, forming a thin sheet opposed to Bruch's membrane. The fibrous basement membrane of the choriocapillaris forms the outermost layer of the Bruch's membrane. The capillaries are 10µm thick at the fovea where the density is the thickest and it thins down to 7µm in the periphery. They arise from the arterioles in the Sattler's layer and give rise to the hexagonal (lobular) domain of a single layer of capillaries, giving rise to its characteristic patchy appearance. They are fenestrated with a large spread of area as the velocity of the red blood cells is 77% of the velocity in the retinal capillaries (Wajer et al., 2000). The fenestrations are highly permeable to proteins contributing to the high oncotic pressure in the extravascular stroma aiding the movement of fluid from the retina into the choroid.

Adjacent to the Sattler's layer, is a fibrous layer connected to the outer fibrous layer of the Bruch's membrane by columns of collagen fibers running between the capillaries. These columns or "pillars" may function to keep the capillary diameter constant (Krebs, 1991).

1.2.2 Choroid vascular layers and the suprachoroid:

The vascular region consists of the outer Haller's layer of large blood vessels and inner Sattler's layer of medium and small arteries and arterioles that feed the capillary network and veins.

The suprachoroid space the transitional zone between the choroid and the sclera contains the elements of, collagen fibers, fibroblasts, and melanocytes.

1.2.3 Choroid Blood flow: Nourishment of the retina:

In spite of the presence of the retinal blood vessels, the major blood supply to the retina is from the choroid. The photoreceptors are extremely, metabolically active and consume over 90% of the oxygen delivered to the retina, especially in the dark when active transport of ions is required for ion homeostasis. In the darkness, ninety percent of the oxygen comes from the choroid (Linsenmeier et al., 1981; Linsenmeier and Braun, 1992).

To obtain this high transport of oxygen from the choroid, despite the barriers of Bruch's membrane the RPE requires a steep gradient of oxygen tension, which is maintained by the high blood flow in the choroid, probably the highest of any tissue in the body and tenfold higher than the brain (Alm, 1992; Alm and Bill, 1973). Consequently, the oxygen tension in the choroid stays high with an arterial/venous difference of only 3% versus 38% for the retinal circulation. The retinal vessels keep the inner retinal PO_2 at about 20 mm Hg

(Wangsa-Wirawan and Linsenmeier, 2003) where the oxygen tension is much lower than it is at the photoreceptors.

In the retina, the capillaries are continuous with no fenestrations constituting the blood-ocular barrier, requiring a special transport system to transport glucose and amino acids. The choroid circulation being fenestrated is crucial to transport nutrients and oxygen across RPE to the retina. The high protein permeability also establishes high oncotic pressure, contributing to the movement of fluid out of the retina through the stroma and suprachoroid and out of the sclera (Bill, 1962; Marmor et al., 1980).

1.2.4 Age-related maculopathy/AMD relevance:

Water, ions, nutrients and plasma -borne protein molecules move in both directions across Bruch's membrane. Impairment of this movement occurs in some disease states and in normal aging which can have serious consequences on visual function. The choroid is approximately 200 µm thick at birth and decreases to about 80µm at the age of 90 (Ramrattan et al., 1994). The thickness of the choriocapillaris and the capillary lumen diameters decreases with age and AMD (Ramrattan et al., 1994; Spraul et al., 1999). If a decrease in choroid blood flow results in decreased clearance of debris from RPE cells, there might be pathological changes in the Bruch's membrane, but it is also possible that the RPE changes might be the primary factor in the underlying change in the choroid (Nickla and Wallman, 2010).

In dry AMD the submacular choriocapillaris degenerates; it is unknown if this is the cause or consequence of the inflammatory response that causes the pathological changes in the

choroidal/RPE extracellular matrix (Zarbin, 2004). However, recent evidence shows that the atrophy of the RPE occurs first (McLeod et al., 2009).

In wet AMD, the choroid neovascularisation (CNV) occurs in response to the synthesis of vascular endothelial growth factor (VEGF) released as a result of the oxidative stress of the RPE. In this form of AMD, choriocapillaris degeneration occurs first in the presence of a viable RPE, suggesting that the neovascularisation is in response to the ischemia induced by the primary capillary degeneration with subsequent effects on the RPE (McLeod et al., 2009).

1.3 Retina:

The retina remains the best-studied part of the human brain, embryologically part of the central nervous system (Duke-Elder, 1963) but readily accessible to examination for both scientists and clinicians. An estimated 80% of all the sensory information in humans is thought to be of retinal origin (Sharma, 2003) indicating the importance of retinal functioning for the ability to interact with the outside world.

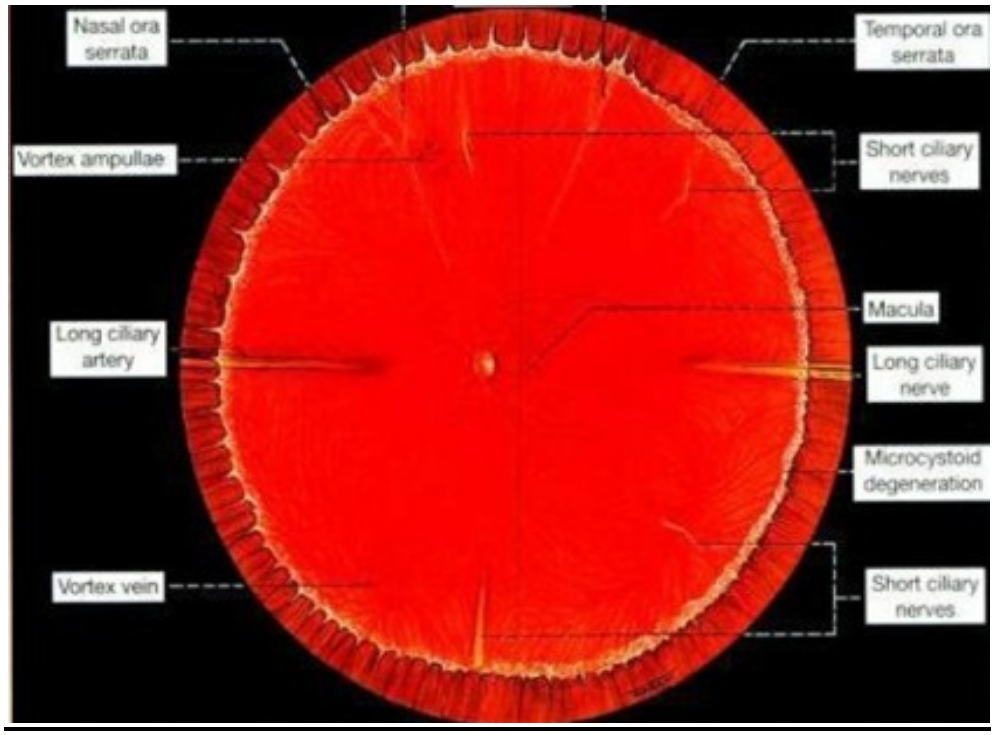

Figure 1.5: Schematic diagram showing the whole retina: an Optic nerve in the center surrounded by the posterior pole, Peripheral retina extending into the ora serrata shown, ciliary nerve, arteries and Vortex veins labelled (www.slideshare.net/retina -preliminary).

The retina extends from the ora serrata in the anterior to the optic discs posterior, it is divided into peripheral retina and the posterior pole (Figure 1.5). The retina has ten layers (Figure 1.6); the innermost layer is the retinal pigment epithelium (RPE) which is a monolayer of pigmented cells transporting metabolic end products from the sub retinal space to blood as well as supplying nutrients to photoreceptors from blood. The second layer after the RPE is the photoreceptor layer which consists of specialized neuronal cells capable of photo transduction and converting the light energy into signals stimulating the biological process of vision. The third layer is the external limiting layer/membrane (ELM)/outer limiting membrane (OLM) which separates the inner segment portions of the photoreceptors from the nucleus in their cells. This is followed by the fourth layer which is the outer nuclear layer (ONL) consisting of the cell bodies of rods and cones. Projections of

the rods and cones synapsing with the dendrites of the bipolar cells form the fifth outer plexiform layer (OPL). The sixth layer, inner nuclear layer (INL) is formed by the nuclei of the amacrine, bipolar and horizontal cells, this is followed by the synapses of the bipolar cell axons with the ganglion cells in the inner plexiform layer (IPL). The eighth layer is the ganglion cell layer (GCL) consisting of the nuclei of ganglion cells, the axons of which become the optic nerve fibres and eventually form the nerve fibre layer (ninth layer). The internal Limiting layer/membrane (ILM) is the tenth layer forming a boundary between the retina and the vitreous body formed by astrocytes and the end feet of Muller cells (retinal glial cells).

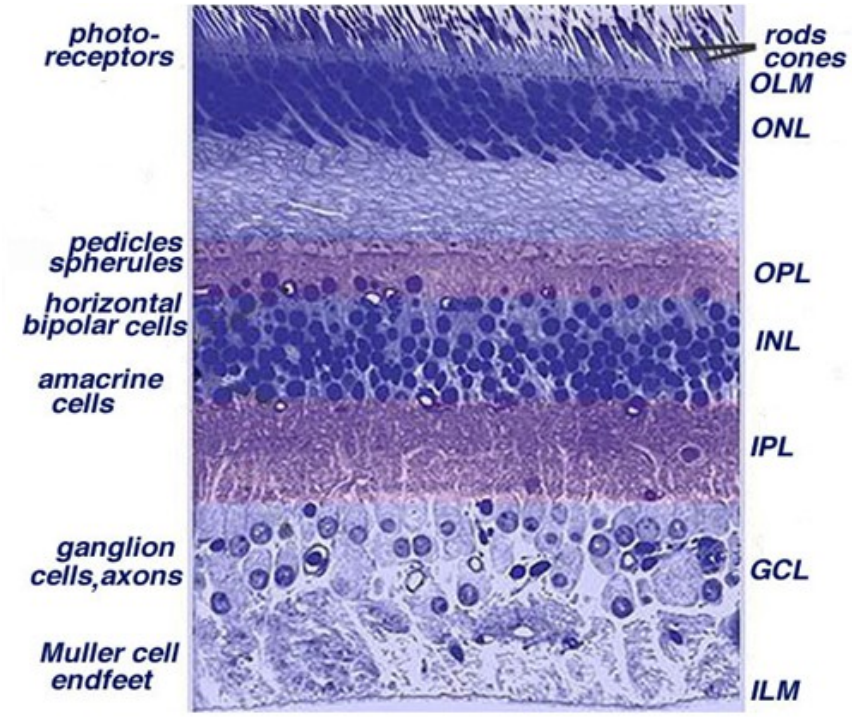

Figure 1.6: Light micrograph of a vertical section through central human retina, the layers of the retina as visualized have been labelled (www.webvision.med.utah.edu). The ten Layers of the retina are; 1. Retinal pigment epithelium (RPE); 2. Photoreceptor; 3.External limiting Layer/membrane (ELM)/Outer limiting membrane (OLM); 4. Outer nuclear layer (ONL); 5. Outer Plexiform layer (OPL); 6. Inner Nuclear Layer (INL); 7. Inner Plexiform layer (IPL); 8. Ganglion cell layer (GCL); 9. Nerve fibre Layer; 10. Internal Limiting layer/membrane (ILM)

1.3 .1 The Macula:

The adult posterior pole (anatomical macula or area centralis) is about 4.5-6 mm in diameter and is centered on the fovea between the superior and inferior arcades. The macula is about 1.5 mm or one disc diameter in size (Kincaid, 1991).

The most central part of the macula, the fovea is formed by a central 0.35 mm wide depression representing the retinal region of greatest visual acuity (Oyster, 1999).

The foveola has the highest density of cone photoreceptors (199,000/mm^2), which are narrowed and elongated in this location to maximize light detection further (Curcio and Allen, 1990). The long axons of the foveal cones form Henle's layer as they radiate out of the central depression. The fovea develops by an opposing process of outward displacement of cells of the inner nuclear and ganglion cell layers, while the cone photoreceptors migrate towards the center (Hendrickson, 1993). Rod photoreceptors are excluded from the foveal outer retina ("rod free zone"). As a result, the foveola contains only the cone photoreceptors and some Muller cells, The central 500µm of the fovea contains no retinal capillaries (the foveal avascular Zone or FAZ), making the fovea dependent on blood supply from the choriocapillaries (Figure 1.7).

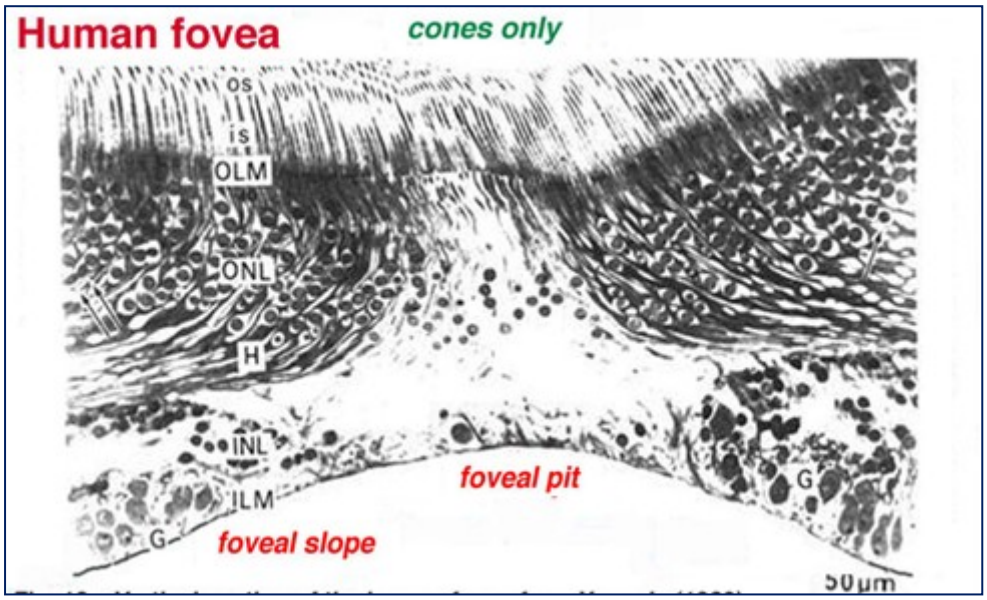

Figure 1.7: Vertical section of the human fovea (Yamada 1969).
Microscopic section showing the layers of the retina at the macula, the foveola contains only cone and some muller cells. OS, IS outer segment and inner segment of photoreceptor cell; OLM, outer limiting membrane; ONL outer nuclear layer; H, Henle fibers; INL inner nuclear layer; ILM inner limiting membrane; G, ganglion cells.

1.3 .2 Peripheral retina:

The peripheral retina comprises of the remaining retina outside the temporal retinal arteries. The central retina is thicker compared to the peripheral retina due to the dense packing of the cone photoreceptors and their associated bipolar and ganglion cells compared to the central retina. The central retina is cone dominated and peripheral retina is rod dominated. The ampulla of the vortex veins lies just posterior to the equator, while the long posterior ciliary arteries and nerves mark the horizontal meridian. The ora serrata marks the anterior termination of the sensory retina and the beginning of the pars plana of the ciliary body, making this space a relatively safe site for surgical access to the posterior segment and also for intravitreal injections.

1.3.3 Retinal Pigment Epithelium:

The retinal pigment epithelium (RPE) is a monolayer of pigmented cells forming a part of the blood/retina barrier (Olaf, 2005). The apical membrane of the RPE faces the photoreceptors outer segments; these long apical microvilli surround the light-sensitive outer segments to make close structural interactions. The outer basolateral membrane of the RPE faces the fenestrated endothelium of the choriocapillaris. Embryologic development of RPE and the photoreceptors are interrelated with RPE secreting factors needed for the survival and differentiation of photoreceptors.

The RPE transports ions, water, and metabolic end products from the subretinal space to the blood and nutrients like glucose, retinol, and fatty acids from the blood to the photoreceptors.

1.3.3a Functions of the RPE:

The functions of the RPE are summarised in Figure 1.8,

1. RPE has a major role in photoreceptor excitability. It performs this function by aiding in the visual cycle and converting all-trans-retinal into 11-cis-retinal, by maintaining voltage dependent ion composition in the sub-retinal space and by phagocytosis of the shed outer segments of the photoreceptors.

2. The secretory function of the RPE is to be responsible for providing a variety of growth factors which help to maintain the structural integrity of choriocapillary and photoreceptors endothelium. RPE also establishes the immune privilege of the eye by secreting immunosuppressant factors (Streilein et al., 2002) as the failure of any of these factors lead to the degeneration of the retina, loss of visual functioning and eventual blindness.

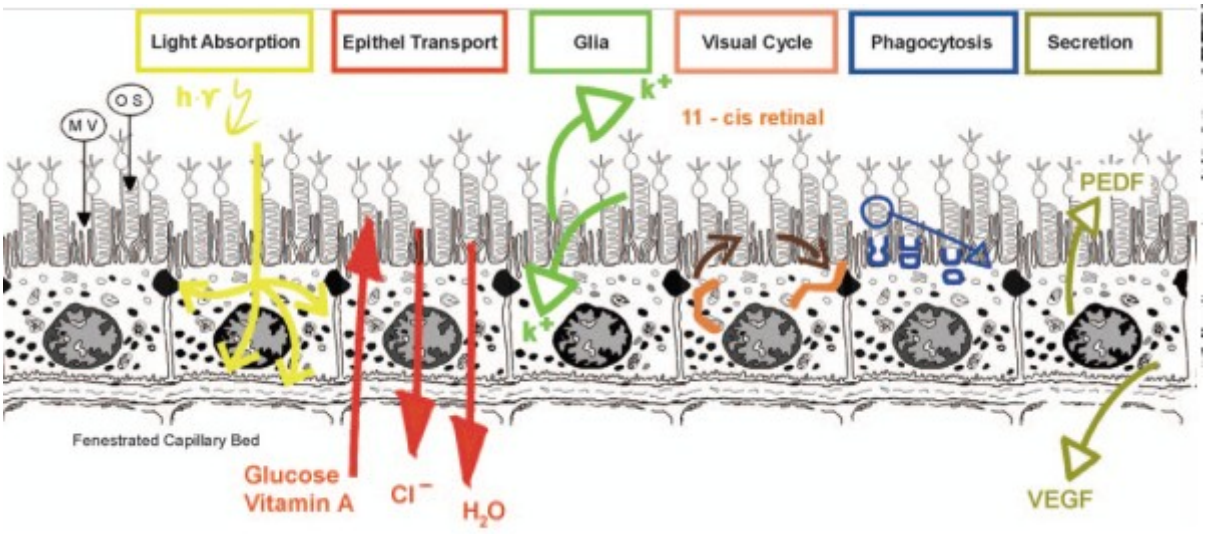

Figure 1.8: Schematic summary of various RPE functions; PEDF, pigment epithelial growth factor; VEGF, Vascular epithelial growth factor; (Olaf ,2005).

3. RPE helps in absorption of light and increases the optical quality of the retinal image by forming a darkly pigmented wall cover which absorbs light that is not absorbed in photoreceptors and scattered light. Light entering the pupil is focused onto the macula lutea by the lens which concentrates the light energy onto the retina. The outer retina is exposed to oxygen rich environment as the blood perfusion of choriocapillaris is high (Alm and Bill, 1972). There is a negligible oxygen extraction along the passage through the choriocapillaris as the venous blood here shows 90% O_2 concentration in comparison to retinal vessels which have 45% O_2 saturation. The retina appears to float on oxygen-rich blood filled vessels which are ideal to allow photo-oxidation and subsequent oxidative damages. The photo-oxidative damage is also increased by a load of reactive oxygen species produced by the phagocytosis of shed photoreceptor outer segments (Miceli et al., 1994).

4. RPE aids in the defense against photo-oxidative stress. This function has been described by Boulton and Dayhaw-Baker (2001) there are three levels of defenses against oxidative damage;

a. Absorption and filtration of light by pigments:

General light absorption is by melanin in melanosomes, absorption of blue light is by carotenoids in photoreceptors which are lutein and zeaxanthin. Blue light is the most dangerous for RPE cells in the adult eye as it permits photo-oxidation of lipofuscin components to cell toxic substances (Ben-Shabat et al., 2001) . As a light absorbing pigment, lipofuscin be beneficial for visual function. However, its concentration reaches a toxic level in older eyes (Olaf, 2005).

b. Anti-Oxidants:

RPE contains high levels of enzymatic antioxidants such as superoxide dismutase (Miceli, 1994) catalase, non-enzymatic antioxidants like carotenoids, ascorbate, alpha-tocopherol, and beta carotene (Beatty,1999). This is supplemented by melanin and glutathione which primarily function as anti-oxidants.

c. Repair Mechanism:

The third line of defense is the cell's physiological ability to repair damaged DNA, lipids, and proteins.

1.3.3b Age-related maculopathy/ AMD relevance:

An increase in the oxidative stress due to reduction in the protective mechanisms or an increase in the number of active photo-oxidative reaction species is believed to contribute to the pathogenesis of AMD (Boulton,1991).

One starting point is the accumulation of lipofuscin in the RPE; age-dependent changes like reduction in the cell density of RPE, accumulation of toxic substances secondary to reduction of alpha-tocopherol, the decline in melanocytes and increase in lipofuscin are seen. Oxidative stress can be seen as an accumulation of advanced -glycation end products (AGEs) in Bruch's membrane which have an important role in inducing CNV.

Drusen which are the most important sign of AMD are metabolic end products from both RPE and photoreceptors. Detailed analysis of the protein composition of drusen has led to alternate theories. In one theory the formation of drusen begins with the loss of RPE that are removed by an inflammatory event. The resultant gap is closed by an adjacent RPE that secretes a new extracellular matrix (Hageman,2001). This is supported by the detection of active dendritic cells and complement system in drusen (Mullins, 2000).The other theory is that the hydrophobic and lipoprotein material may be the debris left from incomplete degradation of cells (Sakaguchi , 2002).

1.3.4: Photoreceptors:

A photoreceptor cell is a specialized neuron in the retina capable of photo transduction and converts light energy into signals that stimulate the biological processes. The two classic cells are cones and rods; there are two to three types of cone photoreceptors and a single type of rod photoreceptor.

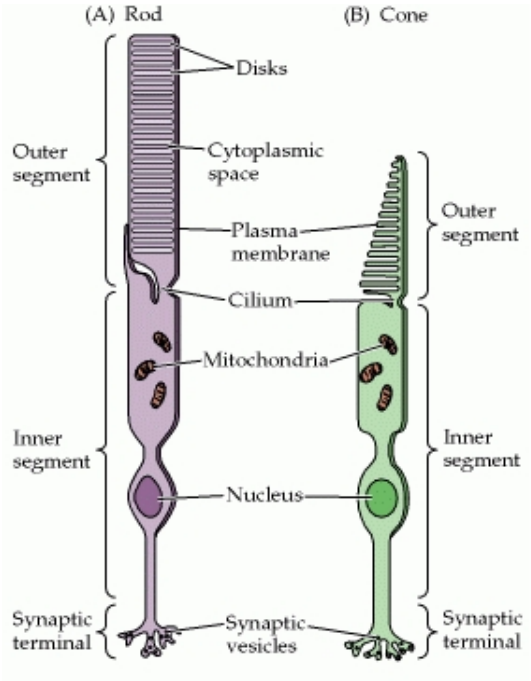

Figure 1.9: Schematic diagram of Rods and Cones. Although generally similar in structure, rods (A) and cones (B) differ in their size and shape, as well as the arrangement of membranous disks in their outer segments (Purves,2001).

As the name suggests cones are conical whereas rods are slim rod-shaped structures arranged in a single row below the OLM (outer limiting membrane) with their inner and outer segments protruding into the subretinal space towards the RPE. Rod/Cone cell bodies make up the outer nuclear layer, while apical processes of RPE envelop the photoreceptor's outer segments.

The photoreceptors (Figure 1.9) consist of an outer segment, an inner segment, a cell body and a synaptic terminal.

The outer segment of a photoreceptor is filled with stacks of membranes containing visual pigment molecules like rhodopsins. The inner segment contains mitochondria, ribosomes, and membranes where opsin molecules are assembled and passed to be part of the outer

segment discs. The cell body contains nucleus of the photoreceptor cell and the synaptic terminal is where neurotransmission to second order neurons occurs.

Outer and inner segments of the rods are generally thinner than of the cones. Rod's inner segments are 2 microns and the cone's about 6 microns in diameter, however at the fovea where there are only cone photoreceptors the central cones are even thinner than the average rods at about 1.5 microns diameter.

The stacks of discs containing visual pigments in the outer segments of the photoreceptors are constantly renewed. New discs are added at the base of the outer segment at the cilium; at the same time, old discs are displaced up the outer segment and are pinched off at the tips and engulfed by the apical processes of the pigment epithelium. These discarded discs become known as phagosomes of the pigment epithelium cells. They are then broken by lysis. Photoreceptor outer segment discs are phagocytosed by the pigment epithelium shortly afterward (Young, 1971).

1.3.4 a Different types of cone photoreceptors:

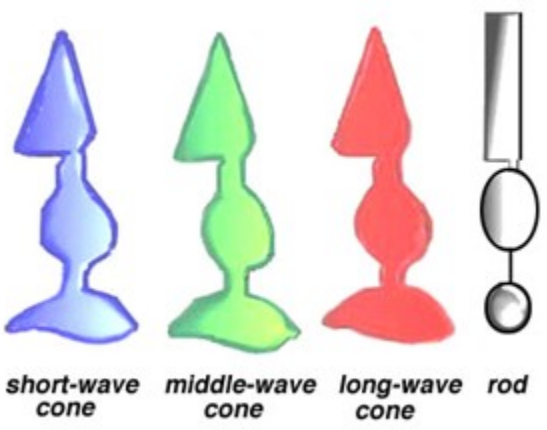

Figure 1.10: Types of Photoreceptor cells.
Short -wavelength cones (blue), Medium cones (Green) and Long wavelength (Red) and rods. Reproduced from (Kolb, 2013).

The long wavelength sensitive, L-cones, are maximally sensitive to wavelengths peaking around 560 nm. Medium wavelengths cones, M-cones, peak around 530nm and short wavelengths, S-cones, have peaks varying from 430 nm (Baylor et al., 1987) to 445 nm (Dobelle et al. 1969) (Figure 1.10)

Colour processing is associated with two main channels that emerge from opponent processing. Colour opponency was initially suggested by Hering in 1874 (translated in 1964) and involves the comparison of signals between different cone inputs. The RG channel utilizes differences between the inputs of L and M Cones, while YB channel compares signals derived from the M and L cones to the signals originating from the S cones. The overlapping sensitivities of the three cone pigments allow an astonishing number of combinations of excitation levels, which in turn lead to the perception of many distinct colours.

S cones have the lowest spatial density in the foveal pit and constitute 3-5% of the cones, reaching a maximum density of 15% on the foveal slope (1 degree from the foveal pit) and forming an even 8% of the total population elsewhere in the retina (Ahnelt et al., 1987).

Marc and Sperling (1977) found the distribution of L -cones at about 33% of the cones throughout the retina, whereas the M-cones peak in the fovea at 64% and vary between 52% and 59% elsewhere in the retina. However, others found the L-cones to outnumber the M-cones in fovea and perifoveal psychophysical testing paradigms (Cicerine and Nerger, 1989). They further established the L: M ratio to be 2:1 in the human fovea centralis. The latest laser interferometry (Roorda 1999; Williams and Hofer et al 2005) found a considerable variation amongst individuals. Roorda et al (1999) found values of 75.8% L with 20.0% M versus 50.6% L with 44.2% M in two male subjects. Hoofer et al (2005) found that males with normal colour vision varied in the ratio of L to M cones from 1.1: 1 to 16.5:1, all subjects had nearly identical S-cone densities. Hoofer et al (2005) suggested that the assignment of L and M pigment, although highly irregular, is not a completely random process and may be a compromise of the visual system between the needs of the spatial and colour vision.

1.3.4 b The density of Rods and Cones in the human retina:

Photoreceptors are organized in a mosaic hexagonal pattern at the fovea and start to break up, while still maintaining an organized architecture of cones evenly spaced with rings of rods. The cone density is highest in the foveal pit and falls rapidly outside the fovea to a fairly even density in the peripheral retina (Osterberg, 1935; Curcio et al 1987). There is a

peak of rod photoreceptors around the fovea at about 4.5mm or 18 degrees from the foveal pit. The optic nerve head forms the 'blindspot' since it is free of photoreceptors.

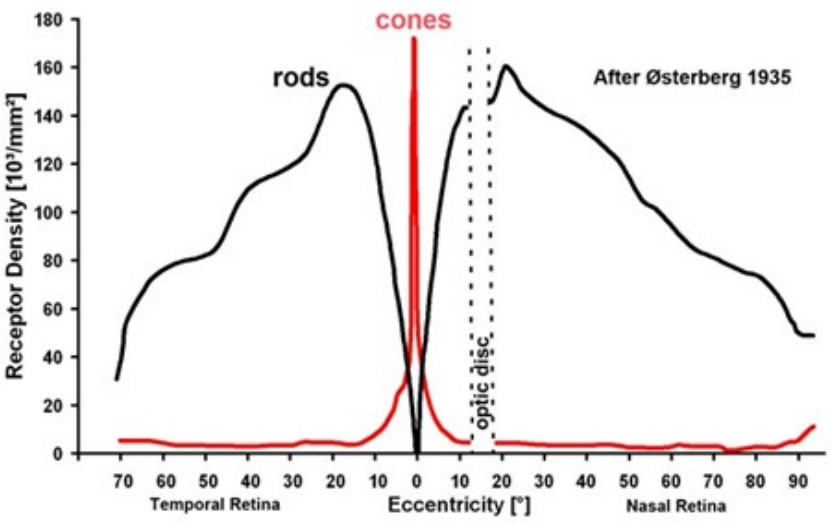

Figure 1.11: Graph showing rod /cone densities along horizontal meridian.
The graph shows that the cone density is highest at the foveal pit, and rod density peaks at about 4.5 mm or 18 degrees from the foveal pit. (Kolb,2013).

Rods are so sensitive that they can actually detect a single quantum of light. Rod sensitivity appears to be achieved at a compromise, since the rods are much slower to respond and the signals from rods may arrive as much as $1/10^{th}$ of a second later than those from cones under lighting conditions where both can be activated (MacLeod, 1972). In addition, the signals from many rods are summed up and converge to single ganglion cells, hence the loss of spatial resolution.

If we consider the macula to be an area of 6 mm in diameter subtending an angle of 21.5°of visual angle centered on the fovea (Klein, 1991), the small cone dominated fovea would be only 0.8 mm (2.75^0) in diameter surrounded by the rod –dominated parafovea (Curcio and

Allen 1990). In young adults, rods outnumber cones in the macula by 9:1. In the entire eye, rods outnumber cones 20:1, so the macula can be considered cone-enriched but not cone dominated.

1.3.4 c Age-related maculopathy and AMD relevance:

In the macula of older adults, lacking grossly visible drusen and pigmentary change, (without any ARM) the cones in the cone-dominated part are stable at approximately 32,000 through the ninth decade (Curcio et al., 1993). In contrast, the rods in the macula of the same eye decrease by 30%. The greatest loss occurs in the parafoveal (1-3 mm from the fovea or 3.5^{o}-10^{o} from the fixation). With respect to photoreceptor topography at different stages of ARM, the foveal cone mosaic of eyes with large drusen and thick basal deposits appears to be similar to age – matched controls (Curcio, 1996) and the total number of cones were normal.

In contrast at the parafovea, the cones appeared to be large and misshapen as few rods remained. Furthermore in eyes with late ARM, virtually all surviving photoreceptors in the macula were cones with a reversal of the normal predominance of rods. The mean scotopic loss is maybe greater in magnitude than the mean photopic sensitivity loss in the majority of ARM patients, as noted by Curcio et al (2000).

1.3.5 Ganglion cells:

Visual signals are transmitted and processed in bipolar, horizontal, amacrine and interplexiform cells within the retina. Finally, the ganglion cells are responsible for transmitting the processed information from the retina to the brain. Because of the anatomical distance between the retina and the brain, the ganglion cell axons require

effective mechanisms for the transport of metabolites and organelles away from (antegrade) and back to (retrograde) the ganglion cell nucleus. Most transportations is slow and anterograde. Axon transportation is an active process that requires adenosine triphosphate (ATP) which is supplied by the mitochondria in the axon.

The ganglion cell layer (GCL) contains about 1.2 million ganglion cells, the thickness of the GCL is greatest in the perifoveal macula consisting of 8-10 rows of nuclei (60-80μm), it decreases to a single row outside the macula (10-2 μm) and is absent from the fovea itself (Sharma 2003; Kincaid and Green1999).

1.3.5 a Aging and Age-related maculopathy/AMD relevance:

The tissues present within the eyes ages along with us and this, in turn, influences the amount of light that reaches the retina (Owsley, 1987). Age-related changes in the optics of the eye contribute to the decline of some visual functions. Changes in the retina and in particular the loss of photoreceptors and ganglion cells in healthy aging also contributes to loss of visual performance (Enoch, 1999, Elliot, 2012). The retinal ganglion cells (RGC) synapse into the lateral geniculate nucleus (LGN) of the thalamus, which in turn relays into the primary visual cortex. Neural changes along the visual pathways from the retina to the striate cortex can also contribute to declining visual function.

MRI of the human LGN shows approximately a 15% reduction in structural volume between 20 and 70 years of age (Li, 2012). Histological analysis of postmortem tissue indicates a more dramatic decline (30%) (Selemon, 2007). Despite these changes in tissue volume, the number of neurons in the LGN regardless of species does not change (Selemon ,2007; Ahmad, 1993; Diaz, 1999), but the RGC neuron itself may be more vulnerable. The

vulnerability is indicted by the diminished size and complexity of RGC axons (Samuel, 2011), slow axonal transport (Karlsson, 1992), and through the age-related shrinkage of the distal superior colliculus volume as seen in animal studies (Crish, 2010) .

Unlike the photoreceptor cells and bipolar cell axons which are unmyelinated, only the short segment of the RGC axon is unmyelinated. Myelination starts once the RGC axon penetrates the laminar portion of the optic nerve. The RGC axons also differ from the photoreceptor axon in being very thin, optimized for minimal firing rate and usage of energy (Niven, 2008, Wang, 2007), but the small size of the RGC axons has implications for susceptibility to Ca^{2+} homeostasis and cytoskeleton degradation. A small axon, especially one with an inefficient and unmyelinated segment, is also at a disadvantage should the available ATP (adenosine triphosphate) diminish due to slow axoplasmic flow. Aging is also associated with a decline in the ATP available for hydrolysis which is necessary for release of stored energy.

Most studies find robust and regular age-related decline in axon number (Mikelberg 1989; Morrison 1990; Jonas 1992). The rate of human axonal loss is 0.5% annually (Harwerth, 2008) resulting in an approximate 40% decline over a life span (Neufeld AH 2003). This suggests that survival of unmyelinated segment in the retina and nerve head is coupled tightly to the survival of distal axon segment in the nerve itself.

2. Age-related macular degeneration:

2.1 Introduction to AMD:

Hutchinson first described the condition in 1874 as "Symmetrical central choroidal-retinal disease occurring in senile persons" (Kolar, 2013). About 25 years ago the term "Age-related maculopathy (ARM)" was accepted and the end stage of the disease was acknowledged as "Age -related macular degeneration (AMD)" (De Jong, 2006) .More recent classifications (Ferris et al., 2013) have classified eyes into normal aging, early AMD, intermediate AMD and late AMD. The term AMD has since been used for both early and late stage of the disease.

AMD is a multi-factorial maculopathy characterized by late-onset progressive neurodegeneration of photoreceptors and retinal pigment epithelium (RPE) (Miller, 2013). AMD is the commonest cause of severe visual impairment or blindness in the developed world. It is estimated that a quarter of a million older adults in the UK alone suffer from blindness due to the condition (Ferris et al., 2013). The World Health Organization (WHO) indicates that AMD ranks third after cataract and glaucoma as a leading cause of blindness globally.

AMD typically is classified into two phenotypic categories: Wet AMD and geographic atrophy (GA). In wet AMD choroid neovascularization breaks through the neuroretina, causing leaky vessels, haemorrhages, and lipid deposits which eventually lead to a scarring process in the macular area. All retinal structures including photoreceptors are destroyed. In GA there is progressive atrophy of RPE and secondary photoreceptors. To the end of the 20th century wet AMD was practically untreatable, however, new pharmaceuticals based on suppression of vascular endothelial growth factor (VEGF) have completely changed the

course of treatment of this condition as nearly 95% of the patients can be prevented from visual loss and 40% of them can improve vision (Lim et al., 2012).

2.2 Epidemiology, risk factors, and natural history:

Many epidemiological studies have been published during the past 30 years. In a meta-analysis of a population-based studies in Caucasians aged 40 and over , the estimated prevalence of early age-related maculopathy was 6.8% and late age-related macular degeneration was 1.5% (Smith et al., 2001). A recent systematic literature review of 39 studies (Wong et al., 2014) showed a pooled prevalence of early, late and other forms of AMD to be 8.01%, 0.37% and 8.69% respectively.

The Baltimore Eye Study in 1999 reported epidemiological data from other ethnic groups, which showed that late AMD was nine to ten times more prevalent in white than in black participant and was almost similar in Asians. However, PCV (polypoidal choroidal vasculopathy) accounts for 50% of wet AMD in Asians and only 8-13% in white people (Laude et al., 2010) . Another variant of wet AMD is RAP (retinal angiomatous proliferans) which accounts for 12-15% of wet AMD; (Gupta et al., 2010) RAP usually does not respond to the standard management of wet AMD.

2.2a Risk factors:

The major risk factor for age-related maculopathy is age; more than 10% of the people older than 80 years have late AMD. Sex has been consistently reported as a risk factor with females being affected the most (Smith et al., 2001).

The major systemic risk factor is smoking (Seddon et al., 1996) .Smoking 20 cigarettes a day doubles the risk of developing AMD. Other systemic risks such as obesity, hypertension, diabetes, and strokes are also found to be associated in people with AMD (Chakravarthy et al., 2010).

Low dietary intake of vitamin A, C, E, Zinc, Lutein and Omega-3 fatty acids can also affect the probability of developing AMD. An unhealthy life style related to cardiovascular risk factors is postulated to be related to ARM and consequent AMD (Lim et al., 2012).

2.2 b Genetic Factors:

In the last ten years several genes have been found to have a role in AMD. The pathogenesis of AMD has been linked to inflammatory and immunological processes, therefore, the complement factor H gene (CFH) have been implicated.
Other confirmed genes in the complement pathway are C2, CFB, C3 and CFI (Penfold et al., 2001). Collagen pathway genes, extracellular matrix pathway gene TIMP3 and finally the angiogenesis pathway genes (VEGFA) have been associated in a Meta -analysis of two AMD genome-wide association studies (Yu et al., 2011).
The gene pathways are associated with onset, progression and bilateral involvement of AMD, but environmental factors may modify individual susceptibility. Genetic variations can also influence differential responses to treatment for AMD which is an emerging research area.

2.3 Normal Aging:

Aging is a physiological process involving all body organs and tissues including the eye. Each body cell has a planned cell cycle leading to apoptosis or cell death but in tissues with no restoration of extinct mitotic cells like the retina, there is a high chance of aging especially after the 75th year of life.

Clinically, aging is the loss of foveal reflex which in effect is the loss of cells from the inner retinal layers around the foveola and FAZ (Foveal avascular zone) (Laatikainen and Larinkari, 1977). In the macular area, there can be a presence of hard drusen which are not ARM but signs of normal aging (Klein et al., 1992). Doppler velocimetry shows a decrease in blood flow to the macular area (Groh et al., 1996). There is a detectable reduction of peri foveolar arterioles and venules together with the enlargement of the FAZ (Ibrahim , 1998) as well as the retinal ganglion cell amounts (Gao and Hollyfield, 1992).

Visual acuity remains relatively unaffected at this stage but there can be a decrease of other visual functions such as adaptation to darkness, contrast sensitivity, colour vision, and stereopsis (Sandberg and Gaudio, 1995).

The macula undergoes a spectrum of changes in the normal eye. In a subset of individuals, these changes can progress to pathology manifest as AMD (Zarbin, 2004). Healthy young maculae tend to have a sharp foveal light reflex on biomicroscopy, caused by the concave shape of the fovea. As the macula ages, this reflex is blunted by possibly the decrease in the photoreceptors density, swallowing of the foveal pit and enlargement of the capillary-free zone (Laatikainen and Larinkari 1977). Several small well-defined drusen are usually present in the elderly (Klein et al., 1992). The irregularity of the RPE may cause a stippled background of varying degrees.

Photoreceptor drop out is caused mostly by the loss of rods (Curcio et al., 1993). Foveal cone density may, however, remain constant until the ninth decade. Lipofuscin accumulates in the RPE and it deteriorates over time. BLamD (basal laminar deposits) are between RPE basal plasma membrane and basement membrane in the subretinal space. BLamD are seen uniformly distributed by the seventh decade, they are considered normal aging if there are focal lesions (Miller, 2013) which are seen as small "hard drusen". However, BLamD is often not visible clinically and represents more of a histological finding. An eye with early BLamD has a normal clinical fundus appearance.

2. 4 Early and intermediate AMD:

Age-related maculopathy (ARM) is a disorder of the macular area of the retina, most often clinically apparent after 50 years of age, characterised by any of the following primary items, without indication that they are secondary to another disorder (International ARM epidemiological study group, 1995) (Bird et al., 1995).

The first primary characteristic item is drusen (Figure 2.1 a) which are discrete whitish-yellow spots external to the neuroretina or the RPE. They may be soft and confluent, often with indistinct borders. Soft distinct drusen have uniform density with sharp edges. Soft indistinct drusen have decreasing density from the center outwards with fuzzy edges. Hard drusen, usually present in eyes with or without ARM, do not characterise the disorder themselves.

The second item is an area of increased pigmentation or hyperpigmentation (in the outer retina or choroid) associated with drusen (Figure 2.1 b). The third are areas of

depigmentation or hypopigmentation of the RPE, most often more sharply demarcated than drusen, without any visibility of choroidal vessels (Figure 2.1c)

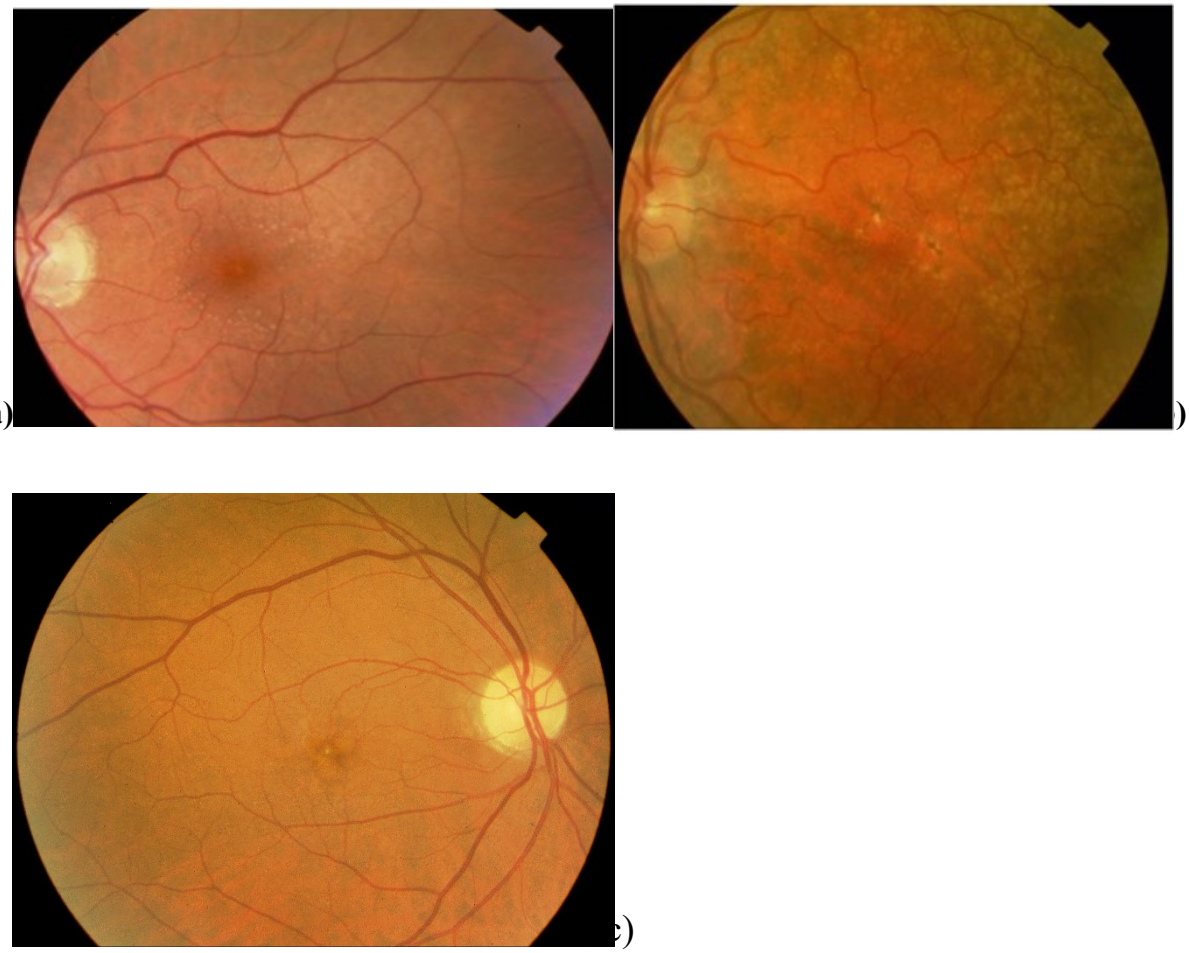

Figure 2.1: Fundus photograph in study patients showing the three primary items in ARM. a) Drusen b) Pigmentary change with Drusen c) Hypopigmentation.

2.4 a Drusen:

Drusen are one of the earliest clinical signs of age-related macular degeneration (AMD) and are characterized based on their texture (hard or soft), borders (distinct or indistinct), and their size: small (<63 μm), intermediate (>63 μm but <125 μm), or large (≥125 μm) (Klein et

al., 2002; Seddon et al., 2006). Lesions similar to drusen, both in histology and clinical appearance, are also seen in choroidal tumors, chronic inflammation and degenerative conditions of the eye. Drusen are yellowish white deposits of extracellular material located between the retinal pigment epithelium (RPE) and the inner collagenous zone of the Bruch's membrane; they are the result of aging. However, drusen seen in varied conditions have a similar clinical and histological appearance. When viewed ophthalmoscopically, drusen appear as dots ranging in colour from white to yellow sometimes with a crystalline, glittering look.

The occurrence of drusen is however not a static phenomenon. Their presence is characterized by dynamic changes. Hard drusen can grow and change to soft drusen. Soft drusen can grow and coalesce into large confluent bodies which lead to detachment of RPE.

Numerous longitudinal studies have demonstrated correlations between total drusen area and the maximum drusen size, with the risk of progression to advanced AMD (Klein et al., 2002; Bressler et al., 1990; Davis et al., 2005; van Leeuwen et al., 2003; Wang et al., 2003). Large, soft, confluent drusen are associated with a higher risk for development of advanced AMD (Klein et al., 2007;Pauleikhoff et al., 1990; Ferris et al., 2005).

2.4 b Changes in RPE:

Irregularities in RPE are associated with all stages of macular degeneration. Focal hyperpigmentation arises from changes at the level of the RPE. Hyperpigmentation can also be seen as the migration of the RPE cells into the subretinal space. Focal hypopigmentation is commonly seen with chorioretinal anastomosis. Focal hypopigmentation is associated with areas of drusen, which leads to the thinning of the RPE cell layer and reduction of melanin

content. Low melanin content has been associated with high risk of transition to wet AMD (Kolar, 2013).

2.4 c Histology:

In AMD with RPE degeneration, the patchy BLam D seen in normal aging develops an overlying layer of diffuse, thick, amorphous and hyalinized material which can become nodular elevations (Bressler et al., 1994). Clinical correlation of this late form is not fully established but its presence can be inferred by pigmentary changes (Sarks et al., 2007). Focal hyperpigmentation correlates histologically with RPE hypertrophy and migration of pigmented cells to sub-RPE and subretinal space and may represent compromised RPE cells that can no longer support the photoreceptors.

BLinD forms layers of membranous debris between the RPE basement membrane and the inner collagenous layer, within the bruch's membrane. BLinD are thought to be lipoprotein particles which appear clinically as soft drusen (Sarks et al., 2007).

Multilayer BLinD cause separation of RPE from the Bruch's membrane leading to CNV making their way into this space.

BLinD can also accumulate as focal aggregations of basal mounds between the RPE basal membrane and plasma membrane, as they do not manifest as drusen but cause pigmentary changes and primary geographic atrophy without the appearance of drusen (Sarks et al., 2007).

2.5: Reticular Pseudo drusen (RPD):

Reticular drusen or subretinal drusenoid deposits represent a subphenotype of AMD that was first identified on blue light (red free) fundus photography (Mimoun et al., 1990) .They

clinically appear as yellowish, faint, interlacing networks that most commonly occur along the arcades and do not fluoresce on FA. Imaging with OCT particularly spectral domain OCT (SD-OCT) has been shown to be effective in detecting reticular pseudodrusen. SD- OCT shows numerous drusenoid deposits above the RPE in the subretinal space (Schmitz-Valckenberg et al., 2010; Zweifel et al., 2010). This is contrary to the previous histological studies which localized the changes to the choroid. The origin of these lesions is unclear but may represent direct photoreceptor damage (Curcio et al., 2013). Reticular pseudo drusen were initially associated with neovascular AMD (Arnold et al., 1995; Cohen et al., 2007) but recent studies show they represent a risk factor for progression to geographic atrophy (Klein et al., 2008b; Pumariega et al., 2011).

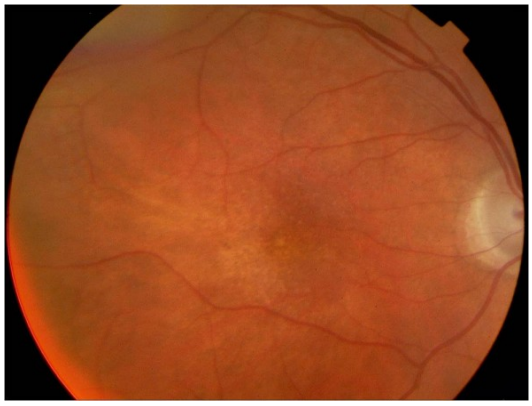

a)

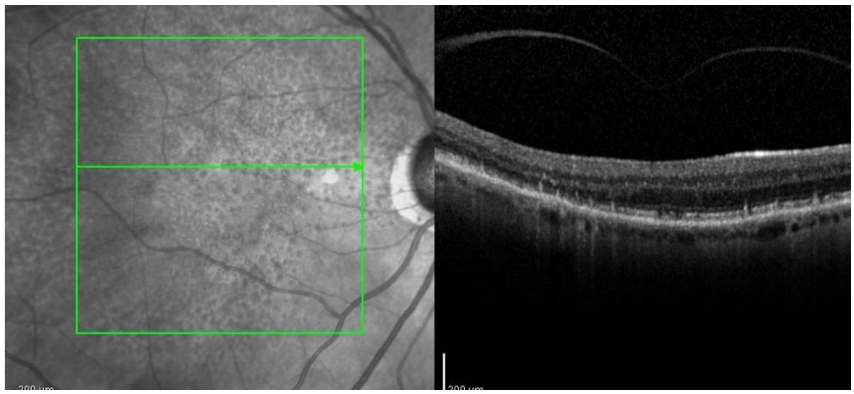

Panel showing b and c

Figure 2.2: Reticular Drusen in a study patient. a) Fundus photo b) Infrared picture C) OCT Scan. Fundus photograph shows the pale yellow lesions of RPD, lesions are seen more clearly and distinct on Infrared imaging (IR) and OCT scan. Reticular IR is seen as groups of hyporeflective lesions against a background of mild hyperreflectance. Spectral domain OCT showing the characteristic subretinal deposits of RPD.

Several multimodal imaging studies showed that RPD are most prevalent in the superior macula and that FAF, IR and SD-OCT are superior to other modalities, like colour fundus photography, in detecting RPD (Alten and Eter, 2015).

Based on a comparison of different imaging modalities used for visualisation of RPD, Sivaprasad et al (2016) recommended that at least 2 modalities be used to detect and confirm the diagnosis of RPD. Currently SD-OCT and IR are preferred for screening of RPD (Smith et al., 2009; Sohrab et al., 2011; Ueda-Arakawa et al., 2013). The sensitivity of IR for detection of RPD has been reported to be about 95% although it has also been found to have

the highest false positives in cSLO imaging (Suzuki et al., 2014), probably due to the similar characteristics shared by RPD and soft drusen. Ueda-Arakawa and colleagues also found high sensitivity (94.6%) and specificity (98.4%) for SD-OCT alone. In addition, red free confocal blue reflectance and ICG were all highly specific (73-100%) for detecting RPD, despite being less sensitive than IR and SD-OCT (Ueda-Arakawa et al., 2013).

2.5a Genetic and environmental factors:

Both groups AMD / ARM and RPD share the same major genetic and environmental factors and showed no significant differences suggesting RPD occurs in the same genotype and epidemiological background as AMD (Puche et al., 2013). Yet, a significant association between ages, later age of AMD onset, gender, and risk of systemic hypertension have been noted (Boddu et al., 2014). The link implies that further genetic studies to verify the exact correlation between RPD and AMD risk alleles are needed.

2.5 b Path physiology:

The exact path physiology underlying the formation of RPD remains unknown but the OCT enface imaging provides information on some of its features. Spaide, Curcio, and co-workers showed through histological examinations that RPD is located internal to the retinal pigment epithelium (RPE) and hypothesized that the biological substrate of the RPD is generated at the level of the RPE and the photoreceptor's outer segments (Curcio et al., 2013; Spaide, 2013).

There has been a relation of RPD to choroidal watershed zone, suggesting choroidal hypoxia in RPD pathogenesis (Alten and Eter, 2015). Reduced choroidal thickness, choroidal volume and narrow and sparse choroidal vessels have been reported in these patients. (Alten and Eter,

2015). The relationship between RPD and choroidal thinning is not expected to be a simple direct correlation and may be related to other factors (Mrejen et al., 2014).

Spaide (2013) showed regression of these lesions with accompanying outer retinal atrophy and loss of underlying choroidal thickness, proposing the term outer retinal atrophy as a new entity to late stage AMD. He suggests that the reduction in RPE function leads to dysfunctional transport of the RPE and the Muller cells, resulting in an accumulation of material in the outer retina. This material also impedes normal transportation of outer segments towards the RPE, with attenuation of the photoreceptor metabolic activity less oxygen is needed resulting in choroidal thinning.

Marsiglia and colleagues (2013) reported that GA expanded particularly in the areas affected by RPD and conclude that RPD represents an early manifestation of the process leading to GA.

2.5 c Histology:

The histological correlate that presumably corresponds to the appearance of the RPD in various imaging modalities was called subretinal drusenoid deposits (SDD). Some of the materials found in soft drusen are also found in SDD, but the lack of opsins suggests that the material is not derived from the retinoids. SDD, unlike soft drusen, are histologically rich in unesterified cholesterol and poor in esterified cholesterol.

Due to the small lesion size, their confluent reticular pattern spreads beyond the central macula, thus quantification of RPD in terms of total affected area is more challenging than the other AMD phenotypes.

Multimodal imaging studies have shown that RPD are more prevalent in the superior macula and that FAF, IR, and SD -OCT yield more information than fundus photographs, fundus fluorescent angiogram and indocyanine green angiography (Alten and Eter, 2015)

2.6. Late or advanced Age-Related Macular Degeneration:

The late stages of ARM, that will be called age-related macular degeneration (AMD), cause severe visual loss and are the most common cause of blindness in people ≥ 50 years in the western world (Amoaku, 2008). Due to the expectation of longer life expectancy in the population, it is anticipated that prevalence of late stages of AMD and its associated visual disability will increase in the 21st century.

Two main forms of AMD occur, Dry and Wet. The dry form accounts for 90%, whilst wet AMD occurs in the remaining 10%. The severe visual loss in 90% of the cases is due to wet AMD (Ferris et al., 1984).

2.6.1. Dry AMD:

The dry form is more prevalent and is a slow and progressive disease, and is characterized by GA as an end-stage disease. GA is any sharply delineated roughly round or oval area of hypopigmentation / depigmentation or apparent absence of the RPE in which choroidal vessels are more visible than the surrounding areas. There is a degeneration of the outer retinal cells (RPE cells) with subsequent profound retinal dysfunction due to the loss of photoreceptors and retinal neurons. The chorioretinal atrophy has no obvious defects in Bruch's membrane. Clinical studies show a decrease in the chorioretinal blood flow (Grunwald et al., 1998). Chorioretinal atrophy includes atrophy of the outer hematoretinal barrier (HRB) without appreciable leakage. It seems that the barrier function maintained and the atrophic area remains dry.

GA not only involves RPE but also the choriocapillaries and the retina. All three entities are inseparable and the atrophy of one of them leads to the irreversible atrophy of the other

two. GA can be primary or secondary based on the absorption of the soft drusen, after flattening of a RPE detachment or as a consequence of a CNV regression, or rupture of the RPE (Kolar, 2013).

Both forms of AMD come with painless loss of central vision with preservation of the peripheral field of vision. Individuals with dry AMD complain of blurred vision and difficulty in seeing minute details clearly. Late GA compromises basic tasks such as recognition of faces, reading signs and other activities of daily living due to the presence of a central scotoma. Wet AMD in turn causes distortion of central vision as sudden distortion or profound loss of central vision indicates the conversion to wet AMD. Self-monitoring with an Amsler grid is critical and can help detect disease progression as early as possible (Noble and Chaudhary, 2010). Systematic review and meta-analysis from small preliminary studies show promising test performance for Amsler grid to rule out wet AMD in the screening setting (Faes et al., 2014). To what extent these findings can be extended to clinical practice needs to be established, as the sensitivity of Amsler charts to detect macular disease is less than 50% because of the phenomenon of perceptual completion, whereby regular objects are “filled in” across the scotoma (Crossland and Rubin, 2007). Patients with primary GA have problems with near vision in particular, which are caused by paracentral scotomas, the inability to adapt to the darkness and deterioration of contrast sensitivity (Sunness et al., 1997). Magnifying aids can be useful in AMD but in GA they might carry the magnified image into the paracentral scotomas and have no beneficial effect. The vision varies depending on the ability to find a central functioning retina within the zone of GA (Sunness et al., 1999). Long-term prognosis depends on the first location of the GA. The interval from first developing the first spot of GA to legal blindness is about 9 years (Maguire and Vine, 1986). The average rate of progression in GA is about 139

microns per year. Affected eyes carry an 8% annual risk of decline in visual acuity from 20/50 to 20/100 (Schatz and McDonald, 1989).

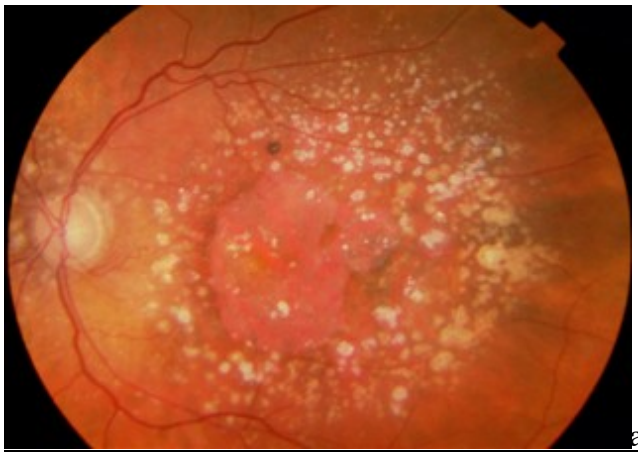

a)

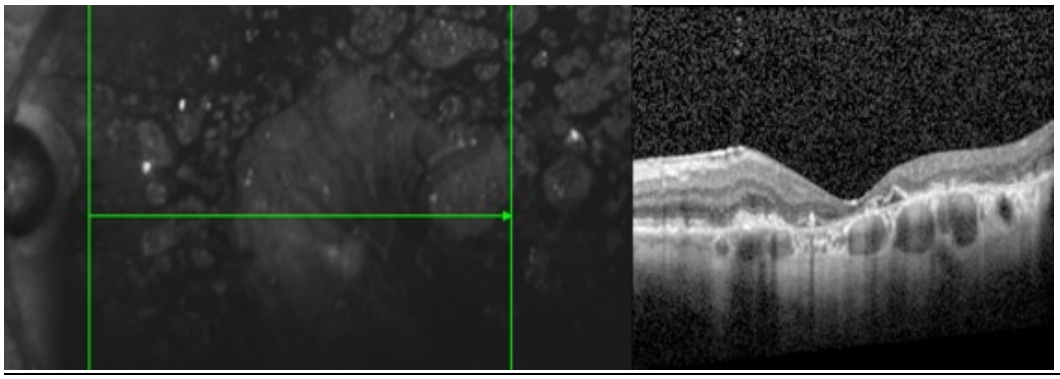

b and c

Figure 2.3: Dry AMD (GA). a) Fundus Photo b) Infra-red imaging c) OCT scan of the macula. Fundus photo shows a sharply demarcated atrophic area and the OCT scan shows the loss of the retina layers in GA. Images are from a study patient who incidentally had early stage AMD in the other eye and was recruited in the study.

GA occurs bilaterally. The second eye is affected in about 50% of the cases. Area covered by GA in the second eye is around 20% smaller. Most cases of GA develop in areas noted to have large drusen. The life cycle of long standing drusen is commonly characterized by the initial development of hyperpigmentation followed by hypopigmentation as the drusen regresses to GA (Klein et al., 2008a).

Research suggests that the RPE oxidant injury and drusen formation recruits macrophages to the site which are beneficial or harmful depending on their activation status. Non-activated or scavenging macrophages may remove deposits without further injury but activated or reparative macrophages can promote complications and progression to late disease through the release of inflammatory mediators and growth factors (Cousins et al., 2004) .

2.6.2 Wet AMD:

Wet AMD occurs less commonly but is far more aggressive than dry AMD.

It is characterized by abnormal blood vessel growth (choroidal neovascularization) in the choriocapillaris through Bruch's membrane, ultimately leading to blood and protein leakage below the macula. Bleeding, leaking and scarring from these blood vessels eventually causes irreversible damages to the photoreceptors and rapid loss to the vision if left untreated. Until recently, no effective treatments were known for wet macular degeneration. However, new drugs, called antiangiogenic or anti-VEGF (Anti-Vascular Endothelial Growth Factor) agents, can stimulate the regression of the abnormal blood vessels and stabilize vision when injected directly into the vitreous humor of the eye

The wet form of AMD is characterized by the occurrence of RPE detachment, choroidal neovascularisation (CNV) and subretinal hemorrhage at the macula.

The terminal stage of wet AMD is a disciform scar. In recent times there have been two more entities added to wet AMD; Angiomatose Retinal Proliferans (RAP) and Polypoid Choroidal Vasculopathy (PCV) (Kolar, 2013).

2.6.2aa Wet AMD Characteristics:

1. RPE detachment/Pigment epithelial detachment (PED):

The RPE detachment is characterized by the elevation of the RPE layer from the Bruch's membrane. The RPE detachment can be a drusenoid PED with multiple soft drusens, a serous PED/RPE detachment with serous elevation but with no leak on FFA or it could be a haemorrhagic PED/fibrovascular PED which contains a CNVM.

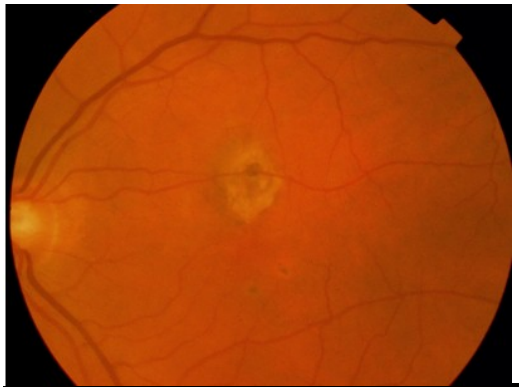

a)

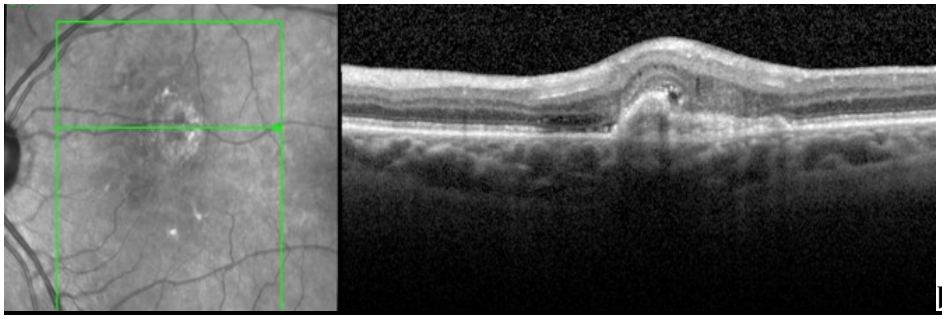

b and c

Figure 2.4: Wet AMD in a study subject. a) Fundus Photo showing the fibrosing PED, b) IR picture and c) OCT scan showing the drusenoid PED with intraretinal fluid. This is the other eye of a study patient and she is already on anti- VEGF treatment and shows a resolving lesion.

The PED can result in a persistent RPE detachment, or a flattened PED leading to GA (Blair, 1975), or a rupture of the PED with CNVM leading to disciform scar (Green, 1983), or may lead lastly to the development of CNVM without rupturing.

The most common complication of a PED is the development of a CNV (Figure 2.4). Increasing age is the basic risk factor in the development of CNV in subjects of RPE detachment. A study showed that elderly people have a larger RPE detachment with more fluid and are more likely to develop CNV (Yannuzzi et al., 2001).

2. Choroidal neovascular membrane:

CNV occurs when there is a breach in the Bruch's membrane leading to the newly formed choroidal blood vessels to grow under the RPE and later into the subretinal space. The presence of neuroretinal oedema in ARM is the sign of CNV activity. A typical picture of a CNV is a subretinally localized grayish lesion which may vary in size, location, and thickness.

Based on its FFA activity it can be classified as classic or occult. A classic membrane is usually well defined and its edges lined with a subretinal hemorrhage. On FFA it can be seen from early stages as a well-demarcated lesion that does not increase in its size in the later stages of the FFA.

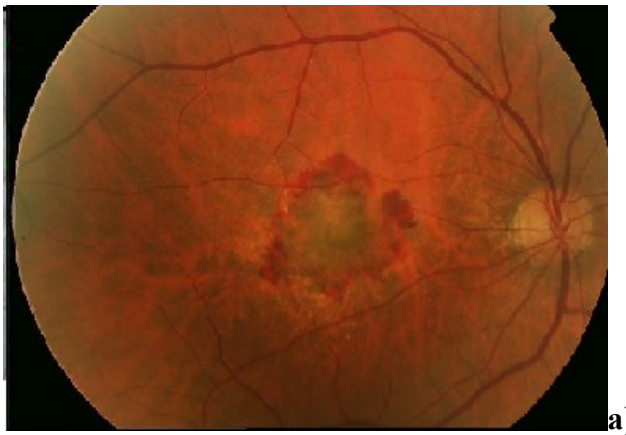

a)

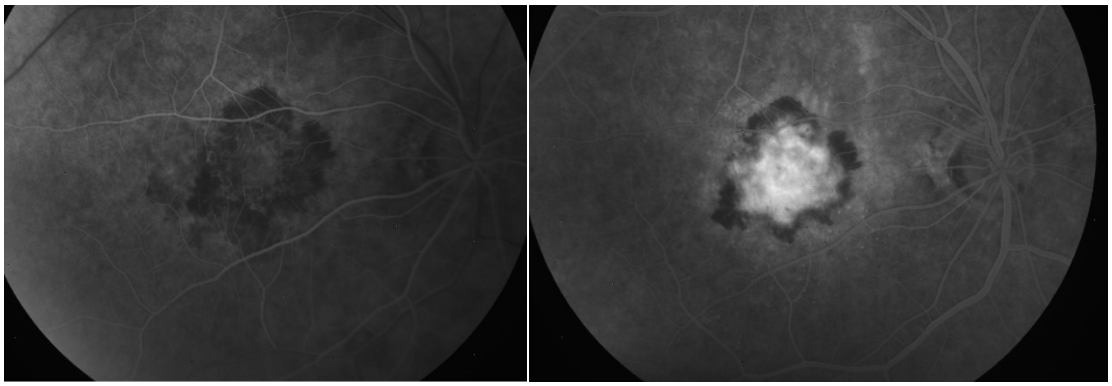

b) **c)**

Figure 2.5: FA of Classic CNV: a) Fundus photo showing a typical grayish lesion lined with subretinal blood. b) early stage of classic CNV with a well-demarcated lesion and block of fluorescence on its border due to subretinal blood.c)Late stages of classic CNV on FA, a well-demarcated lesion that does not increase in its size from an early stage(Kolar, 2013).

Occult CNV is more evident on biomicroscopy and OCT. There may be subretinal haemorrhage or oedema of the neuroretina. Changes are visible at the level of the RPE. FA shows a late mottled leak with an increase in lesion size in comparison to the early stage. According to Gass (Gass, 1967) occult CNVM is characterised by a neovascular complex between the RPE and the choriocapillaris whereas a classic CNVM is the spread of the neovascular complex in the space between the RPE and neuroretina, It does imply that classic arises from the occult in response to the breach of Bruch's membrane continuity (Kolar, 2013).

3. Disciform Scar

Choroid hemorrhage and connective-tissue proliferation between the retinal pigment epithelium (RPE) and Bruch's membrane causes an elevation of the foveal retina resulting in a disciform scar. This reduces visual acuity and results in poor vision (Figure 2.6).

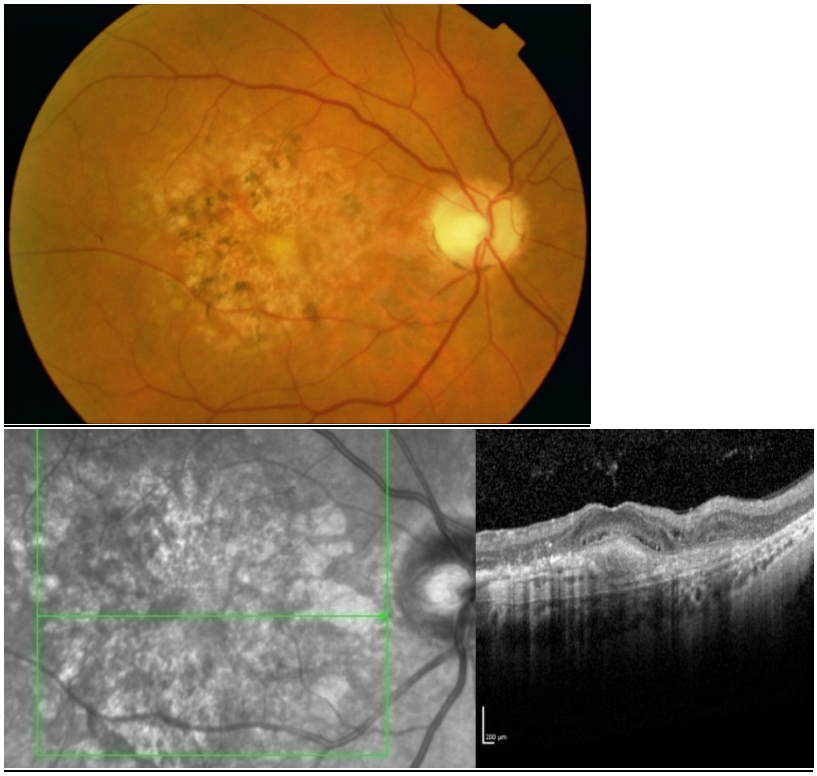

Figure 2.6: Disciform scar in the other eye of a study patient. a) Fundus photo showing extensive scarring in the macular area. b) IR picture and c) OCT showing the subfoveal scar.

2.7 Imaging Modalities in AMD

2.7.1. Grading of ARM /AMD on Fundus photographs:

There are a number of classification schemes for AMD. The aim of these schemes is to provide a common nomenclature so that the prevalence and development of AMD over time can be compared between studies which are often undertaken at different geographical locations.

The main classification schemes share similar features and are largely based on the Wisconsin Age-Related Maculopathy Grading Scheme (WARMGS). This grading system is based on the presence and severity of the characteristic features of AMD namely drusen, pigmentary irregularities, GA, and neovascularisation.

The WARMGS has been in use for over 2 decades and attempts have been made to simplify it for both clinical and research use. The first attempt was in the mid-nineties when a consensus group met and developed the early age-related maculopathy (ARM) international classification system. ARM has now come to be known as early age-related macular degeneration (Ferris et al., 2013).

The Age-Related Eye Disease Study (AREDS) is an ongoing multicenter prospective cohort study of the clinical course, prognosis, and risk factors for age-related macular degeneration (AMD) and cataract. Between 1992 and 1998, 11 retina clinics enrolled 4757 people aged 55 to 80 years in AREDS. An important goal of AREDS has been to develop a severity scale for AMD, to provide baseline risk categories, to allow tracking of progression along the scale, and to define surrogate outcomes for progression to advanced AMD (Davis et al., 2005) (AREDS 17). Various reports on grading have been described in AREDS report 1 to 18 (Ferris et al., 2005). Although ARM has been described for over 100 years, there is neither a

standard agreement on the definition of specific lesions nor a generally accepted classification system.

AREDS report 6 is a simple ARM grading, dividing the ARM into 4 groups.

Further AREDS classifications recognized the importance of drusen size, drusen area and presence of pigmentary changes in each of the 3 nested areas of the grid as a whole, as a risk factor for progression to AMD and included these parameters into the classification (Davis et al., 2005, Ferris et al., 2005).

Described below is AREDS report 6 (Figure 2.7.1 and 2.7.2 and Table 1) as this is the earliest of the AERDS classification and the later grading evolved from the terminologies used in this report.

The severity of ARM has been classified with standard circles and grid as follows:

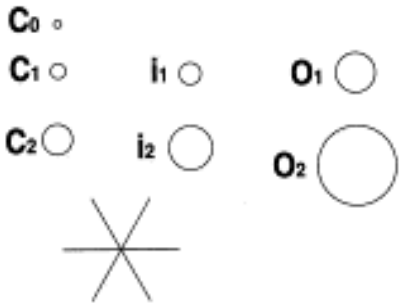

Figure 2.7.1 (AREDS Report 6): The Age-Related Eye Disease Study set of graduated measurement circles, for the estimating area involved by various abnormalities. The symbols designated are; C for central, I for inner, and O for outer subfields. Diameters in the average fundus corresponding to the circles are C-0: 0.042 disk diameter; C-1: 0.083 disk diameter; C-2: 0.167 disk diameter; I-1: 0.120 disk diameter; I-2: 0.241 disk diameter; O-1: 0.219 disk diameter; O-2: 0.439 disk diameter. Disc diameter is 1500 µm by clinical convention but the most accurate estimate is 1800-2000 µm. Transparent grid templates with graduated measurement circles made for disc diameter 1, 500, 1800 and 2000 µm for our study.

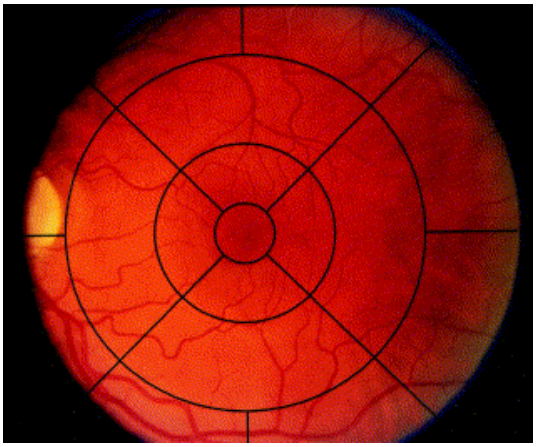

Figure 2.7.2 (AREDS report 6): The Age-Related Eye Disease Study (AREDS); Maculopathy Grading Grid. The radius of the inner circle corresponds to 1/3 disk diameter in the fundus of an average eye; the radius of the middle circle to 1 disk diameters; and the radius of the outer circle to 2 disk diameters.

AMD Level	Criteria
1	Drusen maximum size < circle C-0 (63 µm diameter) and total area < circle C-1 (125 µm diameter)
2	Presence of one or more of the following: (a) Drusen maximum size ≥ circle C-0 but < circle C-1 (b) Drusen total area ≥ circle C-1 (c) Retinal pigment epithelial pigment abnormalities consistent with AMD, defined as one or more of the following in the central or inner subfields: (1) Depigmentation present (2) Increased pigment ≥ circle C-1 (3) Increased pigment present and depigmentation at least questionable
3	Presence of one or more of the following: (a) Drusen maximum size ≥ circle C-1 (b) Drusen maximum size ≥ circle C-0 and total area > circle I-2 and type is soft indistinct (c) Drusen maximum size ≥ circle C-0 and total area > circle O-2 and type is soft distinct (d) Geographic atrophy within grid but none at center of macula
4 (*Advanced*)	Presence of one or more of the following: (a) Geographic atrophy in central subfield with at least questionable involvement of center of macula (b) Evidence of neovascular AMD (1) Fibrovascular/serous pigment epithelial detachment (2) Serous (or hemorrhagic) sensory retinal detachment (3) Subretinal/subretinal pigment epithelial hemorrhage (4) Subretinal fibrous tissue (or fibrin) (5) Photocoagulation for AMD

Table 1. Age-related macular degeneration abnormalities included in the Age-Related Eye Disease Study Grading System and their codes (AREDS Report 6).

The international classification for ARM and AMD recognised the need for an internationally accepted nomenclature for ARM. They recognised a need for a uniform grading system useful in cross-sectional, longitudinal or case-control epidemiological studies. It stimulates researchers to use their system or modifications derived from it that will permit more comparable data collection.

The international ARM classification graded drusen, morphology, type, number, size, the area covered by drusen and the main location of the drusen. It also included a severity grading for hypo and hyperpigmented lesions. The modified international ARM classification used in this study has been described in the methods section of the dissertation.

Both WARMGS and the ARM classification give considerable details on the size and surface features of drusen and the presence or absence of pigmentary irregularities. Although the severity scales are moderately good at predicting the progression from early to late AMD, these groupings cannot be achieved without the standardised systematic grading of stereoscopic fundus images, thus restricting their applicability in the clinical setting.

The initiative for macular research classification committee 2013 (Ferris et al., 2013) proposed a basic clinical classification scale to predict the risk of late AMD that can be used in clinical practice and classified eyes into normal aging, early AMD, intermediate AMD and Late AMD.

Ferris et al (2013) acknowledged that several AMD classification schemes, grading systems and severity scales have been developed in literature in an effort to provide standards to assist clinicians and researchers in the diagnosis and management of this important disorder. There has been no universally accepted precise definition for diagnosis and staging of the AMD phenotype. There is not even consensus on basic terminology with

some groups using AMD and others using age-related maculopathy or ARM or ARMD. Furthermore the terms such as early and intermediate have different meanings in various classification systems. The AMD classification proposed by Ferris et al (2013) focuses on the development of large drusen and pigmentary abnormalities leading to neovascular AMD, geographic atrophy (GA) or both. Ferris et al (2013) hoped that consensus recommendations from their committee will result in a simple unified classification scheme that can be used worldwide.

2.7.2 Optical coherence tomography (OCT):

OCT is a medical imaging technology that can perform high-resolution cross-sectional imaging of tissue morphology in situ and in real time. OCT imaging is in principle similar to ultrasound, except that it uses light rather than sound and measures the echo time delay and magnitude of reflected or backscattered light using low-coherence interferometry. Cross-sectional images are generated by directing an optical beam onto a tissue and scanning it in the transverse direction, thus yielding a data set that can be displayed as false-colour or grayscale images.

In ophthalmology, OCT has become a standard diagnostic technique and provides detailed images and quantitative morphometric information on retinal structure (Huang et al., 1991). It has become an essential tool to diagnose wet AMD and to help treatment decisions in wet AMD.

Time domain OCT (TD-OCT) (eg StratusOCT, Carl Zeiss Meditec, Dublin, California) acquires two-dimensional cross-sectional retinal images consisting of 512 A-lines with axial resolutions of 10 μ in 1.28s. Ultra-high resolution (UHR) OCT imaging also utilizes time

domain technology and could achieve axial resolutions of about 3 µm, but needs longer acquisition times to obtain a scan (Wollstein et al., 2005; Drexler et al., 1999). Repeatability of retinal thickness and volume measurements are important to make the important retreatment decisions. Eriksson et al (2012) found that in eyes affected by wet AMD, there were small differences in repeatability and reproducibility when comparing quantitative maps in Stratus and Cirrus OCT. However, they found that when the software for manual correction for foveal position in Cirrus OCT was used, the variability decreased markedly, the repeatability was close to what has been reported in normal eyes. This demonstrated a significant, potential advantage of spectral –domain over time domain OCT.

In spectral Domain OCT (eg Spectralis, Germany, Heidelberg engineering; Cirrus, Dublin, California, Carl Zeiss Meditec) (SDOCT) technology, the light from the reference arm interferes with the light reflected from the layers of the retina, generating spectral interference fringes. The SD-OCT acquires in-depth information by analysing the interference pattern in the spectrum of mixed reflected lights (Wojtkowski et al., 2004). SDOCTs use a fundamentally different detection method which utilizes a spectrometer which is more efficient allowing for a 150-fold improvement in sensitivity compared to TDOCT (Nassif et al.; 2004, Yi et al.; 2009). The axial resolution of about 2µm is possible with the latest SDOCT.

The multi-layered structure of the retina is clearly visible and the RPE and Bruch's membrane are also partially delineated (Figure 2.8). Most of the incident light from the OCT is reflected before it reaches the RPE. Variations in RPE pigmentations may allow some light to reach the choroid, but it is insufficient to resolve choroidal structure in detail. Although functions such as 'Enhanced Depth imaging" facilitate assessment of choroidal features such

as choroidal thickness. OCT is excellent in detecting separation of the retina from the RPE, its basement membrane and any interruptions in the RPE layer. Thickening of the retina and the presence of intra-retinal fluid are easily detected, CNV can be visualised and its position in relation to RPE can be ascertained. The composition of tissues like RPE proliferation, perfusing CNV, fibrosis or organised haemorrhage cannot be ascertained, as all of these have similar characteristics. Some OCT systems have combined FFA and ICG capabilities which will improve the correlation of the different information.

Currently, in vivo imaging of drusen has been limited to fundus photography which is the gold standard of phenotyping for epidemiologic studies and fluorescein angiography in selected cases. Optical coherence tomography (OCT) allows imaging of drusen (Figure 2.9) and other areas of RPE elevation in cross-section and could be an easy and useful tool in epidemiological studies.

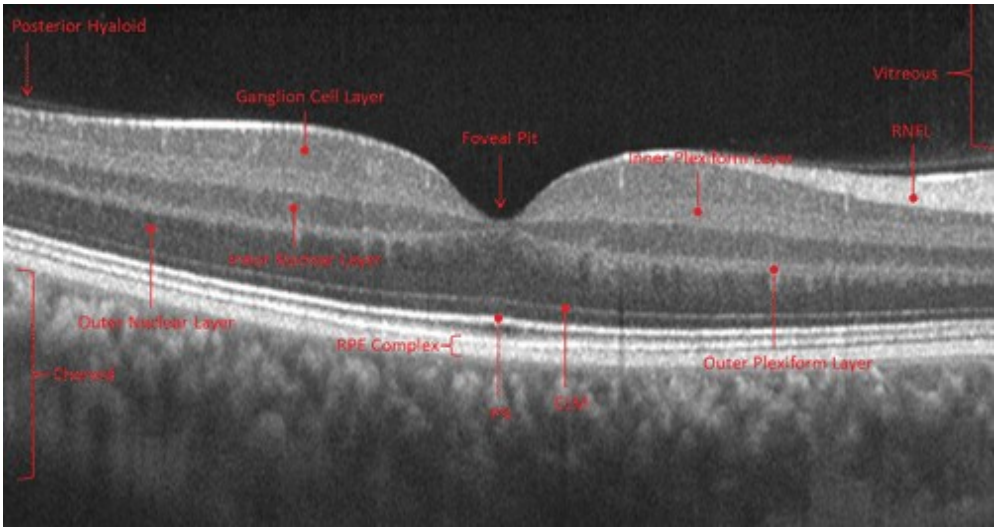

Figure 2.8: Normal in Vivo OCT scan of the human retina. Multilayered structure of the retina visualised and labelled. (Sherman and Epshtein 2012)

Furthermore, recent studies have shown the potential of SD-OCT to quantify geometrical parameters of the RPE such as deformations associated with drusen. SDOCT has also been

used for manual measurement of drusen volume, semiautomatic measurement of drusen area, size as well as for automatic detection and measurement of drusen area, height and volume (Yehoshua et al., 2013; Khanifar et al., 2008).

Yehoshua et al (2013) used an automated algorithm and found poor agreement between drusen area measurements obtained from SD-OCT images and colour fundus photos. Drusen area measurements on colour fundus images were larger than those through SD-OCT scans. This difference can be attributed to the fact that the OCT algorithm defines drusen in terms of RPE deformations above a certain threshold, and will not include small, flat drusen and subretinal drusenoid deposits. The two approaches provide complementary information about drusen.

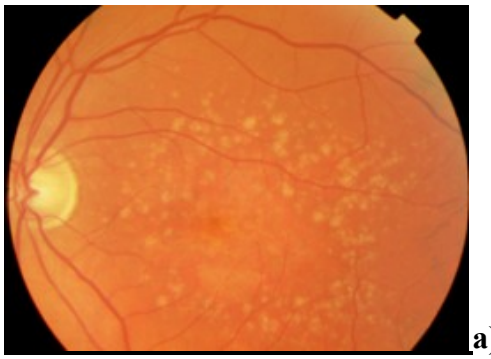

a)

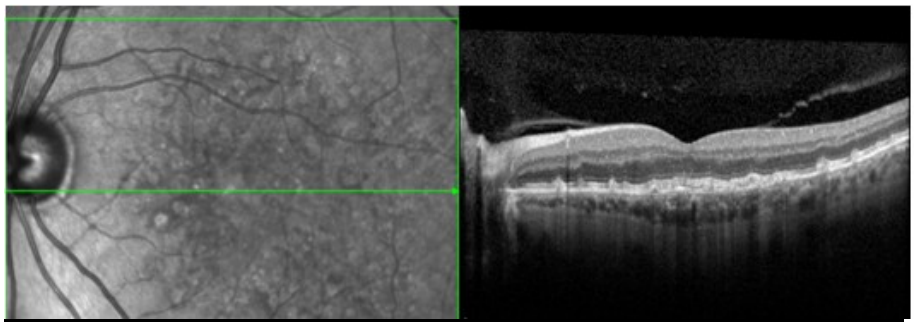

b)

Figure 2.9: OCT scan in AMD showing drusen in study patient. a) Fundus Photo, b) IR picture, c) OCT scan. The drusen were seen on fundus photo, IR and OCT scan helps correlate the information.

2.7.3 Fundus Autofluorescence (FAF):

Fundus autofluorescence (FAF) topographically maps lipofuscin distribution of the retinal pigment epithelial cell monolayer. Confocal Scanning laser ophthalmoscope (cSLO) allows imaging FAF over larger retinal areas up to 55 degrees using low-power laser source to scan the retina in x and y directions (Webb et al., 1987). To reduce the background noise and to enhance image contrast, a series of several single FAF images are usually recorded (Schmitz-Valckenberg et al., 2009). For the final FAF image, a number of frames (usually 4 to 32) are averaged and pixel values normalised. Given the high sensitivity of cSLO and high frame rate up to 16 frames per second, FAF imaging can be performed within seconds and at low excitation energy levels, that are well below the maximum retinal irradiance limits of lasers established by the American National standards Institute and other international standards. The HRA2 system is the commercially available FAF system with excitation wavelength of 488 nm and emitted light detected above 500 nm. Fundus camera uses different excitation and emission filters compared with the cSLO,535-580 nm excitation bandwidth, and 615-715 nm emission bandwidth (Spaide, 2007). Thus, due to the use of different filters compared to cSLO, it might show other retinal fluorophores, though the evidence is still lacking. Per definition low pixel values (dark) illustrates low intensities and high pixel values (bright) illustrates high intensities respectively.

2.7.4 Normal Fundus on FAF: The topographical distribution of FAF in normal eyes demonstrates a consistent pattern. A diffuse FAF signal over the posterior pole can be seen. Retinal vessels and optic nerves are seen dark, characterised by the very low signal, which could be because of the absorption of haemoglobin in the retinal vessels and the absence of autofluorescence material in the optic nerve. Figure 2.10 shows the minimal change pattern

of FAF due to AMD at the macula and normal appearance of optic disc and retinal vessels as described above.

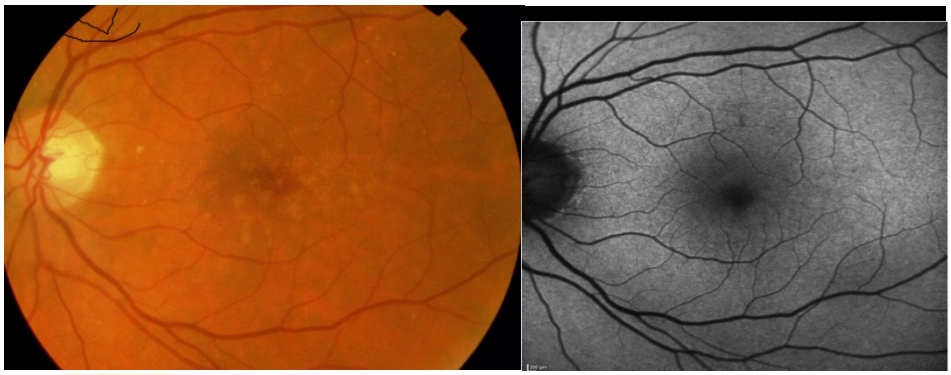

Figure 2.10: FAF in AMD subject from the study. The subject showed a minimal change pattern, topographical distribution of FAF intensity shows typical background signals with shadows on optic disc (absence of autofluorescent material) and retinal vessels (absorption), intensity is markedly decreased over the fovea due to absorption of the blue light by yellow macular pigment.

FAF gives an indication of the health of the RPE (Figure 2.10). Lesions causing visual loss in age-related maculopathy (ARM) are related to ageing changes in the retinal pigment epithelium (RPE), Bruch's membrane, and the choroid (Pauleikhoff et al., 1990; Bird, 2010). These changes play a key role in the pathogenesis of the disease. Diffuse and focal deposits of debris in Bruch's membrane (focal and diffuse drusen) are hallmarks of ageing (Bressler et al., 1990). In post-mitotic RPE cells, autofluorescent lipofuscin granules accumulate with age in the lysosomal compartment. These are mainly by-products of constant phagocytosis of disc sheds from photoreceptors outer segments. It is suggested that the photo-oxidation of RPE lipofuscin could serve as a trigger for the complement system predisposing the macula to pathological alterations, contributing to chronic inflammation over time (Delori et al.,2000).

Drusen are composed of a variety of materials including lipids, proteins, and advanced glycation end products (Dorey et al.,, 1993). With the advent of confocal scanning laser ophthalmoscopy it is possible to visualise in vivo fundus autofluorescence (FAF) which is mainly mediated by accumulation of lipofuscin in the RPE (Delori et al., 2000, Lois et al., 2002). The Fundus FAF in Age-related Macular Degeneration Study Group (FAM-Study Group) (Einbock et al., 2005) aims to identify FAF changes as predictive factors for the progression of age-related macular degeneration (AMD).

Different FAF patterns may be related to high-risk characteristics and may provide new predictive factors for the development of late ARMD and visual loss. The identification of these high-risk FAF patterns in patients with AMD may be helpful in identifying those to be targeted for monitoring and those to be segregated for future therapeutic intervention (Einbock et al., 2005). Einbock et al (2005) discussed that the aim of their study was to correlate between FAF changes and the natural history of AMD. They argued that all previous classification schemes for AMD use fundus photography to identify pigmentary changes and the type or the size of the drusen. FAF provides additional information on the status of the RPE and expands the spectrum of possible risk factors.

In general, FAF changes are not strongly correlated to the visible fundus changes in patients of AMD as the changes are indicative of the lipofuscin accumulation and the health of the RPE. Einbock et al (2005) found that areas of increased FAF may correlate to areas of hyperpigmentation, yellowish soft drusen or normal fundus appearance. However not all drusen exhibited increased FAF as only large drusen exhibited increased FAF in their study. They also found areas of reticular drusen showing a reticular pattern of decreased FAF surrounded by normal FAF. Hypopigmentation was associated with decreased FAF suggestive of absence of RPE or degeneration. The speckled pattern showed no correlation to

drusen or visible fundus change and indicated the presence of different fluorophores contained by lipofuscin and different states of RPE degeneration (Delori et al., 2000).

2.8 Drusen not related to AMD:

"Soft Drusen" are defined as deposits located between RPE and the inner collagenous layer of Bruch's membrane. These lesions usually appear after the age of 50 and are associated with AMD.

2.8.1. Early onset Drusen (EOD):

Younger people can have similar deposits called "Early Onset Drusen"(EOD). These lesions have been recently classified into three entities called Large Colloid Drusen (LCD), Malattia Leventinese Doyne honeycomb retinal dystrophy (ML-DH), and Cuticular Drusen (CD) (Guigui et al., 2011). Studies have described the multimodal morphological features of EOD as deposits classically located under the RPE similar to soft drusen observed in AMD (Piguet et al.; 1995, Stone et al., 1999; Leys et al., 1991).

Large colloid drusen (LCD) are identified on fundus examination as large, bilateral and yellowish lesions in the macular areas and/or in the periphery of the retina. LCD's are hyperautofluorescent and appear in the late stages of ICGA as hypoautofluorescent centre surrounded by hyperfluorescent halo which is again bordered by a hypofluorescent ring.

In ML-DH, colour fundus shows drusen of different sizes. The smaller drusen have a radial distribution whereas the larger drusen are located in the macular area. FAF shows hyper autofluorescence of large drusen showing a hypofluorescent halo. Cuticular Drusen's (CD) are small, round and yellowish lesions randomly scattered in the macula and in the middle periphery of the retina. In the late stages of FA, the drusen are hyperfluorescent with a typical "star in the sky" pattern.

The diagnosis of EOD is classically based on fundus examination and angiographic features. Recently SD-OCT has been used to detect the different EOD entities and to define drusen as deposits observed under the RPE. There has been an association between reticular pseudo drusen and EOD. SD-OCT with high resolution allows histological imaging of drusen located above and below the RPE. Curcio et al (2013) hypothesized that the RPE is polarized and bidirectional secretion of lipoproteins participating in lesion formation above and below the RPE, explaining the simultaneous soft and reticular drusen in patients of EOD and AMD.

2.8.2. Sorsby's fundus Dystrophy:

This dominantly inherited dystrophy originally described by Sorby has been well characterised (Sorsby and Mason, 1949). In some patients, a confluent yellow deposit at the level of the RPE is associated with GA or CNV (Polkinghorne et al., 1989; Steinmetz et al., 1992).

Drusen like deposits are seen along the arcades and nasal to the optic disc rather than at the central macula. The diffuse nature of the change is revealed by FFA. Drusen over the fovea is not a frequent finding in this disorder, making the visible distinction between Sorsby's fundus dystrophy and AMD.

2.8.3. Adult Onset Vitelliform Macular Dystrophy (AVMD):

AVMD was first reported by Gass in 1974 and is characterised by a yellow, solitary, round or oval subretinal macular lesion that resembles juvenile onset macular dystrophy and Best's disease. Other characteristics include the age of onset between 30-50 years, an asymptomatic or mild decrease of visual acuity and normal or subnormal electrooculograms (EOGs) (Gass,

1974). Clinicopathological studies show massive accumulation of lipofuscin pigments within the RPE and a loss of RPE and the photoreceptor cell layer with infiltration of pigment-containing macrophages in the central area (Arnold, 2003). Multifocal ERGs (MfERG) were found to be impaired not only in the macular areas but throughout the posterior pole in AVMD. OCT showed a highly reflective fusiform-thickened layer at the level of RPE and choriocapillaris in patients with a submacular vitelliform lesion (Gass et al., 1985; Cohen et al.,1994).

3. Visual Psychophysics:

Visual psychophysics (Psycho=perception, physics=physical nature of the stimuli) is the science of studying visual perception and sensation by determining the relationship between controlled visual stimuli and a subject's response (Brenton, 1989). Psychophysical tests which depend on the functional status of the photoreceptors, may detect subtle alterations in the macula before morphological changes are apparent on ophthalmoscopy or before traditional measures of visual acuity show deterioration. These tests have the potential to be useful tools in assessing and monitoring patients with an early stage of AMD and maybe of predictive value with respect to progression onto wet AMD or geographic atrophy.

In this chapter, the various psychophysical tests which help in early detection of AMD, including the colour vision test used in our study, are discussed.

The majority of psychophysical tests are based on the concept of threshold testing where the threshold is the point where a given visual stimulus may just be detectable or undetectable. The investigator has a large degree of freedom to vary the stimulus patterns in space, time, brightness and colour. The method of adjustment, the method of limits, the modified methods of limits (staircase) and the method of constant stimuli represent just a few modes of presenting the stimulus during testing (Kalloniatis and Luu., 2005). During the testing, the subjects need to commit to an answer to minimize variations in obtained threshold. There can be a Yes / No segment or a "Forced choice" procedure where the subject chooses one from two or more intervals as the one corresponding to the stimulus (Kalloniatis and Luu., 2005).

Testing in scotopic conditions involves responses from rods which mediate retinal sensitivity in the periphery at low light levels. Photopic conditions test mostly cone responses which

mediate central retinal sensitivity at higher light levels. Furthermore, the psychophysical tests assess rods and cones simultaneously under mesopic conditions.

The psychophysical tests study spatial vision, temporal responses such as rapid flicker and motion perception, visual adaptation, visual field testing and chromatic sensitivity.

3.1 Spatial vision:

Examines how the patterns of light on the retinal are resolved and detected by the visual system. The various tests of spatial vision examine high contrast VA, low contrast VA, hyperacuity, reading speed and contrast sensitivity (Neelam et al., 2009).

3.1.1. High contrast Visual acuity (VA):

Visual acuity, the acuteness of vision, is a measure of the spatial resolving ability of the visual system under conditions of very high contrast. In terms of contrast sensitivity (CS), VA is a measure of the highest spatial frequency that can be detected at 100% contrast (Owsley, 2003). Visual acuity is the identification or the recognition stage of the visual pyramid and if this stage is intact then we can safely assume that the stage of detection and resolution are intact. The detection stage is limited by optical attenuation and spatial summation of neural receptive field, the resolution stage is limited by spacing of receptive fields of visual neurons (sampling) and the identification stage is limited by several factors such as attention, memory and cognitive functions (Thorndyke,1977).

VA is the standard test of visual functions and is the most commonly used indicator of spatial vision in clinical practices and research studies. When the recognition stage is measured for

the purpose of research, the patient is encouraged to guess as he/she approaches the limit of resolution (forced choice methodology) in order to ensure the threshold measure is recorded. The Snellen optotype test chart remains the most popular method of assessing vision in clinical practices and the ETDRS LogMAR has emerged as the test of choice for measuring threshold acuity in vision research (Neelam et al., 2009).

3.1.1 .1 Visual Acuity and AMD:

Patients with GA and CNV, the two most advanced forms of ARM exhibit a significant loss in VA. The loss is seen mostly when the signs of advanced ARM involve the central or inner subfields of the ETDRS grid (Neelam et al., 2009).

Geographic atrophy progresses gradually over time, sparing the foveal center until the late stage of disease and is associated with slow and gradual deterioration in VA. The percentage of fovea involved within the atrophic area is the most important predictor of VA. The photoreceptor mosaic is at the front end of the neural system as the processing of visual information starts with a sampling of the retinal image by this mosaic. Death or dysfunction of photoreceptors in ARM causes reduced density and/or increased irregularity of the mosaic. Furthermore, VA is limited by the density of the cone and by the spacing between the cones, as predicted by the sampling theory of Nyquist. The sampling theorem states that a signal that is sampled at regular intervals can be reconstructed from its samples without loss of information if the original signal has no frequencies above ½ the sampling frequency. This critical frequency is commonly referred to as the Nyquist limit of the sampling array (William , 1987), therefore to decrease VA by one-half (i.e., to reduce spacing by 50%), the sampling density must be reduced by approximately 75%. In other words, a majority of the

photoreceptors in the fovea must become dysfunctional or die before significant loss of VA is evident in ARM (Geller, 1992), causing inconsistency between the severity of morphological changes in advanced ARM and VA.

In conclusion, VA is a poor indicator of the quality of life such as face recognition and mobility in advanced ARM and incapable of quantifying functional deficits in early ARM. Nevertheless, despite its limitations, VA measured under standard conditions using logMAR charts is the most common outcome measure in clinical trials.

3.1.2 Low Contrast Visual acuity (LCVA):

Low contrast visual acuity, which is related to contrast sensitivity with a correlation range of 0.3 to 0.5 (Owsley,1990; Regan,1988) is assessed using low contrast or variable contrast letters charts. These charts have a similar design to conventional acuity charts and have letters decreasing in size down the chart, although the letters are presented at relatively low contrast (<85% contrast). Some commonly used low-contrast visual acuity (LCVA) charts with good test - retest variability include the Regan chart and Bailey-Lowe chart

Four studies investigated LCVA in patients with AMD, and the data from all these studies suggests that there is a reduction in LCVA in AMD. Kleiner et al (1998) investigated LCVA using Regan letter charts in 52 patients with drusen, and demonstrated a significant decrease in LCVA in AMD patients when compared with age-matched controls. This reduction was magnified as the contrast of the chart was further lowered to 9% and 3% (Kleiner et al., 1988). Furthermore, patients with AMD demonstrated a significant trend of decreasing number of letters read correctly with increasing number of drusen. Similarly, Lovie -Kitchin and Feigl, Abadi et al and Cheng et al in three different studies observed that LCVA is

reduced in patients with AMD (Lovie-Kitchin and Feigl, 2005; Abadi and Pantazidou, 1996; Cheng and Vingrys, 1993).

3.1.3 Hyperacuity

Hyperacuity measures the ability to detect misalignment of objects at the fovea and is approximately 10-fold higher than VA (Hogg et al., 2003). The tasks of hyperacuity include detection of offset between two lines, recognising space discrimination (SD), radial frequency patterns (RF), identifying deformed patterns from a cluster of perfect circles to assess hyperacuity (Wang et al., 2002) . Although extra striate cortex maybe responsible for processing SD, it needs uncontaminated information from lower levels of the visual system reflecting the integrity of the photoreceptor mosaic.

SD involves integration across a wide retinal region and therefore is more sensitive than conventional VA to irregular sampling or under sampling caused by photoreceptor dysfunction or death in patients with AMD.

Wang et al (2002) observed that patients with early stage AMD had significant deficits in performing SD in spite of good VA and CS. Hyperacuity testing has emerged as an early detecting tool for patients with AMD, especially at home, in order to catch wet AMD early. A study by Chen and Adelman (2016) explored the Hyperacuity App (HAC) as a potential screen and showed 92.3% sensitivity and 61.5% specificity in distinguishing patients who required treatment and those who did not in wet AMD.

3.1.4 Contrast sensitivity:

The term contrast is a physical dimension and refers to the light-dark transition of a border or an edge in an image that delineates the existence of a pattern or object (Owsley, 2003). The amount of contrast required by an individual to either detect a sinusoidal grating or to

recognise letters or to make some spatial judgement as to the location or the presence or absence of spatial features in the target is known as contrast threshold. The reciprocal of this threshold contrast is known as contrast sensitivity (CS).

The CS function refers to a curve where CS is plotted as a function of spatial frequency (SF) on log-log coordinates and represents minimum contrast required for detection of sine-wave (SW) gratings of various SF. The most common way of measuring CS in clinical research is by varying the contrast of SW gratings, which consists of striped patterns matched with uniformly gray targets of similar luminance. Although these tests measure CS over a range of SFs they are relatively expensive and time consuming, and, therefore unsuitable for clinical practice (Woods and Wood, 1995). Letter - optotype charts, such as Pelli-Robson chart, represent an alternative and common method of measuring CS in clinical studies. CS measured by these charts is moderately associated with VA and highly predictive of reading performance (Whittaker and Lovie-Kitchin, 1994, Rohaly and Owsley, 1993).

Studies that investigated CS function in patients with ARM (Neelam et al., 2009) suggest that there is a loss of CS across all SF in patients with ARM. Three studies found a significant correlation between the disease severity of ARM and loss of CS (Kleiner et al., 1988 ,Midena et al., 1997; Stangos et al., 1995). A plausible mechanism underlying loss of CS function in early stage AMD may reflect decreased efficiency for lateral inhibitory mechanisms that are mediated by horizontal and amacrine cells (Brown, 1983). Loss of CS greatly influences the vision-related quality of life by impairing activities of daily living such as eating, dressing pouring drinks etc. CS may alter the reading speed and may alter the understanding of printed words and most vitally may affect the task of face/object recognition. Patients with AMD also complain of visual disability associated with changing levels of luminance suggesting a

compromise of adaptation mechanism in the disease process of AMD (Brown and Garner, 1983). Maynard et al (2016) found mesopic Pelli-Robson CS functional deficits before photopic CS in early and intermediate AMD that can be differentiated from aging and they proposed this test for early detection of retinal dysfunction.

In conclusion, patients with AMD have significant disruption of CS function at high and medium SF, measurable up to eight degrees of retinal eccentricity. Furthermore, a progressive loss of CS function may reflect disease progression; however such a loss is unable to identify eyes at a particularly high risk for developing wet AMD. Lastly measurements of CS function may provide insight into the extent of functional disability in AMD patients with no apparent loss of VA (Neelam et al., 2009).

3.2 Temporal Function :

Temporal function represents the response of an eye to a flickering stimulus, and can be assessed for non-periodic stimuli. Temporal summation refers to the eye's ability to sum the effects of individual quanta of light over time which occurs at a critical period. A flickering light stimulus may detect functional changes in the retina of AMD patients earlier than static stimuli (Phipps et al., 2004). The flicker stimulus induces an increased metabolic demand (Kiryu et al., 1995) which is not met in an AMD eye and has a decreased oxygenation from a compromised choroidal circulation (Arden et al., 2005).

3.2.1 Temporal Resolution:

When intermittent stimuli are presented to an eye, the stimuli appear to stay on, but only with a change in intensity or motion (flicker). However, if the rate of presentation of intermittent stimuli exceeds a certain rate/frequency, then the perception of flicker ceases and is replaced

with a sensation of steady light, and such a frequency is known as critical flicker frequency (CCF) (Kalloniatis and Luu 2005). Hammond et al (1998 and 2005) demonstrated that subjects with the highest macular pigment (MP) density have about 25% higher CFF values than subjects with lowest MP density, suggesting that MP optical density may exert a protective effect on visual health across lifespan.

3.2.2: Temporal contrast sensitivity (TCS):

The temporal contrast sensitivity (TCS) measures the temporal frequency characteristics of the human eye by varying the modulation depth of a sinusoidal flicker, and can be analysed in a manner similar to the measurement of contrast thresholds for a spatially modulated stimulus. Brown and Lovie-Kitchin (1989) found TCS function in AMD patients to be significantly decreased across a wide range of frequencies with predominant disruptions at low and medium frequencies, which might be related to alterations in photoreceptors, their connections or reduced function due to functional loss in the RPE.

3.3 Visual adaptation in ARM:

Visual adaptation refers to a remarkable ability of the eye to function over a wide range of luminances (greater than 9 log units) and is made possible through a coordinated action of the mechanical, photochemical and neural process in the visual system (Lamb and Pugh,2004; Barbur and Stockman, 2010). The integrity of these visual processes can be assessed using psychophysical tests such as the dark adaptation of rods, cones, and the glare recovery test.

3.3.1 Dark adaptation (DA);

Dark adaptation refers to the slow recovery of visual sensitivity in the dark following an exposure to intense light that bleaches a large percentage of the visual pigments in the photoreceptors and includes recovery /regeneration of photoreceptor pigments. The dark adaption curve consists of two distinct regions of recovery; photopic, scotopic and kinetic state functions. In biochemical terms, this process includes recovery of visual threshold, resumption of circulating currents in the photoreceptors and regeneration of the photoreceptor pigment.

With increasing age, there is progressive thickening of the Bruch's membrane acting as a barrier to transport vitamin A to RPE and the transportation of 11-cis retinal from RPE to rod's outer segments delaying the regeneration of rhodopsin. Although both rods and cones degenerate in AMD, rod's loss precedes cone's loss in 75% of early and late ARM eyes (Curcio et al., 2000).

Patients with AMD often complain of difficulty in performing various activities at night under low levels of illumination such as driving and reading in spite of good vision (Steinmetz et al., 1993) suggesting abnormal DA.

Neelam et al (2009) reviewed twelve studies that investigated DA function in ARM where all except two found reduction in scotopic retinal sensitivity (RS), furthermore, five of the six studies evaluating kinetic function observed prolongation in the time course for pigment regeneration in patients with AMD. These findings confirm the greater vulnerability of rod photoreceptors in AMD. Eisner and co-workers (1992) reported that the prolonged time course for foveal photopic DA in combination with abnormalities in colour matching may identify eyes at risk for wet AMD.

Flamendorf et al (2015) found impairments in DA increased with age, worse visual acuity, presence of RPD, AMD severity and decreased subfoveal choroidal thickness, with the presence of RPD conferring the largest parameter estimate.

3.3.2 The Photostress Test:

The Photostress test (PST), also known as glare recovery or dazzling test, refers to a technique for assessing the dynamic response of the retina following exposure to a controlled glare source and measuring the time course required for the return of retinal sensitivity, in terms of two most common predefined visual tasks, the VA and CS (Collins, 1989). The recovery is believed to be largely due to the regeneration of cone pigments and is presumably dependent on the anatomical and biochemical events that occur at RPE-photoreceptor complex following the photopic process of vision (Alpern et al., 1971). It is believed that a higher degree of functional recovery is required for restoration of baseline VA than for CS (Severin et al., 1963). The PST is quantitative and involves precise delivery of photo stress. Though easy to perform, the PST lacks standardized techniques for performing the test and also has wide variation in the observed recovery time. Any macular disease is capable of altering the PST's response, and the pathology can reside in the photoreceptors, the RPE, Bruch's membrane or the choriocapillaris.

Fourteen studies have investigated PST in AMD patients and all except two have demonstrated prolonged PST (Neelam et al., 2009). It is unsurprising that patients with AMD may become acutely symptomatic while going indoors on a bright day, driving through a tunnel in day time or viewing oncoming headlights at night due to slow recovery of vision after exposure to glare (Sandberg et al., 1998).

3.4 Perimetry:

The term perimetry is interchangeable with visual field testing. This psychophysical test measures the visual function of the eye at topographically defined loci in the visual field and is based on the concept of visual threshold testing. The visual field (VF) is that portion of the external environment of an observer wherein the steadily fixating eye can detect visual stimuli, and the normal subject extends 110 degrees temporally, 60 degrees superiorly, 65 degrees nasally and 75 degrees inferiorly. In three-dimensional view, the VF is represented as a "hill of vision" with a peak sensitivity at the fixation and a gradual decline towards the periphery (Lynn et al.,,1980).

Furthermore ,when VF is mapped topographically on the surface of the striate cortex, the projection is largest for the central VF, and decreases progressively towards the peripheral VF (Mora et al., 1989). In other words, there is decreasing amount of visual cortex devoted to each degree of the VF as one proceeds from the fixation into the periphery. According to De Valois et al , the eventual cortical magnification of the central retina is such that approximately 25% of the striate cortex is devoted to the processing of the central 2.5 degrees of the VF (De Valois , 1988).

Conventional perimetry also known as white-on white perimetry is static peimetry used in the clinical setting. Conventional perimetry has evolved to give way to flicker perimetry, SW automated perimetry (SWAP), frequency doubling technology (FDT) and fundus perimetry (microperimetry). Microperimetry has evolved as a useful tool in AMD as it is the diagnostic technique which allows us to exactly correlate, in real time, the sensitivity threshold of any individual point of the retina with its clinical (biomicroscopic and OCT) appearance which

was made possible by the introduction of the scanning laser ophthalmoscopy (Midena and Pilotto, 2017).

A systematic review of 16 studies (Neelam et al., 2009) showed that 14 studies revealed that early stage AMD is associated with a decrease in the mean retinal sensitivity in the central VF. Furthermore, the VF defect is prominent in the parafoveal region and spares fixation till the end.

Midena et al (2007) examined retinal sensitivity over areas of drusen and pigment abnormalities using microperimetry and patients with early stage AMD. He found a statistically significant decrease in retinal sensitivity over large drusen and pigment abnormalities and this was more noticeable when large drusen and pigment abnormalities were found together.

With 52% of ARM patients having large VF defects and 84% of the ARM patients having localized depression of greater than 10db in the foveal region, Phipps et al (2004) discovered that flickering perimetry produces larger and deeper defects than static perimetry.

3.5 Colour Vision (CV):

Colour vision (CV) represents the ability to discriminate between stimuli, which differ in spectral composition, regardless of other dimensions such as intensity. External objects reflect a variety of wavelengths and the observer constructs a colour percept based on the photoreceptor responses to the wavelength distribution and spatial variables (Swanson and Cohen, 2003).

Normal colour vision is called trichromatic as it relies on three different cone photopigments. Photopigments can be maximally sensitive to short-, middle- or long wavelength sensitive or S, M and L respectively.

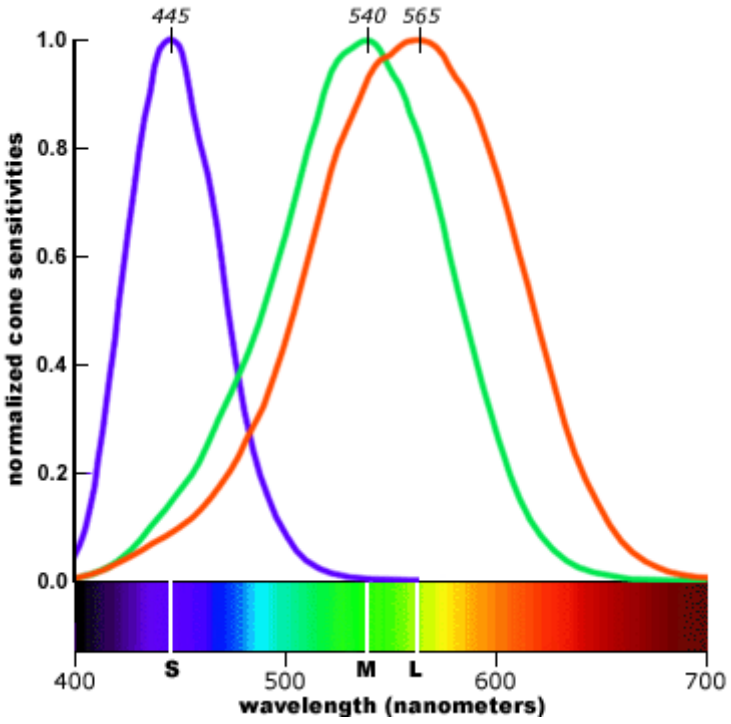

Figure 3.1 : The Stockman & Sharpe (2000) 10^0 quantal fuundamentals, normalized to equal peak values of 1.0 on a linear vertical scale. S cones show maximum sensitivity at ~ 445 nm, M cones at ~ 540 nm and L cones at ~ 565 nm (data from www.cvrl.org).

Colour processing is associated with two main channels from opponent processing. The RG channels utilizes differences between the inputs of L and M cones whilst YB channel compares signals from M and L cones with the signals generated by the stimulus in S cones (Hering 1964). The overlapping sensitivities of the three cone photopigments allow for an astonishing number of combinations of these signals and hence the perception of a large number of different colours. Normal colour perception depends on the normal functioning of the photoreceptors as the primary requisite alongside the functioning of the rest of the visual apparatus. It can be interpreted that early changes in the photoreceptors can be affected via the colour vision before manifesting on the routine clinical tests such as the visual acuity.

It is proposed that S cones are more vulnerable to damage in AMD due to the following reasons:

Firstly, the S-cone pathway is prone to damage due to its territorial nature of overlapping receptive fields, resulting in corresponding area of scotoma with not even a single S bipolar/ganglion cell damage (Boycott and Wassle, 1991).

Secondly, psychophysical pathways of SWS (short wave sensitive) cones have a more limited response range resulting in larger disease related changes in thresholds and apparent vulnerability to retinal disease (Hood et al., 1984).

Thirdly, the S-cones may be more susceptible to alterations in the metabolic environment of the RPE –photoreceptor complex, such as photopigment turnover due to an increase in the diffusion distance compared to other cone system (Spraul et al., 1999). Lastly the SW sensitive pathway may be selectively damaged during the pathogenesis of ARM attributable to relatively lower levels of MP.

Haegerstrom-Portnoy et al (1988) observed a relative preservation of S-cone sensitivity at the fovea where the MP density is highest, compared to the para fovea in the elderly. AMD represents a gradual transition from aging to degenerative change and suggests a role for MP in preserving S-cone sensitivity and possible prevention of development of ARM. Eisner et al (1991, 1992) demonstrated in two different studies that lower S-cone sensitivities was associated with high risk features (confluent drusen, pigmentary changes) with subsequent development of CNV in the fellow eye of patients with unilateral CNV.

3.5.1 Colour vision tests :

A CV test examines the ability of an observer to discriminate different wavelengths and describes a defect in terms of abnormality in colour matching, colour discrimination, colour detection and spatial arrangements based on minimum colour differences. The most common colour tests and the CAD test are discussed below:

3.5.1 .1The Ishihara test (IT):

The Ishihara pseudoisochromatic plates makes use of static luminance and chromatic contrast masking to isolate the use of colour signals and reveal red-green (RG) chromatic sensitivity. The test does not assess loss of YB sensitivity (Barbur et al, 2016). The IT cannot be used reliably to determine the severity of colour vision loss (Rodriguez-Carmona, 2012). The Ishihara pseudoisochromatic plates consists of a series of numbers outlined by different coloured dots and uses camouflage to exploit the expected colour confusions of colour deficient observers (Belcher et al., 1958). The most common IT test is a 38 –plate edition recommended for clinical use. The first 25 plates contain single or double –digit numerals and the remaining 13 plates are for non-verbal subjects. The Ishihara test employs a range of designs, such as transformation, vanishing or hidden digits to detect and analyse colour deficiency. Plate 1 is for demonstration, 2-9 are for transformation plates, 10-17 are for vanishing plates, 18-21 are for hidden plates and 22-25 are for classification plates. (Figure 3.2)

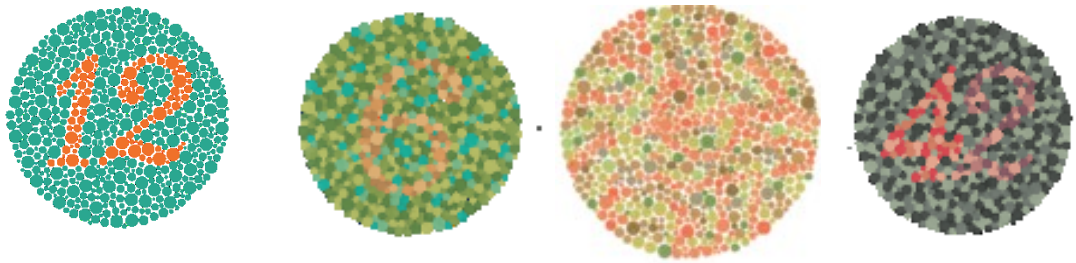

a) b) c) d)

Figure 3.2: The Ishihara pseudoisochromatic plate test; a) Demonstration plate which is visible to normal and colour deficient persons b) Vanishing plate which only persons with normal colour vision can recognise the figure c) Hidden plate which only persons with colour vison defect can identify the figure. d) Diagnostic plate which is intended to determine the type of colour vision defect and severity of it. (Creative commons CCO1.0 universal public domain dedication)

3.5.1.2 Nagel anomaloscope:

The Nagel anomalsocope is based on colour matching and is often regarded as the standard clinical reference test for identifying and diagnosing red/green colour deficiency (National Research Council-National Academy of Sciences, 1981). This instrument produces a disc stimulus that consists of two half fields which are viewed in an optical system.
Subjects are then asked to use two control knobs to completely match the two halves of the circle in both colour and brightness. The ratio of the red/green mixture field is altered systematically by the examiner until the limits of the matching range are found. The matching range and the match midpoint should also provide an indication of the severity of the RG colour vision loss. An observation was made, in this regard, that subjects with variant L-M cone pigments make relatively normal matches but exhibit reduced RG chromatic sensitivity (Barbur, 2008). These observations and need for an experienced examiner makes the Nagel anomaloscope less attractive, particularly when some level of colour deficiency may go un-noticed.

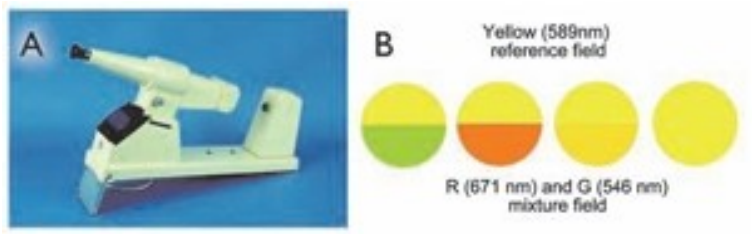

Figure 3.3: A, Nagel anomaloscope B. The stimulus as seen by the subject. (Model 1, Schmidt and Haenach, Germany)

3.5.1.3 Farnsworth – Munsell 100 Hue test:

This system was developed by Dean Farnsworth in the 1940s and it tests the ability to isolate and arrange minute differences in various colour targets with constant value and chroma that cover all the visual hues described by Munsell colour system (Figure 3.4). There are several variations of the test, one featuring 100 colour hues and one featuring 15 colour hues.

The test was originally taken in an environment with physical hue tiles, but now it is undertaken on computer consoles. An accurate quantification of colour vision accuracy is particularly important to designers, photographers and colourists, who rely on accurate colour vision to produce quality content.

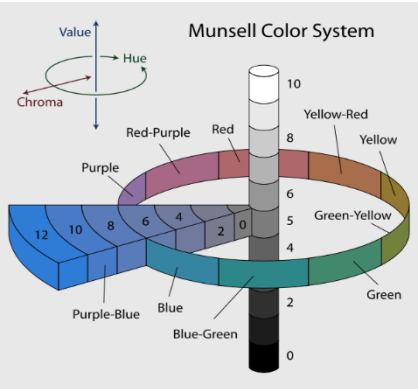

Figure 3.4: The Munsell colour system. It shows a circle of hues at value 5 chroma 6, the neutral values from 0-10,and the chromas of purple-blue (5PB) at value 5 (Creative Commons Attribution).

3.5.1.4The Colour Assessment and Diagnosis (CAD):

The Colour Assessment and Diagnosis (CAD) test was developed at City, University of London. The CAD test measures the smallest colour signal strength needed to just see different colours. The test has been explained in the Material and Methods (4.2.4). The CAD test has a number of advantages over conventional tests, in terms of isolation of colour signals as well as sensitivity and accuracy (Barbur et al , 2016).

a) Isolation of colour signals is achieved by masking luminance contrast signals generated by the moving coloured stimulus that are only photopically isoluminant for the standard CIE normal observer. This is particularly important since there is a large variation in L: M cone ratio within normal trichromats (Carroll, 2002) and the colour deficient observers will introduce variations in the perceived luminance contrast of most coloured stimuli. When using dynamic luminance contrast masking, the applicants cannot make use of any other cues apart from colour to see the moving target and to carry out the task.

b) The severity of both red-green (RG) and yellow-blue (YB) colour vision loss is quantified in standard Normal Units (SNU) which are easy to understand (Barbur, 2006).

c) The CAD test has close to 100% sensitivity and specificity in detecting congenital colour deficiencies and in classifying the type of deficiency involved. In terms of sensitivity, the CAD can detect even minimal colour deficiencies (particularly in subjects with acquired loss of chromatic sensitivity) that may produce variable results or pass unnoticed in conventional colour vision test. (Barbur, 2006).

d) The availability of built in, monocular and binocular normal, upper threshold limits from 6 to 85 years of age makes the CAD test particularly useful in allowing for normal aging changes and in diagnosing acquired loss of RG and YB colour vision.

3.5.2. Acquired colour vision deficiency:

Acquired colour vision deficiency occurs as a result of ocular, neurologic or systemic disease. A wide array of conditions may affect colour vision, ranging from disease of the ocular media through to the pathology of the visual cortex. Traditionally, acquired colour vision deficiency is considered as a separate entity from congenital colour vision deficiency, although emerging clinical and molecular genetic data would suggest a certain degree of overlap (Simunovic, 2016). The below section on acquired deficiency is not exhaustive and reviews common conditions without a large hereditary component to the disease.

3.5.2.1 Disorders of the ocular media:

Possibly the most common mechanism of acquired colour vision deficiency is a so-called absorption mechanism secondary to the age –associated increase in optical density of the lens pigments (Norren and Vos, 1974). Intraocular lens is characteristically yellow in colour and absorbs short wave-length visible light, because of the gradual nature of such changes, patients seldom notice any change in colour. Further-more, there is evidence to suggest that increased media absorption may be offset by increased S-cone sensitivity (Johnson et al., 1988). Implanted intraocular lenses with yellow tints modulate the spectral quality of light when compared to aphakia (van de Kraats and van Norren, 2007) and the empirical evidence supports this assertion (Simunovic, 2012).

3.5.2.2 Retinal disorders:

a) Age related macular degeneration:

Our ability to monitor retinal structure in AMD has improved with the advent of modern imaging techniques and quite a few attempts have been made in this regard to relate this progress with functions in terms of colour vision.

Systematic review of studies which have investigated chromatic function in patients with ARM (Neelam et al., 2009) reviewed a total of 15 studies from 1978 to 2005. The studies used Farnsworth -Munsell 100 hue test, Farnsworth D15 test, anomaloscope and colour contrast sensitivity using computer graphics system. They performed colour tests in ARM case groups and control groups and the sample size ranged from 10-47 cases. Most studies concluded on an optimistic note and found a blue yellow defect (Bowman et al., 1978; Smith et al., 1988; Feigl et al., 2005; Frennesson et al., 1995). A positive relationship between severity of retinal changes and elevation of YB colour thresholds were found in some studies (Applegate et al 1987, Eisner et al 1994, Cheng et al 1993, Holz et al 1995, Arden et al 2004). Two studies found no difference in the colour thresholds of ARM group and the control group (Atchinson et al., 1990; Midena et al., 1997). The chromatic sensitivity loss as a result of disruption of cone receptors and subsequent neuronal pathways can be classified as an acquired defect in AMD. Furthermore, YB loss is the most common acquired colour vision defect in macular pathology (Verriest, 1963).

Midena et al (1997) could not demonstrate a colour abnormality using FM100 hue test in 47 patients of ARM. Their observation were not consistent with the majority of the studies and according to the investigators, one possible explanation is the lack of commercially available tests to detect the subtle changes in early ARM. Similarly Atchinson et al (1990) failed to elicit a colour defect in their 10 ARM patients probably because of the presence of hard drusen/pigmentary changes which represent normal aging changes.

The test of colour sensitivity (FM100, D15) determines colour contract thresholds in protan, deutran and tritan confusion axes and three studies used Ardens computer graphic system. It

podiscrimination and tests like the CAD system quantifying saturation and thresholds will be useful to determine early ARM defects.

The pilot study by O'Neill–Biba (O'Neill-Biba et al., 2010) tested colour vision using the CAD system in 18 AMD subjects (36 eyes). They found 30 (83%) eyes to have elevated M-L mechanism and tritan thresholds. They concluded that the initial loss was YB followed by both RG and YB loss of sensitivity in the later stages of the disease. They graded AMD into 5 categories and found a positive correlation between chromatic sensitivity loss and disease severity.

b) Diabetic retinopathy:

Diabetic retinopathy is commonly associated with acquired colour vision deficiency. About half of the patients in the Early Treatment of Diabetic Retinopathy Study were found to have abnormalities on the F-M 100 (Fong et al., 1999). Andrade and colleagues (2014) found diabetic patients as a group showed higher FM 100 scores then the controls but the FM 100 test was not able to differentiate the diabetic group with retinopathy from the diabetic group without retinopathy. A Pilot study at City, University of London using the CAD test observed that diabetic subjects exhibited equal and highly correlated reduction in RG and YB sensitivity using the CAD test (O'Neill-Biba et al., 2010).

3.5.2.3 Optic nerve disorders:

a)Glaucoma:

Glaucoma is the term applied to a collection of optic neuropathies that may have acute or chronic forms and share common features of loss of retinal ganglion cells and

excavation/cupping of the optic nerve head (Weinreb et al., 2014). Several early studies suggested that glaucoma causes an acquired M-L mechanism deficiency (Pokorny et al.,, 1979). However, such studies concentrated on patients with advanced diseases as it is now generally accepted that glaucoma first causes an acquired S-mechanism deficiency on conventional colour vision tests such as FM 100 Hue and desaturated D-15 (Sample et al., 1986). Much of the attention over the past few decades has been directed at detecting loss of function before evident on conventional perimetric visual fields. SWAP, which is short wave length blue on yellow perimetry generated interest for early detection of galucoma (Monhart, 2007) .

There are other miscellaneous causes of loss of colour vision such as drugs, toxins and hypoxia.(Simunovic, 2016).Acquired colour vision deficiency is a common condition and even though its precise prevalence is unknown ,the available evidence suggest it is more common than congenital colour deficiency in populations aged 40 and more (Schneck et al., 2014).

4. Material and Methods:

All subjects were recruited from the medical retina clinic at Kings College Hospital, London. The study was approved by the NRES ethical committee London-East and City, University of London. The prospective study included patients / subjects of AMD aged 55 and over. Ninety eyes of 67 participants were included. They had AMD in one or both eyes with vision of 6/12 or better. All subjects with bilateral AMD were asymptomatic and were referred from their opticians for a routine opinion. AMD patients with the other eye treated for wet AMD were recruited from the Anti -VEGF clinics.

4.1 Inclusion and exclusion criteria:

Subjects were excluded for diabetes, glaucoma, significant cataract or any other significant ocular pathology by ophthalmic history and examination. The significance of cataract was determined by the symptomatic history, visual acuity, examination and was based on the clarity of fundus details. Any lenticular opacity which obscured fine fundus details and imaging was excluded. A careful selection of subjects was made based on their mental ability to understand the test and physical ability to perform the test using the keypad. A short test programme which is a teaching mode on the CAD system was used to determine suitability for the actual definitive test and for inclusion into the study.

4.2 Study design:

Suitable subjects (AMD and early onset drusen) in the Medical Retina Clinic who were attending a routine appointment were approached and the study was discussed with them. They were handed a patient information leaflet about the study and given one hour to read and consider it. The interested subjects were given a choice to perform the CAD test during the same day or at another convenient time. The subjects who were keen to perform the test on the day were seen as part of their clinical care. After receiving informed consent, they underwent a detailed history; both ophthalmic and general medical history was taken including drug history and smoking status. Ophthalmological examination, best corrected visual acuity, colour fundus imaging and OCT scans were performed as a part of their routine ophthalmological care and the CAD test was performed as a part of the study. The patients had their pupils dilated for OCT, fundus photograph and ophthalmological examinations. The CAD test was performed either dilated or undilated depending on the availability of the patient's time during the course of the clinical appointment to aid effective use of patient's time. The negligible effect of pupil size and mild lenticular opacity has been discussed in confounding factors of the CAD test (4.2.4.1). The subjects were recruited over a period of 2 years and a follow up of only the clinical notes was conducted at the end of 12 months for each subject.

4.2.1 Visual acuity measurements:

The subjects had both monocular and binocular visual acuity recordings by a trained nurse/ ophthalmic assistant on an ETDRS letter chart. Vision was recorded with their distance glasses on and when they reached the letter that they could last identify, a pinhole was introduced to check for the best corrected VA. VA was recorded separately in each eye using

an occluder. The patient was encouraged to guess any letters that were difficult to read and instructed to make a definite decision and were allowed to move on to the next line, only if they had identified at least one letter on the previous line in order to access the threshold of visual acuity testing.

ETDRS score was calculated as follows; each letter correctly identified was circled on the visual acuity form. Any letters read incorrectly was deleted and letters for which no guess is made were left unmarked. Each letter scores one point. The total for each line is recorded in the right –hand column (maximum 5), the scores for each line were added at the bottom. If the score was 20 or more, then 30 points were added automatically and the final score was then recorded.

4.2.2 Photographic imaging of the Retina:

Fundus photographs were obtained using Topcon fundus camera which was performed by experienced medical photographers as part of routine care. The protocol was one single 30 degree shot of the posterior pole which included the disc and the macula. The photographers used the same magnification for all subjects. The disc was included in the picture for the investigator to compare the disc among subjects and ensure that a uniform magnification was used for all subjects.

4.2.3Optical Coherence Topography (OCT): SDOCT (Spectralis; Heidelberg Engineering, Heidelberg, Germany) allows high-speed, high resolution, confocal laser imaging of the retina. It allows for simultaneous cross sectional OCT and infrared imaging (870 nm) as well as simultaneous OCT and FAF imaging (488 nm excitation and 500 nm barrier). The beam of a super luminescence doide (SLD) scans across the retina to produce a cross sectional B-scan image (Spectralis Catalogue, 2007).

The protocol for OCT was a volume scan on a 20 × 20 degrees cube, with 49 raster lines, each containing 1064 pixels, separated by 125µm, used to acquire macular scan centred on the anatomical fovea. The OCT measurements were carried out by experienced medical photographers as a part of clinical care. The scans were analysed qualitatively to identify drusen and RPD along with the fundus photographs. Infrared reflectance imaging done alongside the macular scans was used to confirm the presence of RPD.

4.2.4 Colour Assessment and Diagnosis (CAD) test:

Every subject was assessed for colour vision using the Colour Assessment and Diagnosis (CAD) test. The test was performed in a dimly lit room with sufficient ambient light. The test was performed binocularly and then monocularly in each eye for 15 patients, this protocol was time consuming and exhaustive for the subject. After reconsidering this protocol it was decided that only monocular tests be done to obtain useful data needed for analysis.

The CAD was initially devised as a binocular test when it was primarily used for congenital colour blindness diagnosis. The software has since been modified for use in monocular conditions for acquired colour deficiency and the test has been named monocular medical on the CAD system. The monocular test results obtained have been compared to monocular normative data to give a diagnosis at the end of the test. The system used in this study had the monocular medical mode installed on it.

The patients were seated at a 3 meters distance from the CAD system and they used their best corrected glasses for the test. The concept of the test and the procedure of response was explained to the patient. They were allowed to practice on the short test programme which produces highly saturated colour stimulus to understand the test. If a subject scored 100

percent on this practise they were ready to take the definitive test programme. The test programme was divided into RG and YB programmes to allow for rest between the tests.

The CAD test ideally takes up to 12 minutes to complete and to produce a result. The test can last up to 20-25 minutes in the event of abnormal thresholds, which increases the confusion of patient performance. The test can also be prolonged when the subject fails to press the response button at the beep. Using only monocular tests, without repeating test on binocular programme and divided RG / YB programmes helped prevent patient fatigue.

The CAD test made it possible to isolate the use of colour signals and to measure small changes in chromatic sensitivity. The fundamental principles of the Ishihara pseudoisochromatic plates had been employed in novel tests generated on visual displays to test for RG and YB chromatic sensitivity (Barbur 2004, 2011.). The colour assessment and diagnosis (CAD) test enhanced the masking of luminance contrast signals by employing dynamic, random, luminance contrast noise without changing the time-averaged, local luminance of the checks. The CAD test has been used in several studies to investigate variability in RG and YB sensitivity in normal trichromats and in subjects with congenital and/or acquired loss of chromatic sensitivity (O'Neill-Biba et al., 2010). The CAD test employs a dynamic spatiotemporal masking technique that isolates the use of colour signals without affecting the subject's chromatic sensitivity. The colour-defined stimulus is buried in dynamic luminance contrast noise (as shown in Figure 4.1a) and travels diagonally across a square region defined by the noise. The use of dynamic, luminance contrast noise ensures that detection of any residual luminance contrast signals in the 'isoluminant' colour-defined stimulus is masked so that the subject can only perceive the moving target by processing chromatic signals (Barbur, 1994). In the absence of chromatic signals, the subject fails to see the coloured target, even

for chromatic displacement amplitudes that are limited only by the phosphors of the display (Barbur et al., 2006). The standard CAD test employs sixteen interleaved directions specified in the CIE 1931 – (x, y) colour space. After each presentation (Figure 4.1a), the subject's task is to press one of four buttons, to indicate the direction of motion of the colour-defined stimulus. The randomly interleaved staircases produce colour thresholds (Figure 4.1.b) for each of the directions measured. This distance is proportional to the cone contrast signals generated by each colour (Barbur and Rodriguez-Carmona, 2012).

Typical data for a normal trichromat are shown by the coloured symbols in (Figure 4.2**)** and the solid black symbols show median threshold values of 330 normal trichromats. The area of the diagram associated with normal colour vision is shown in grey and represents the 2.5 and 97.5% statistical limits of RG and YB thresholds in normal trichromats (Rodriguez-Carmona 2006, Barbur, 2006) The pattern of colour vision loss for the 16 directions measured with the standard CAD test provides the information needed to diagnose normal trichromacy and to detect and classify accurately both congenital and acquired colour deficiency.

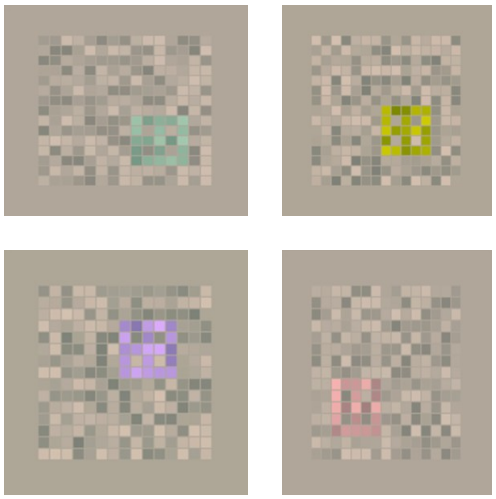

Figure 4.1_a: Shows screen dumps of suprathreshold CAD test stimuli that correspond to the RG and YB axes; Colour defined stimulus buried in in luminance contrast noise

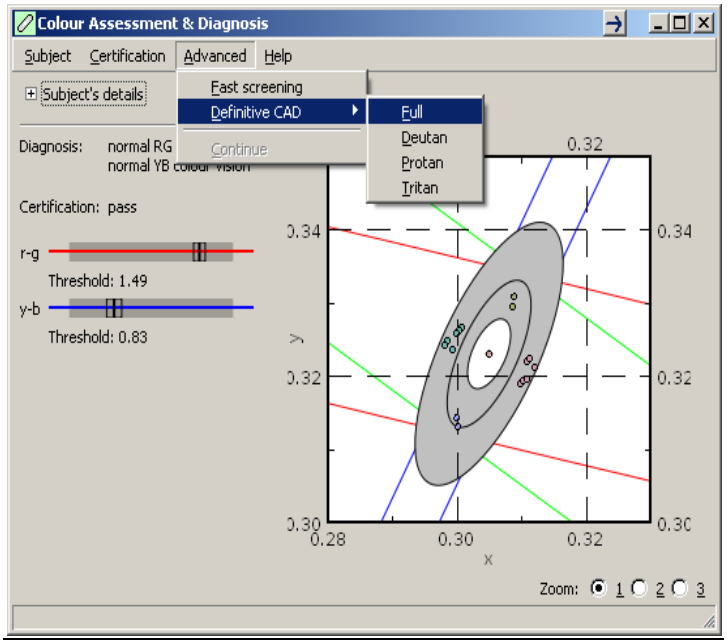

Figure 4.1 b: Screen shot of CAD test result; the colour thresholds are produced at the end of the test.

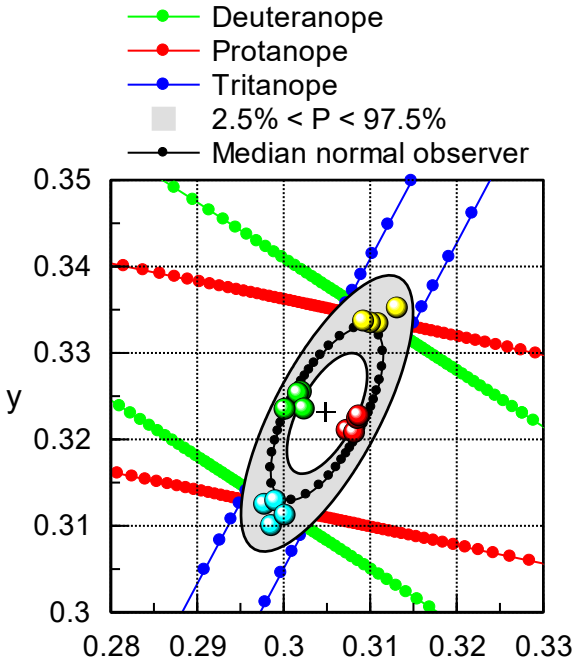

Figure 4.2: Normative data for CAD test shows the mean ellipse for young, normal trichromats (solid discs) together with the corresponding confidence limits measured in 333 subjects. The green, red and blue lines show the colour confusion bands for deutan, protan and tritan-like observers and the coloured symbols show CAD test thresholds for a typical, normal trichromat.

4.2.4.1Confounding factors:

a) Pupil size: CAD test was done irrespective of pharmacological pupil dilatation, Corrections have not been made to account for changes in effective retinal Luminance caused by the Stiles–Crawford effect, because the change in luminous efficiency at either extreme is (i.e., 2.75 and 7.1 mm) with respect to the efficiency computed for the mean pupil size (i.e., 4.36 mm) is less than 0.14 log units (Barbur, 2012). The mean luminance employed in the CAD test (i.e., 24 cd/m^2) is well above the range of the luminance effects (Barbur, 2006).

b) Lens opacities: Subjects with nuclear sclerosis, significant cortical or posterior subcapsular cataract dense enough to obscure the details of a dilated fundal view were not included in the study. A grading scale like the LOCS III was initially adopted to grade any lenticular changes noted in spite of clear fundus details. This grading was discarded after discussion among the investigators. Experiments at City, University of London found that YB remain independent of absorption of short wavelength by the lens (Rodriguez-Carmona, 2006) provided sufficient ambient light is available to avoid large reductions in retinal illuminance for blue light.

4.2.5 Severity grading of AMD using fundus photographic imaging

a) International Classification and grading system (Bird etl al 1995)

Drusen morphology	Drusen Number	Drusen Size	Drusen Main location	Drusen Area Covered
1)Questionable	1)Questionable	1) <63µm	1)Outside outer circle	1)>10%
2)hard Drusen(<125µm)	2)1-9	2)≥63 µm <125 µm	2)in the outer subfield	2)>25%
3)Intermediate,soft Drusen (>63µm≤ 125 µm)	3)10-19	3)≥125 µm<175µm	3)in the middle subfield	3)50%
4)Large,soft Drusen(>125 µm)	4)>20	4)≥175µm<250µm	4)in the central subfield	4)>50%
5)Large,soft indistinct drusen(>125µm) crystalline/calcified/ serogranular		5)≥250µm		

Hyper-Pigmentation	Hypo - Pigmentation	Location of pigmentation
0)Absent	0)Absent	1)Outside outer circle
1)Questionable	1)Questionable	2)in the outer subfield
2)Present (<63µm)	2)Present (<63µm)	3)in the middle subfield
3)Present(≥63µm)	3)Present (≥63µm	4)in the central subfield

Table 2: International classification and grading system for ARM /AMD (International ARM/AMD study group Bird et al 1995)

Bird et al (1995) proposed the above grading scheme to encourage researchers to use the grading system or the modifications derived from the grading to permit improved understanding and comparison of results. This classification is elaborate and takes into consideration the drusen morphology, size, number, area covered and main location of the drusen on the ETDRS grid.

All aspects of the classification except 1.2 in the original classification were used, this sub classifies the predominant drusen type in the outer circle of the grid. After analysing the macular area using the three circles of the ETDRS grid (Figure 2.7.2) Drusen morphology (1.1), number (1.3), size (1.4) and area covered (1.6) were analysed mainly for the inner circle. The inner grid was analysed for the drusen parameters as the CAD system theoretically measures the central 5 degrees of the fundus which lies in the inner circle of the grid.

Bird et al (1995) discussed that 30 to 35 degree photographic field is the standard use in AMD studies and the magnification provided by a 30 degree field is usually adequate to determine most lesions with AMD. They called for variations to be limited between 25 to 40 degree and for a grid template to be used for uniformity of results between studies.

In the present study 30 degree photographic field was used and fundus transparencies were prepared with ETDR grid and circles C_0,C_1,C_2,C_3,and C_4 measuring 1/24, 1/12, 1/8.6, 1/6 and 1/3 of the disc diameter, according to the measurement of the disc on the photograph. The same computer monitor was used for all subjects to maintain uniformity. RV was the main investigator performing the measurements after a formal meeting and agreement with SS. SS was also sought, in case of doubt in measurement of any subject.

b)Clinical classification:

We used clinical classification by Ferris et al (2013), initiative for macular research classification Committee, for a broader and simpler view of colour thresholds over the range of AMD.

Grade	AMD Severity grade	Drusen size in µm	Pigment
0	No signs	nil	Absent
1	Normal	≤63 µm	Absent
2	Early	(>63≤125)	Absent
3	Intermediate	(>125 >250µm)	Present
4	Late	Geographic atrophy/Wet AMD	

Table 3: Clinical classification of age related macular degeneration; Macular Research classification committee added category 3.5 for classification in our study, to get more detail in correlation.

4.3 Optical Cohorence Topography (OCT): Heidelberg Spectralis (Spectral domain OCT) for drusen volume calculation, identification of drusen morphology and FAF imaging.

a)Drusen volume calculation:

Drusen volume in mm³ was calculated across 9 OCT sections and 480µm on either side of fovea using J Image (NIH public domain software). This corresponds to centre of the grid and central 5degree of vision. On each of the 9 scans any drusen seen was calculated for volume using the image J software and the total volume across the 9 scans was recorded. Drusen volume for each eye classified as grade 1 (no drusen), grade 2(<0.1mm^3) grade3 (0.1-0.5mm^3), grade 4 (>0.5mm^3).

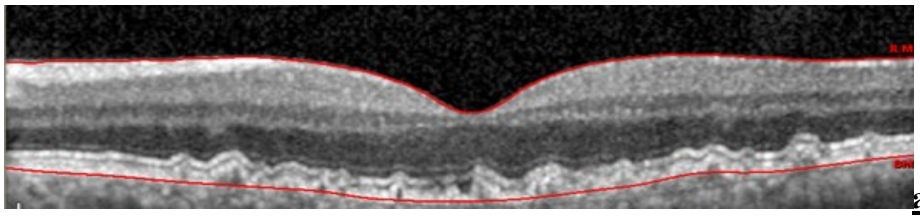

a)

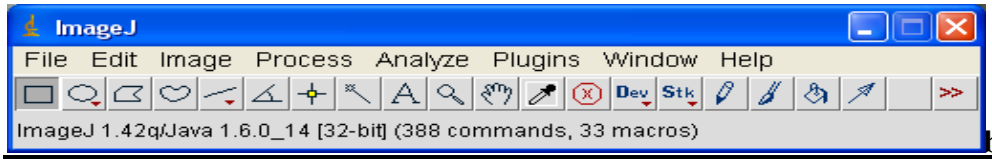

b)

Figure4.3: a) Example of an OCT scan analysed on Image J. b) Image J (NIH public domain soft ware) which was used to anlalyse drusen colume.

b)Drusen Morphology on OCT scan:

We used OCT scan for IR images, AF and identification of drusen deposits / reticular pseudodrusen on OCT sections. We have mainly used IR and SD-OCT scan to identify our subject's eye with reticular pseudodrusen (RPD).

We divided our patients into:

a) Reticular drusen only without soft drusen

b) Soft drusen only without Reticular drusen

c) Combined lesion: CR- predominant reticular (>50%),

d) Combined lesion CS- Predominant soft drusen (>50%).

CR and CS were included under RPD for analysis.

Reticular pseudodrusen were identified on IR imaging as groups of hypo-reflectant lesions against a mildly hyper-reflectant background and as well-defined and regular patterns reticular pseudodrusen. RPD were confirmed by the presence of subretinal drusenoid deposits on SD-OCT imaging obtained on the same instance as IR imaging. Large (≥125 μm) soft drusen were identified on colour photographs by their characteristic yellow, indistinct appearance and confirmed by the presence of mounds of deposits under the retinal pigment epithelium on SD-OCT imaging.

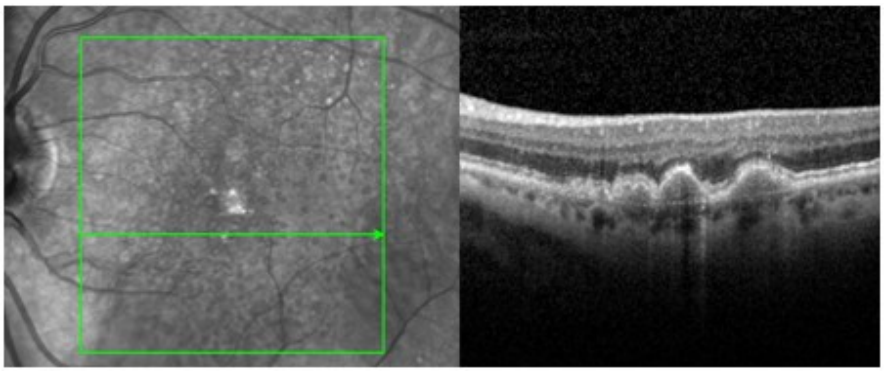

Fig 4.4.A)Soft Drusen (SD) in a study subject

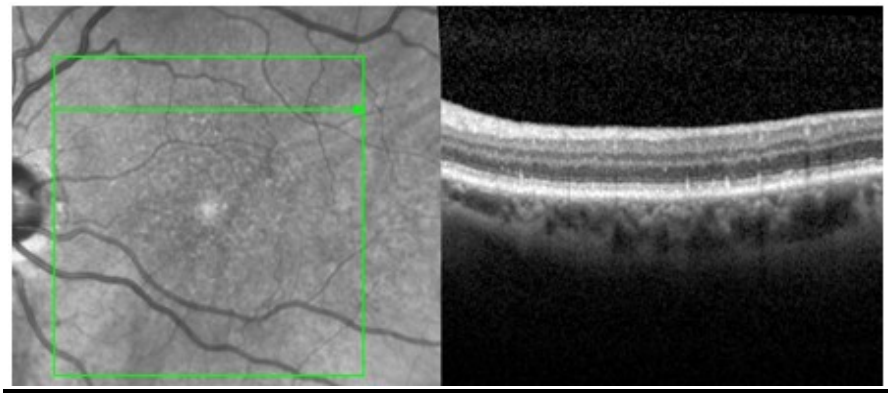

Fig 4.4.B) Reticular Drusen (RD) in a study subject

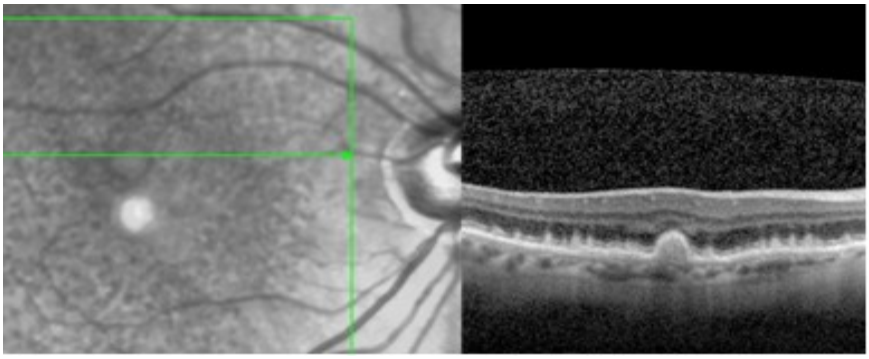

Fig 4.4.C) Combined drusen -predominance of soft drusen (CS) in a study subject

Figure 4.4 : Three divisions of reticular drusen subjects graded for the study. A) SD- Soft drusen only. B) RPD Reticular drusen only C) COMBINED -predominance of soft drusen . All three images are from study subjects.

c) Autofluroscence (FAF):

FAF of the macula was performed using the infrared mode. The Fundus AF in Age-related Macular Degeneration Study Group (FAM Study Group) (Einbock et al., 2005) aims to identify AF changes as predictive factors for the progression of age-related macular degeneration (AMD). Different AF patterns maybe related to high-risk characteristics and may provide new predictive factors for the development of late AMD and visual loss. The identification of these high-risk AF patterns in patients with AMD may be helpful in identifying those to be targeted for monitoring and for possible future therapeutic intervention.

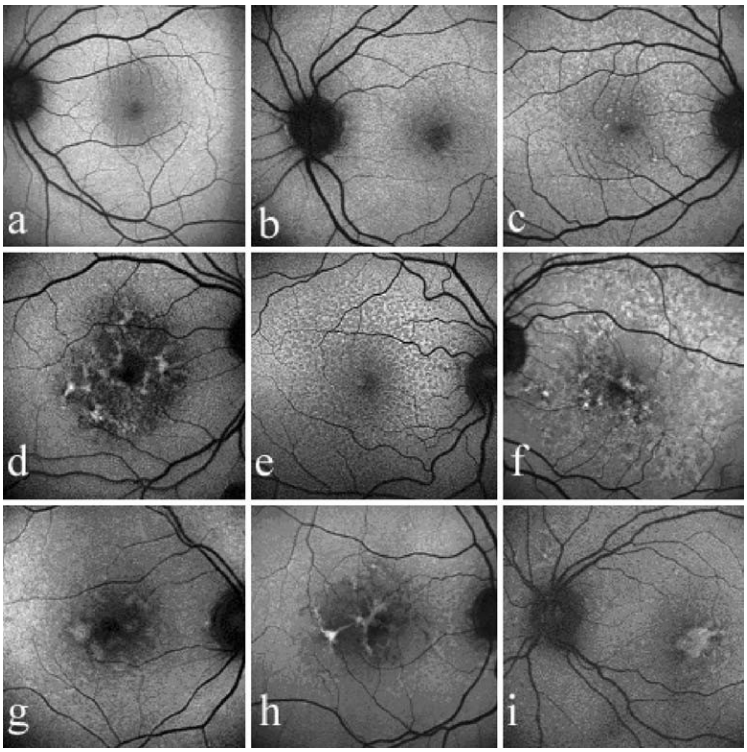

Fig 4.5: AF pattern according to the classification of the International Fundus Autofluorescence Classification Group: a. normal pattern, b. minimal change pattern, c. focal increase pattern, d. lace- like pattern, e. reticular pattern, f. speckled pattern, g. patchy pattern, h. linear pattern, i. focal plaque-like pattern

Statistics: All statistical tests were carried out using SPSS V.17.0 (SPSS, Chicago, IL, USA). Measured RG and YB thresholds in patients with AMD were compared against age-matched normative data. The measured thresholds were related to the severity of AMD grading. Thresholds measured in eyes with RPD were also compared against those measured in eyes without RPD. Student tests were used to determine if the two set of data are significantly different from each other as $P < 0.05$ was considered significant.

At the start of the study apriori calculation made the following assumptions; normal monocular threshold of 1.29 (SD 0.63) and normal group size of 32. Using these parameters 81% power could be achieved with an alpha of 0.05 for a sample size of 38. It was proposed

to double the sample size (38x2) to assess accurately the variability in chromatic sensitivity loss (RG and YB) within each disease group.

During the analysis of the study it was realised that the sample size needed to demonstrate a significant effect, does not apply well to the present study as every subject tested had thresholds outside the normal range. However, a large sample size can provide useful information on the distribution of patients within clinical categories. It was concluded that given the large variability observed in clinical categories, it would have been impossible to compute sample size with any credibility.

5. Results:

5.1:Demographics:

5.1.1. Subjects :

We recruited a total of 67 subjects with AMD for the study. CAD tests were conducted in 90 eyes out of the 134 present in 67 patients (26 males and 41 females). Age of the patients ranged from 55 to 88 years, the median age being 75 years.

Subjects	Eyes tested	Age (Median±SD)	Range	Male: Female	VA range
67	90	70± 7.73	55-88 yrs	1:1.57	6/5-6/18(Snellen chart) (91-61 ETDRS lettters)

Table 4: Demographics of the study group.

Out of the 67 subjects, 23 subjects who had bilateral AMD were eligible for the study had monocular CAD test performed on both the eyes, while 44 subjects who were eligible in one eye performed monocular CAD test in that eye. This was because the other eye had either wet AMD or advanced dry AMD with vision less than 6/18.The Visual acuity (VA) ranged from 6/5 to 6/18**,** VA in most cases was recorded on ETDRS letter chart and converted to Snellen visual acuity.

All the subjects were recruited from AMD clinics at Kings College Hospital. All subjects were deemed asymptomatic in the study eye, as they did not report difficulty in vision and were not aware of any colour or contrast difficulties in everyday life. The subjects with bilateral AMD were in the hospital setting for a regular check after a referral from the optometrist for AMD. The subjects with other eye late AMD were in the hospital for treatment of the affected eye.

5.1.2 History of Smoking:

History of smoking was available in 25 subjects, 3 of the subjects were non-smokers although one admitted being a passive smoker. All except one had given up smoking at the time of the study. The average amount consumed was 10 cigarettes per day for an average of 20 years. The average duration since cessation of smoking was 20 years. Smoking is the most important modifiable risk factor for AMD development and progression (Velilla et al., 2013). Quitting smoking reduces the risk of AMD, and after 20 years of cessation the risk of developing AMD is the same as for non-smokers (Hughes et al., 2007, Rennie et al., 2012). Beaver Dam Offspring study confirmed that smoking 11 or more packs (level of smoking is classified as pack years) was associated with early stage AMD (Klein et al., 2010). Other studies in Korea and Japan also demonstrated that level of smoking was associated with early and late AMD (Moon et al., 2012, Tamakoshi et al., 1997).

5.1.3 Range of Visual acuity in the study sample:

Eyes with best corrected visual acuity of 6/18 (61 ETDRS letters) or better were recruited for the study. This cut-off was chosen to make sure that early stages of AMD were recruited. This level of vision also made sure that the stimulus of the CAD was seen accurately at 3 meters for reliable performance of the test. The distribution of visual acuity across four grades of clinical classification of AMD has been described in Figure 5.1. There was no statistically significant difference in the visual acuity measurements among the different severity scales.

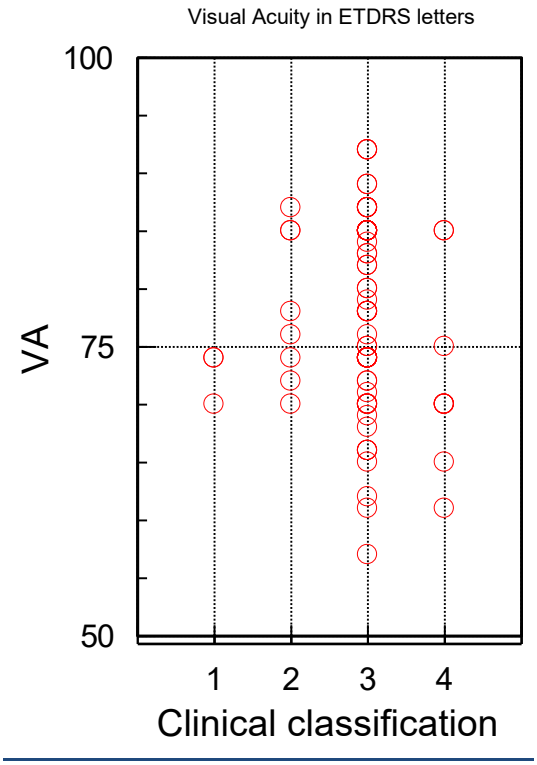

Figure 5.1: Distribution of visual acuity in ETDRS letters in our study sample shown in the four severity grades of clinical classification of AMD.

5.2 Chromatic sensitivity results in the AMD study group

All 90 eyes with AMD had subnormal age corrected colour vision either RG/YB thresholds or both in comparison to the age corrected normative data. The distribution of thresholds spread over the whole scale of severity and ranged from 2.5 to 36.59 CAD units (for RG) and 2.7 to 18.21 (for YB). This is a significant loss as the normative monocular CAD limits for 55 - 88 years is YB= 1.2 to 2.7 ± 2SD; RG= 1.3 to 2.4± 2SD (Barbur et al., 2015).

A. B.

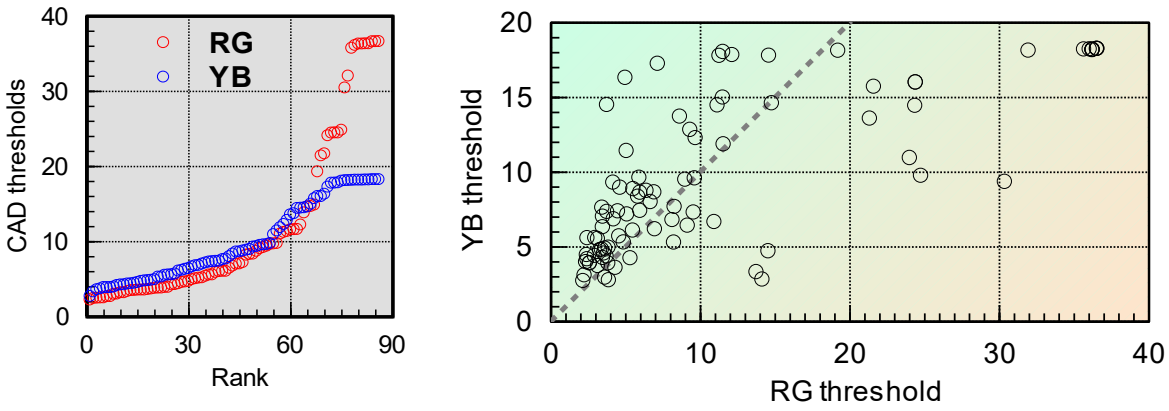

*Figure 5.2 (A, B): Distribution of RG and YB thresholds measured in the 90 eyes examined in the study. Panel A shows the independent ranking of RG and YB thresholds. The thresholds span the full range from just greater than the upper normal limits to the maximum chromatic saturations possible in the RG and YB directions. Panel B shows the relationship between the RG and YB thresholds measured in the same eye. Although in general, most eyes exhibit greater YB losses, when the correlation is limited to a maximum of 18.2 CAD units (i.e., the largest YB threshold limit imposed by the largest chromatic saturation possible on the visual display), linear regression analysis yields an r2 value of 0.35 (YB = 3.482 + 0.724*RG) and the two tailed is P< 0.001.*

The Figure 5.2 (A) shows the distribution of the CAD thresholds in the study group of 90 AMD eyes. The results are interesting as the loss seems to cover the whole scale of severity with some eyes having a mild loss and some having a very severe loss, with the latter being limited only by the phosphors of the visual display employed in the CAD test. The corresponding RG and YB thresholds in 5.2 (A) describe the independent ranking of RG and YB thresholds within the examined eyes. The results show the saturation of both RG and YB thresholds caused by the limits of the visual display.

The lower normal sensitivity for detection of yellow-blue changes may be due to the much reduced S-cone density in the retina but when expressed in SN CAD units, the median thresholds corresponds to one unit for both RG and YB discrimination. The lower upper limit

for YB thresholds is caused by the much larger YB colour signals needed at threshold by comparison with the RG colour signal.

In Figure 5.2 (B) the patient's RG threshold in each of the eyes examined in the study is plotted against the corresponding YB threshold. The results illustrate the proportional increase in both RG and YB thresholds. The independent ranking of RG and YB thresholds of AMD eyes, after eliminating those with thresholds above 18.2 CAD units to account for the maximum possible YB limit, reveals higher YB thresholds when compared to RG ($P > 0.0019$) suggesting that loss of YB sensitivity tends to precede RG. The linear regression analysis limited to data below 18.2 CAD units, yields an r^2 value of 0.35 (Panel B). The two thresholds are therefore correlated.

5.2.1 Chromatic loss in AMD compared to age matched normals.

The results were compared to the monocular normative CAD data for age matched normal's available (Barbur and Rodriguez -Carmona, 2015).The normative data were obtained for a large sample size of 720 eyes and included subjects from 4-90 years of age. The large majority of the subjects were from Damme Optometri practice (Kersteren,Netherlands) and they were filtered for congenital colour vision deficiency, with medical conditions such as diabetes, hypertension, abnormal fundus appearance including drusen (Figure 5.3).

There is a gradual and linear increase in sensitivity from younger age groups and the best chromatic sensitivity corresponds to approximately 20 years of age, depending on a number of factors including improvements in attention ability and performance. The second phase must be linked to healthy aging and is likely to involve physiological changes that also follow a gradual linear decline in sensitivity.

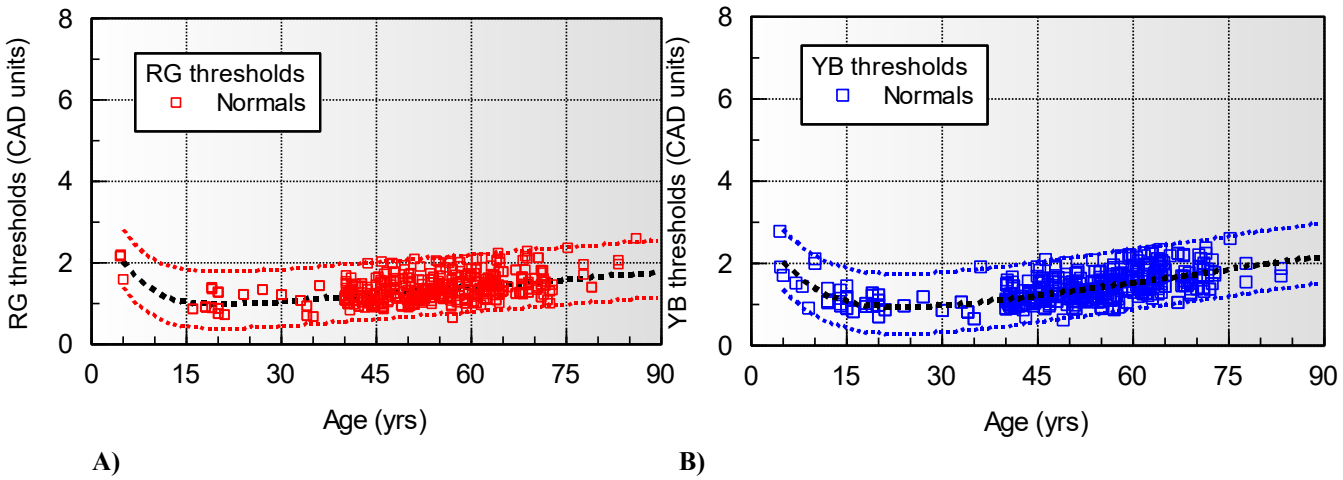

Figure 5.3(A,B) : RB/YB monocular CAD thresholds in age corrected normal population. The original monocular data measured at City University London and the Damme Optometric practice in Netherlands (Kresteren). CAD thresholds obtained in 720 eyes,The age range of subjects was from 4 to 90 years of age. RG and YB CAD thresholds were measured separately for each eye. Exclusions criteria were applied to 'filter' out subjects with congenital and acquired colour vision deficiencies. The filters were defined according to the following criteria:1. Congenital colour deficiency (exhibiting elevated RG and normal YB thresholds). 2. Subjects with medical conditions (MC) such as diabetes, hypertension and ocular abnormalities which may cause acquired loss of chromatic sensitivity.3. Subjects with abnormal fundus appearance or drusen. 4. Subjects who exhibited a statistically significant difference in RG and or YB chromatic sensitivity between the two eyes. The indexes employed to describe the asymmetry between the two eyes were the difference in monocular thresholds referenced to the best eye.

The results show a linear increase in colour thresholds of 1% per year for RG and around 1.6% for YB over the remaining life span. The loss of myelinated RGC axons and cell bodies with increasing age follows a similar trend and may account in part for the observed loss. As the colour vision relies largely on normal cone signals and integrity of retina and visual pathways, the small changes in optics of the eye caused by small changes in refraction, pupil size and scattered light have little effect, on the colour vision, when the task is to measure

colour thresholds with large stimuli against a background of high luminance (Barbur et al., 1997; Barbur and Rodriguez-Carmona, 2012).

The study by Barbur et al 2015 establishes the reliable upper threshold limits for RG and YB colour vision which enables detection of the earliest signs of acquired loss of chromatic sensitivity and hence the presence of anatomical and physiological changes other than those attributable to normal aging.

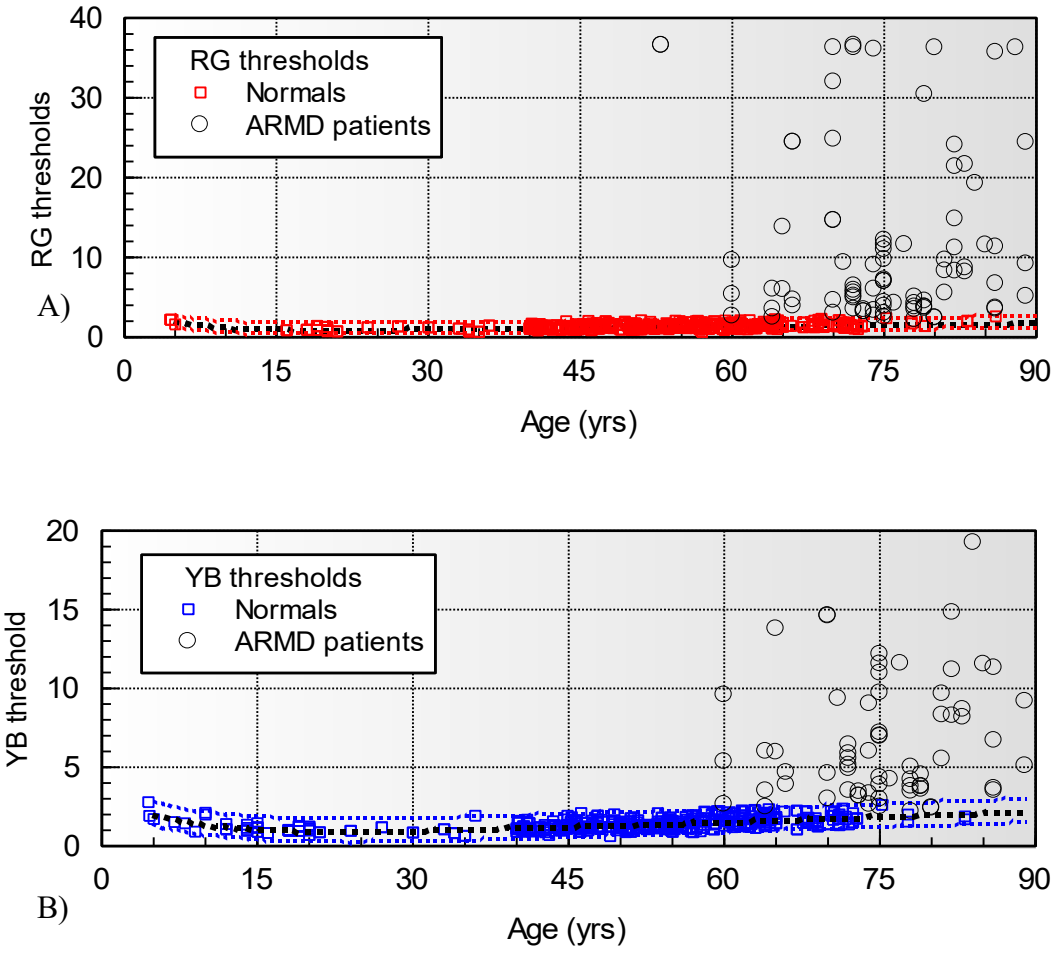

Figure 5.4(A): RG CAD values of AMD subjects plotted against age matched normals; (B): YB CAD values of AMD subjects plotted against age matched normals. The normative data are based on 720 eyes filtered for congenital and acquired colour deficiencies. RG/YB thresholds of 90 eyes with AMD were significantly higher than the normative data.

When chromatic sensitivity was measured in standard normal CAD units, the AMD subjects were significantly higher than the normal population. The two- tailed P value was less than 0.0001 for both RG and YB thresholds of AMD subjects compared to RG and YB of normative data. This difference was considered to be highly significant, which was equivalent to saying that one can be certain that RG and YB colour vision is strongly affected in AMD.

5.2.2. Grading the Severity of Chromatic loss in AMD group:

The AMD subject group had been stratified according to severity of chromatic sensitivity loss as they presented with in the study. Severity grading has been described in methods section 4.1.

	Mild	Moderate	Severe	V.Severe
RG	46%(n=42)	25.5%(n=23)	6.6%(n=6)	21.1%(n=19)
YB	33.3%(n=30)	33.3%(n=30)	14.4%(n=13)	18.8%(n=17)

Table 5: showing the distribution of severity of chromatic loss in AMD subjects.

46% of the eyes had mild loss of chromatic sensitivity with RG thresholds where as only 33.3% of the eyes had mild loss of chromatic sensitivity with YB thresholds. This shows that the YB thresholds were affected and progressed earlier than RG as suggested by various studies in the past (Neelam et al., 2009).

A majority of the AMD subjects had mild to moderate chromatic sensitivity loss with both RG/YB thresholds rather than having severe to very severe loss. This could be the reason that chromatic sensitivity loss has not been recognised so far, however we have made an attempt

in further sections to identify causes of severe to very severe chromatic losses in these subjects.

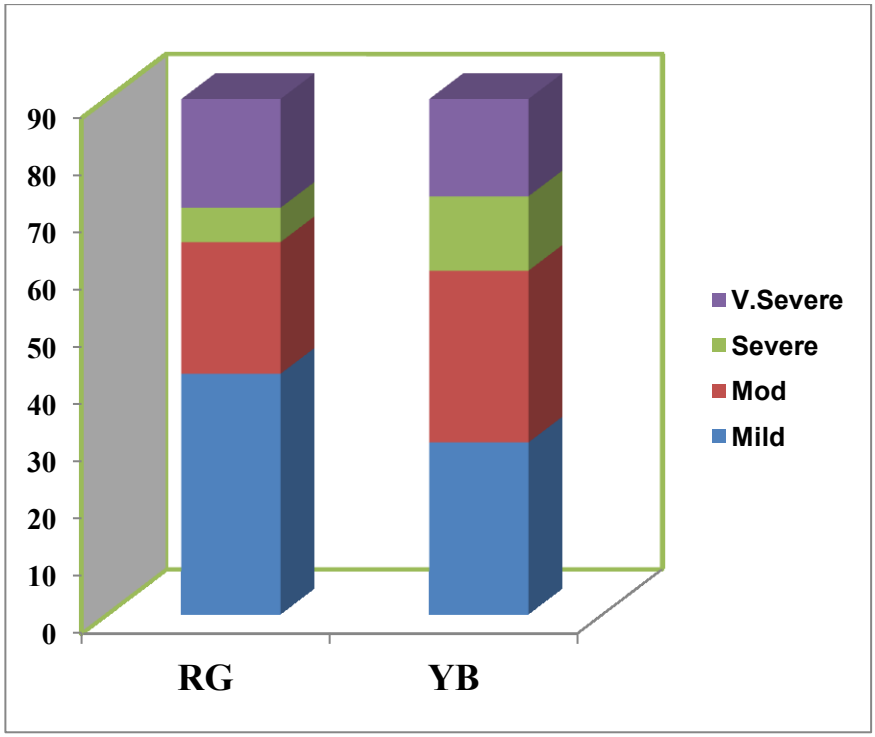

Figure 5.5: Stratification of AMD subjects based on CAD thresholds. AMD subject divided according to the severity of their CAD threshold losses. Majority had mild to moderate losses; YB showing early progression in comparison to the RG thresholds

5.3: Correlating Clinical classification on fundus photographs to chromatic sensitivity:

To understand the distribution of AMD pathology in our study group we separated the subjects according to clinical classification of AMD (Ferris et al., 2013).This is a quick and basic clinical classification aiding clinicians to assess risk of progression to late AMD. This classification mainly used the size of the drusen. Eyes with drusen size ≤63 µm were considered as normal aging, whereas eyes >63≤125 were considered as early aging, and size

larger than this, with or without pigmentary changes, as intermediate aging. They included wet AMD and GA as late AMD.

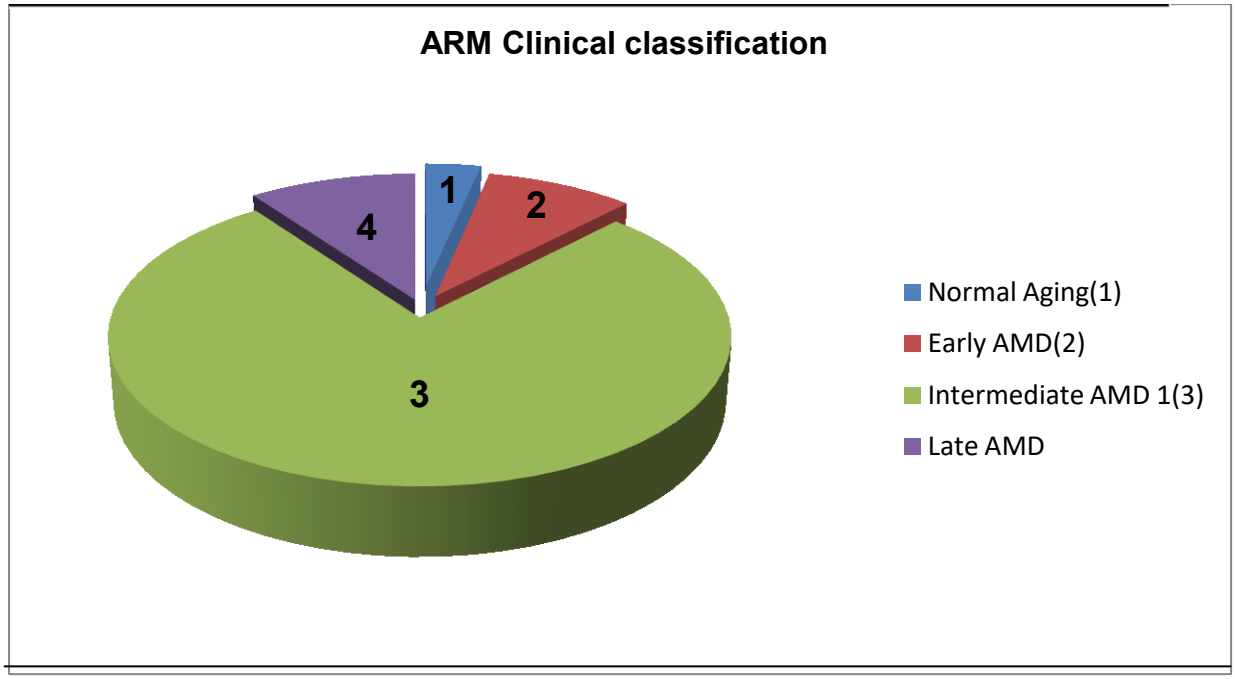

Figure 5.6: AMD Demography in the study group: The 90 AMD eyes classified according to clinical classification of AMD and the most common group of subjects who performed the CAD test were in the intermediate AMD stage.

A majority of our AMD group was classified as intermediate AMD (77.7%, n=70). Three eyes met the criteria for normal aging (3.33%), 8 eyes for early AMD (8.88%) and 9 eyes for late AMD (10%). Eyes classified as late AMD were recruited as an early stage of the disease but found to have incidental early geographic atrophy or an isolated cyst on OCT during result analysis, in spite of good visual acuity. The grades were correlated with the RG/YB thresholds to look for any correlation as the severity of grades increased on the clinical classification. There was a gradual increase in the mean of the thresholds with increasing severity of grades. There was a wide variablity in thresholds with large SD in each group of

the classification as a result of which the P value comparing the eyes with early AMD to the

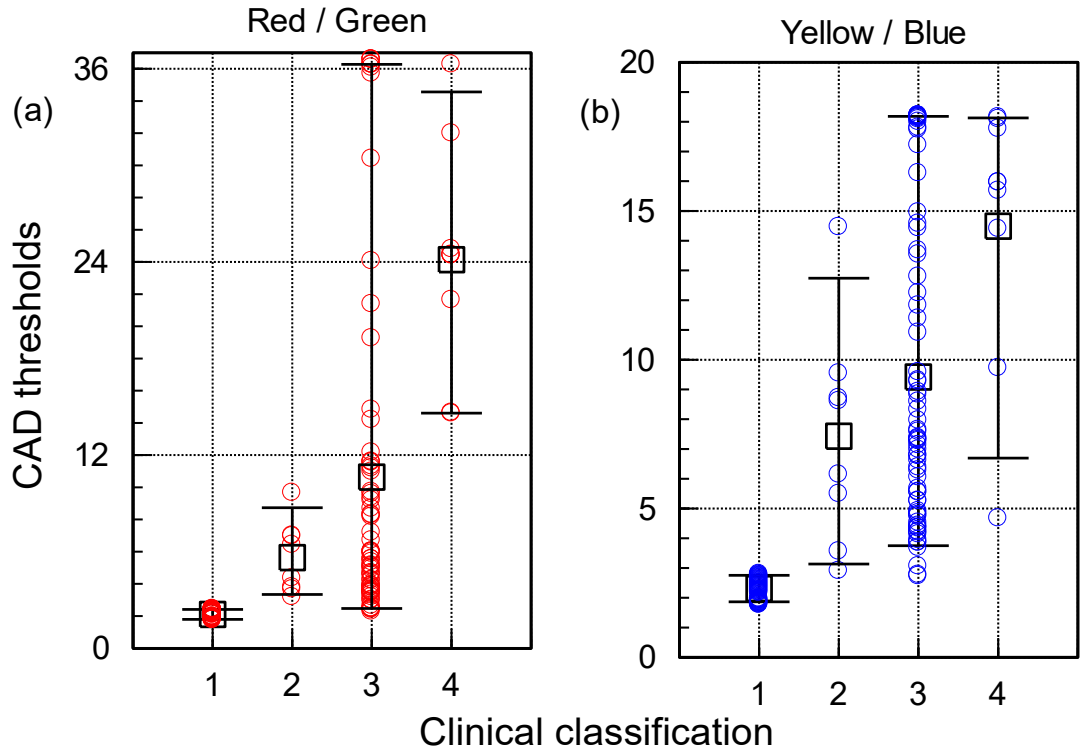

eyes with higher intemediate AMD was not significant.

Figure 5.7: Spread in RG and YB thresholds within the four groups formed using the clinical classification criteria. 1 = Normal, 2 = Early, 3 = Intermediate, 4 = Late. Individuals CAD thresholds of each eye are plotted for each of the 4 groups, the whiskers show the 5th and 95th percentile, while the mean value is plotted as an outline square. Although the results show a gradual increase in mean thresholds, the difference between group 2 and 3 was not statistically significant due to large inter subject variability. The 'Late' AMD group in eyes with early GA had more severe loss of both RG and YB colour vision.

CC	1	2	3	4
n	3	8	70	9
RG	2.43(0.3)	5.63(2.2)	10.63 (10.3)	24.14(7.0)
YB	3.27(0.8)	7.43(3.7)	9.42(5.2)	14.49(14.4)

Table 6: Showing mean chromatic sensitivity in each grade of the clinical classification with Standard deviation (SD).

5.4: Chromatic sensitivity correlated to Age related Drusen Categories:

The AMD group had been further subdivided to examine the effect of different types of drusen on chromatic sensitivity and to study chromatic sensitivity while soft drusen had been classified and graded in detail according to the international classification and grading system for ARM (Age related maculopathy)/ AMD (Bird et al., 1995).

Seventy one eyes were available to grade for drusen morphology grading, after excluding eyes with only pigmentary change but no drusen, eyes with early GA and eyes with coincidental cysts on OCT.

49 eyes had only soft drusen, 9 eyes had reticular drusen, 11 eyes had reticular drusen with soft drusen and 3 eyes had small drusen (<63µm), which is not classified as AMD.

	Normal Aging	Soft Drusen	Reticular Drusen
n	2	49	20
RG(SD)	2.43(0.3)	7.69(7.4)	18.85(12.6)
YB(SD)	3.27(0.8)	7.85(4.3)	14.03(4.4)

Table 7: Showing number of eyes under each category of Age related Drusen; mean chromatic sensitivities in each category with standard deviations shown.

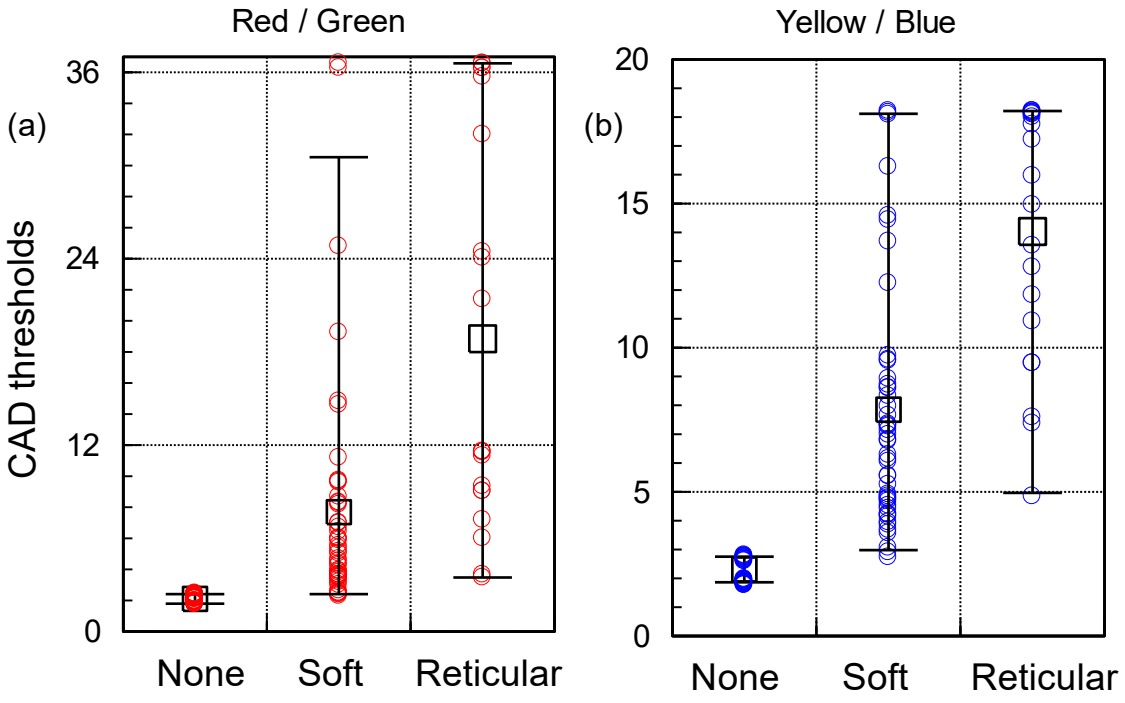

Figure 5.8: Spread in RG and YB thresholds in eyes classed as normal aging, soft drusen and those with reticular drusen. The latter showed significantly larger RG and YB thresholds. The 'None' group included 3 subjects classed as having changes attributed to normal aging as well as age matched normal eyes from normative database. The whiskers show the 5th and 95th percentile, while the mean value is plotted as an outline square. This box plot shows the eyes with reticular drusen have worse CAD thresholds and the chromatic sensitivity worsen as we move from normal aging to Soft Drusen to Reticular Drusen.

Subjects with reticular drusen had the highest mean CAD thresholds (i.e., RG = 18.9 and YB = 14 CAD units). Subjects within the soft drusen group had mean RG CAD thresholds of 7.7 and YB thresholds of 7.9. Typical examples are shown in Figure 7a and 7b.

Both the SD and the RPD groups showed significantly larger thresholds when compared with the normal group ($p<0.0001$). The mean difference between the SD and RPD groups was also statistically significant ($p< 0.0001$ for both RG and YB). The subjects within the reticular drusen group were more affected than those in the SD group.

(1)

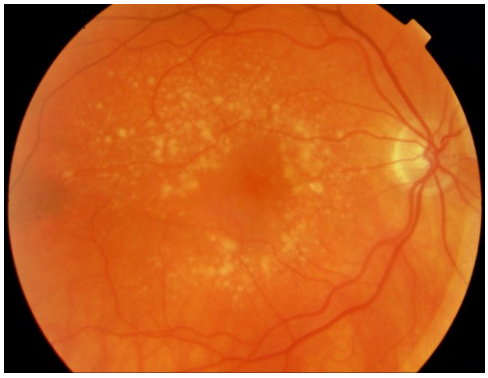

CAD Thresholds
RG: 4.53
YB: 7.34
(Moderate loss of colour vision)

(2)

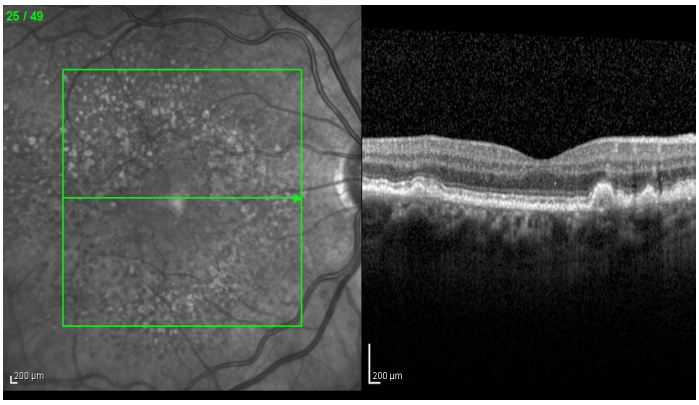

(3)

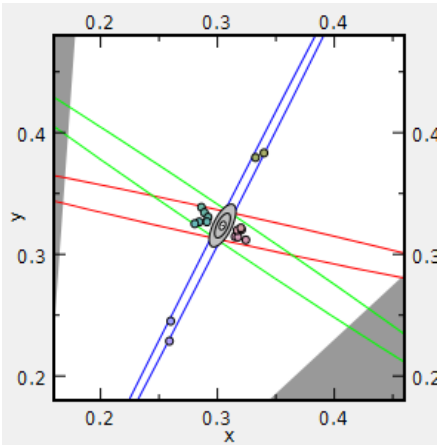

Figure 5.9a: Example of eye with soft drusen showing a moderate loss of chromatic sensitivity.1. Fundus photo 2.OCT scan 3. CAD results

(1)

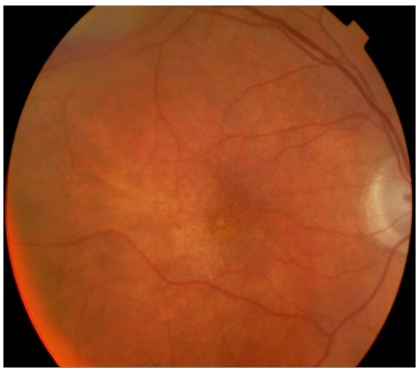

CAD thresholds
RG:21.38
YB: 13.54
(Severe loss of colour vision)

(2)

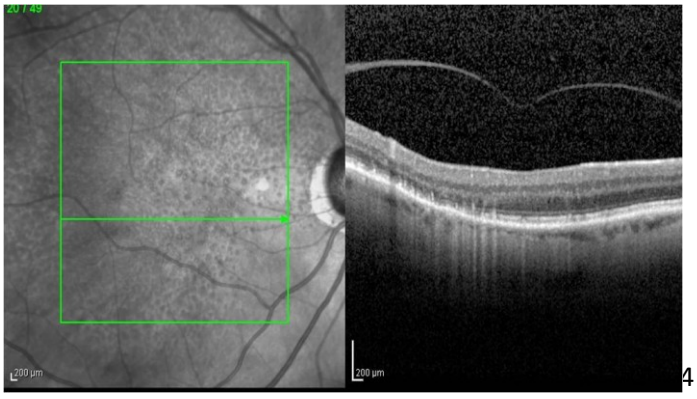

(3)

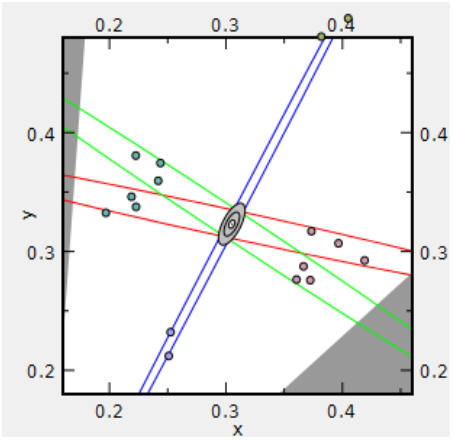

Figure 5.9b: Example of images from eye with reticular drusen showing severe loss of chromatic sensitivity. 1. Fundus photo, 2.OCT scan, and 3. CAD results

5.5: Chromatic Loss correlated to Fundus Grading in Soft Drusen:

All eyes with soft drusen (49 eyes) were stratified based on soft drusen morphology, size, number, area covered and main location of the drusen on the ETDRS grid. The grading was first applied to the central subfield of the ETDRS grid, and then on the whole grid. The findings were not conclusive for the central subfield, thus the results of the whole grid are mentioned.

5.5.1 Drusen Morphology:

Drusen morphology was graded from 0-5 and classified according to the International Classification and Grading System for AMD (Please see Table 2).

	Questionable(1)	Intermediate(3)	Large(4)	Soft/serogranular(5)
n	1	10	16	22
RG	2.29	4.7(1.8)	6.2(3.3)	10.36(1.8)
YB	3.06	5.6(1.6)	8.3(3.9)	5.6(1.6)

Table 8: Showing CAD thresholds in soft drusen eyes classified according to increasing drusen morphology grades. Mean CAD units with SD displayed. R^2 for the mean CAD thresholds over increasing grade of morphology showed a good linear trend of 0.9 for both RG and YB thresholds, but there was a wide variability of CAD units as indicated by the SD.

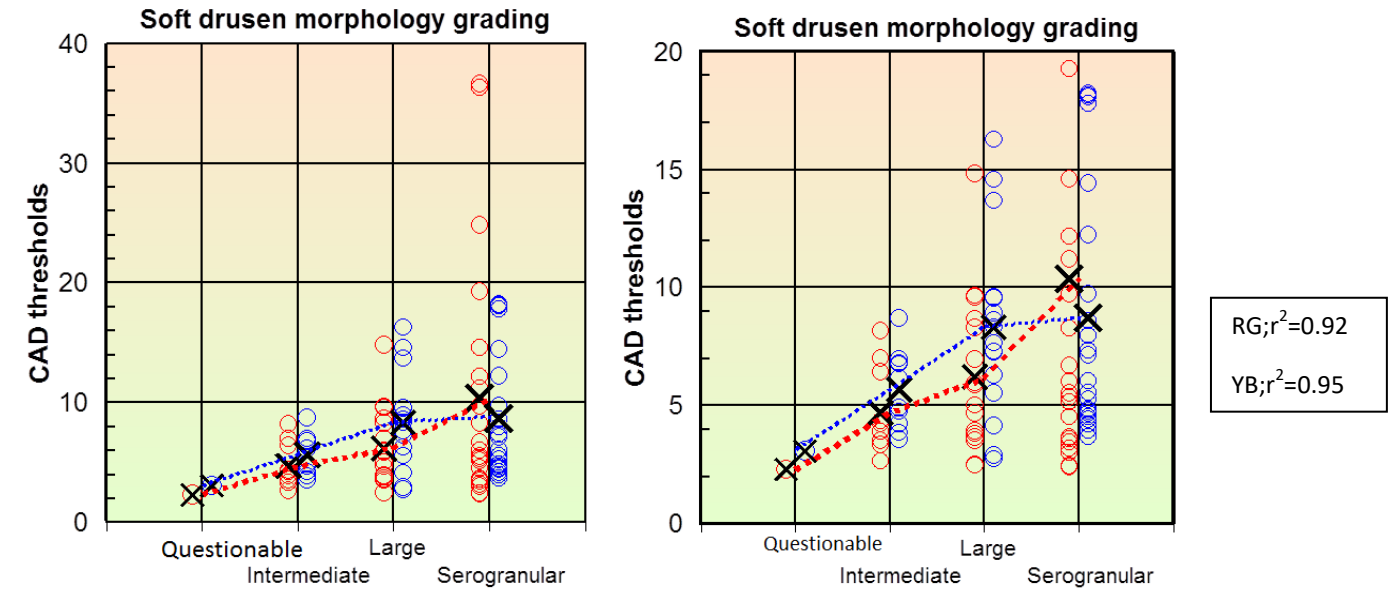

a) b)

Figure 5.10: Trend of chromatic loss in increasing drusen morphology grading: a. Results plotted up to 40 CAD units, b: Results magnified up to 20 CAD units

Comparison of CAD thresholds of Grade 5 with the rest of the grades showed a significant difference for RG ($p = 0.02$), while the comparison of CAD thresholds for YB of Grade 5 eyes with YB thresholds for the rest of the grades did not show significant p value. This may be due to the increased variability in YB thresholds and the upper limit of loss imposed by the phosphor limits of the display.

5.5.2 Drusen Number:

Drusen number was graded from 1-4 and classified according to the International classification and grading system for ARM /AMD (Please see Table 2)

Grade	1	2	3	4
n	2	0	7	40
RG	2.29 (0.3)	0	5.7(2.2)	8.0(8.1)
YB	3.06 (0.2)	0	6.3(1.7)	8.0(4.5)

Table 9: Showing the Chromatic sensitivity in grades of drusen number with SD, R squared for the mean thresholds showed a linear trend (0.9) and again a large variation in the thresholds with large SD noted. The CAD thresholds of Grade 4 eyes was not statistically different from the CAD thresholds of all other grades.

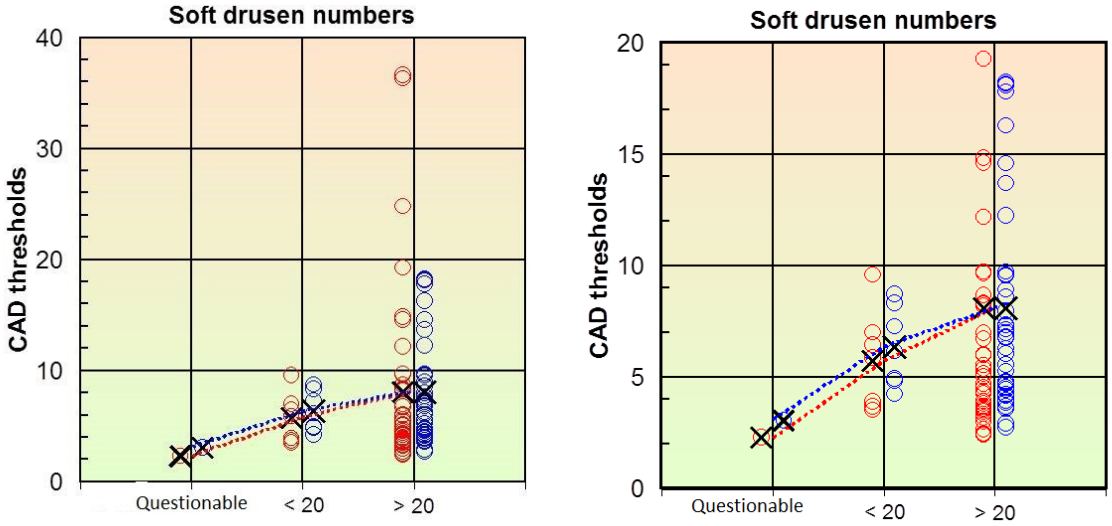

a) b)

Figure 5.9: Trend of chromatic loss in grades of increasing drusen number. a) Results plotted upto 40 CAD units, b) Results magnified up to 20 CAD units

5.5.3 Drusen size:

Drusen size was graded from 1-5 and was classified according to International classification and grading system for AMD (Please see Table 2).

Grade	1	2	3	4	5
n	1	6	13	14	15
RG	6.4	6.3(2.1)	4.4(2)	5.7(3.4)	13.2(11.2)
YB	3	6.8(2.5)	5.5(1.8)	8.4(4.1)	10(5.6)

Table 10: showing the Chromatic sensitivity in Grades of drusen size with SD. R squared for the mean thresholds did not show a linear trend, but the CAD thresholds of Grade 5 eyes was statistically different from the CAD thresholds of all other grades.

The P value comparing the CAD thresholds of RG and YB of Grade 5 to the rest of the grades was statistically very significant with P value <0.0003 for RG and 0.02 for YB.

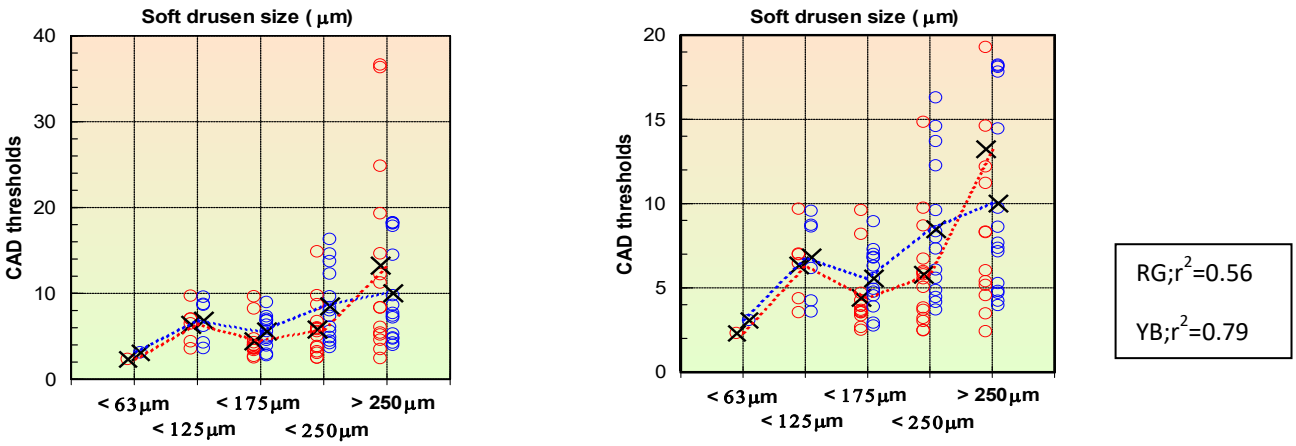

Figure 5.11 : Trend of chromatic loss in grades of increasing drusen size. a) . Results plotted upto 40 CAD units, b) Results magnified upto 20 CAD units .The R squared did not show a linear trend but the P vaule comparing chromatic sensitivity of grade 5 eyes was statistically different from the chromatic sensitivity of eyes with other grades(1 to 4).

5.5.4 Main Location of the Drusen(1.4):

Location of drusen was graded from 1-4 and was classified according to International classification and grading system for ARM /AMD (Please see Table 2).

We examined the eyes with drusen involving the central subfield in comparison to the rest of the locations. This was done to test the hypothesis that drusen involvement in the centre might be associated with greater severity in terms of AMD grading and chromatic sensitivity.

Grade	Druen in central subfield	others
n	14	25
RG	8.8(9.3)	6.6(4.6)
YB	7.9(5.0)	7.6(3.9)

Table 11: The Chromatic sensitivity of eye with drusen in the centre and other eyes. There was no statistical difference between the two groups.

There was no significant difference between the CAD thresholds of the eyes with drusen involving the centre of the macula and eyes with drusen in other ETDRS subfields besides the center.

5.5.5. Area covered by the Drusen(1.5):

Soft drusen eyes were further classified into 1-5 grades depending on the percentage of area covered and classified according to the International classification and grading system for

AMD (Table 2). The p value comparing the CAD thresholds of Grade 5 to the rest of the grades was not statistically significant.

Grade	1	2	3	4	5
n	3	4	9	28	5
RG	6.1(3.6)	6.1(3.8)	5.7(2.3)	8.1(9.2)	10.84(5.8)
YB	6.3(2.9)	7.7(4.4)	8.4(4.7)	7.8(4.7)	8.0(5.8)

Table12: showing chromatic sensitivity in increasing grades of drusen area. R squared of the means did not show a linear trend and there was no statistical difference between eyes of larger area of drusen involvement and other eyes.

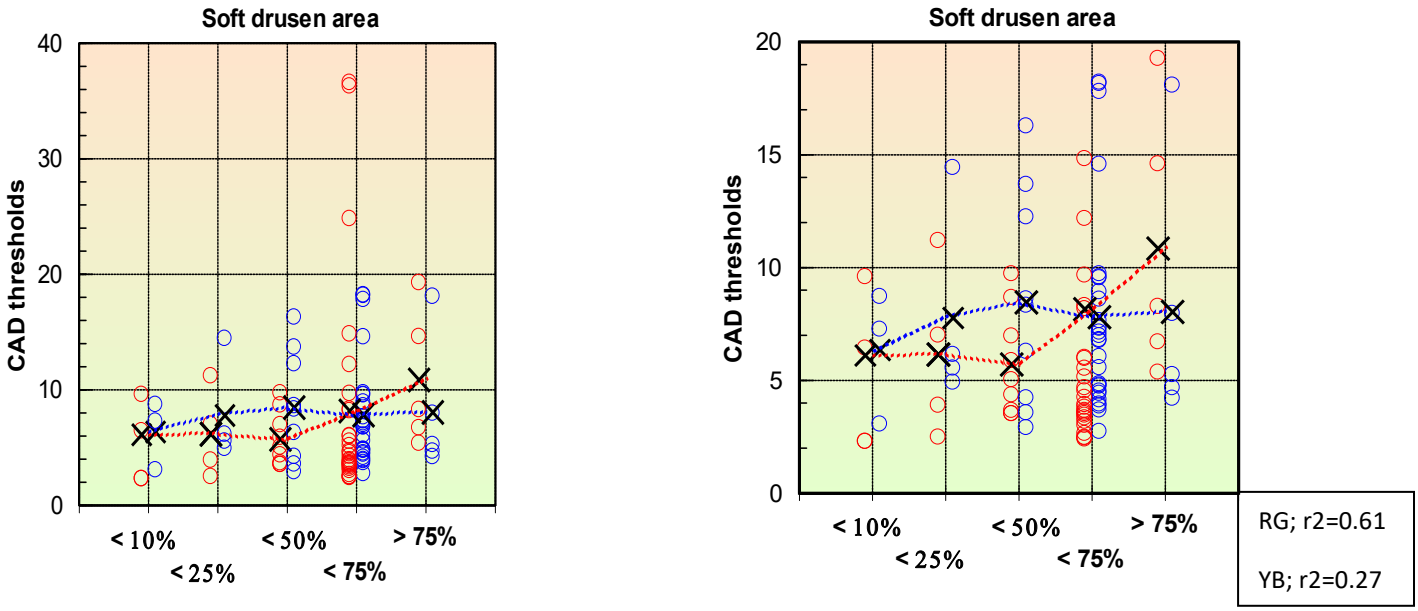

Figure 5.12: Trend of chromatic loss in grades of increasing drusen area. a) Results plotted up to 40 CAD units, b) Results magnified up to 20 CAD units. The R squared did not show a linear trend but the p value comparing the grade 5 eyes was statistically different from the chromatic sensitivity of eyes with other grades.

5.6 Fundus Autofluroscence(FAF):

FAF was performed in 76 eyes which underwent the CAD test. We stratified our patients depending on the FAF pattern in the study by the FAM study group (Einbock et al., 2005).

The most common pattern was the minimal change pattern (32%, n=25) followed by the specked pattern (21%, n=16).

AF Pattern	n	RG	YB
1. Patchy	10	20.9(14.4)	14.1(4.9)
2. Lace -Pattern	8	20.1(15.3)	11.17(6.0)
3. Speckled	16	11.3(10.6)	10.2(5.3)
4. Focal plaque-like	7	10.9(12.7)	8.3(5.6)
5. Linear	3	9.2(2.1)	11.7(2.9)
6. Reticular	7	8.3(9.9)	6.9(1.9)
7. Minimal change	25	8.2(6.2)	9.0(5.2)
8. Focal increase	1	3.5	6.9

Table 13: The FAF pattern of 76 AMD eyes arranged in decreasing order of chromatic sensitivity in CAD units. Patchy pattern had the worse change in sensivity followed by the Lace-Pattern of FAF.

Patchy pattern of FAF was evaluated as this was the high risk pattern in the study according to the FAM study group criteria. This group had the largest CAD thresholds in accordance with the FAM group results.

50% of patients with a patchy pattern of FAF had very severe loss of RG and YB CAD thresholds. Patchy pattern of FAF had the worst CAD thresholds, and the next group to have larger CAD thresholds was the Lace-pattern of FAF.

5.7 Central macular thickness:

We had the central macular thickness (CMT) available for 90 eyes which was correlated to their RG/YB thresholds. Three eyes were noted to have early GA on careful examination of the fundus and OCT but a CMT more than 200µm (203,205 and 266µm), these eyes showed very severe loss of RG / YB thresholds.

The P value correlating the CAD thresholds of eyes with CMT<200 and the rest was statistically significant with P<0.01 for RG and <0.002 for YB.

	GA	CMT<200µm	CMT>200µm
n	3	11	76
RG	25.1(10.8)	18.3(13.0)	10.2(10.0)
YB	17.2(1.1)	14(4.7)	8.9(5.0)

Table 14: showing chromatic sensitivity in relation to central macular thickness: Eyes with GA and CMT less than 200 microns have significantly worse chromatic sensitivity than the other eyes.

5.8 Drusen Volume:

Drusen volume calculation was done in 25 eyes and further calculations were abandoned as manual measurements were time consuming and preliminary calculations showed poor correlation between chromatic sensitivity and drusen volume.

Drusen volume in the central grid was calculated using the image J program (NIH public domain software) and classified as grade 1 (no drusen), grade 2 (<0.1mm^3) grade3 (0.1-0.5mm^3), grade 4 (>0.5mm^3).

Eyes (n=9) with grade 1 volume showed chromatic sensitivity ranging from 2-36 CAD units for RG and 2-18 CAD units for YB which shows that chromatic sensitivity can range from mild to very severe even when there was no drusen recorded in the centre of the grid. No statistical significance could be obtained for other grades of drusen volume and chromatic sensitivity.

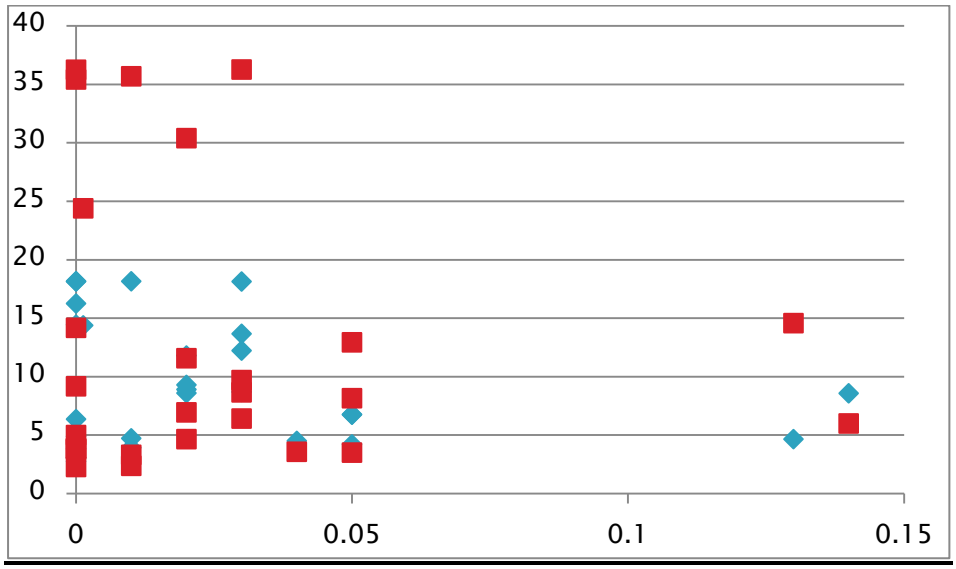

Figure 5.13: Manual Drusen volume calculation in 25 eyes using Image J program. A scatter graph for correlation between chromatic sensitivity and drusen volume.

SD OCT provided for better quantification of drusen and attempts had been made to correlate to the fundus photographs which have been the gold standard so far.

Yehoshua et al (2013) found only fair agreement between drusen area measurements obtained from SD OCT and colour fundus photos. Drusen area measurements on colour fundus images

were larger than those with SD-OCT scans. They attributed the difference to the fact that OCT algorithms define drusen in terms of RPE deformations, above a certain threshold and will not include small, flat drusen and subretinal drusenoid deposits. They recommended a combined approach using both the OCT and fundus photographs for information on drusen.

5.9 Clinical follow-up at one year:

It is of great clinical interest to establish whether eyes with severe and very severe CAD thresholds do progress to wet AMD. A year after the initial test, follow-up data was available for 45 eyes from routine hospital appointments and this information was reviewed. The study had ethical approval to review hospital notes and patients were made aware of this beforehand, during the consent process. The results showed that 6 eyes had converted to wet AMD; the CAD thresholds recorded 12 months ago in these eyes were studied to look for any pattern of chromatic loss. No conclusive pattern of loss was seen with the eyes having all grades of severity of chromatic loss.

4 eyes had mild RG loss and the remaining 2 eyes had severe and very severe loss. 3 eyes had moderate YB loss and among the remaining eyes, 2 had mild and one had severe chromatic loss.

5.10 Chromatic sensitivity in Drusen not related to AMD:

Ten eyes of subjects with drusen not related to ARM/ Early onset drusen (EOD) were included in the study. The p value was not significant in comparison to normative data but was statistically significant in comparison to the soft drusen group (p=0.03 RG and p=0.01 YB) and the reticular drusen (RPD) group (<0.001) for both RG and YB CAD thresholds. This implies that CAD in EOD / not AMD eyes was not very different from normative data but significantly different from soft drusen and RPD groups.

Diagnosis	Age	RG (RE)	YB (RE)	RG (LE)	YB (LE)
EOD	48	1.14	0.96	1.38	1.96
EOD	40	1.91	2.68	3.18	3.86
BLD	46	2.73	2.58	1.42	1.39
Sorsby	70	2.54	8.49	3.39	3.09
AVMD	79	3.3	10.69	5.06	4.12

Table 15 a: Chromatic sensitivity in Early onset Drusen. The CAD thresholds were not statistically different from normative data and had statistically lower thresholds than the AMD eyes.

EOD	n	RG(SD)	YB(SD)
	10	2.61(1.2)	3.98((3.16)

Table 15 b: Table showing the number of EOD and their mean CAD thresholds with SD.

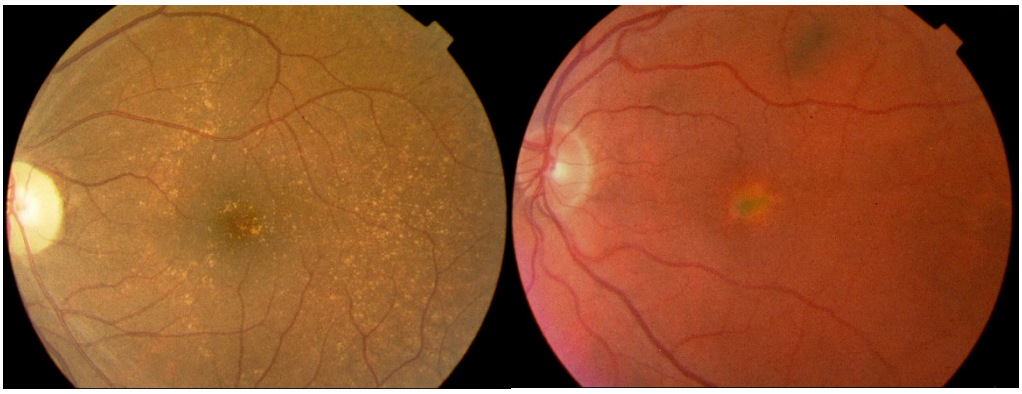

a) **b)**

Figure 5.14: Examples of Drusen not linked to AMD etiology: a) BLD (Basal Laminar drusen) b) Adult vitelliform macular degeneration. In spite of significant drusen (a) and macular pathology (b) the colour vision remains normal to mild loss unlike in AMD.

Even though the EOD/not AMD eyes had drusen morphology similar to AMD the colour thresholds were not as adversely affected as in AMD concluding that just the appearance of drusen in these eyes does not suggest the same degenerative disease as in AMD.

6. Discussion

6.1 Abnormal chromatic sensitivity in early and intermediate AMD:

The hypothesis that psychophysical tests like colour vision depend on the functional status of the photoreceptors and may detect subtle alterations in the macula before the morphological fundus changes and traditional measures of vision, exhibit any deterioration, is well illustrated in Figure 6.1

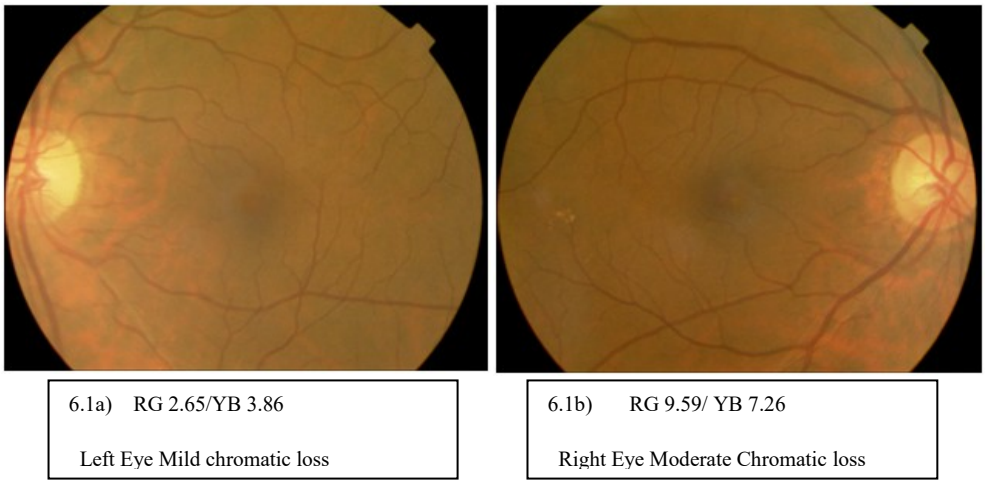

Figure 6.1(a,b): Shows CAD thresholds of a study patient . The Left eye(a) of a subject has no signs of AMD and shows only mild loss of colour discrimination; The Right eye(b) of the same subject has early stage AMD and shows Moderate loss of colour vision. This is illustrated to demonstrate the chromatic change a eye might experience with the onset of Aging. It is of interest to note that although the loss of chromatic sensitivity is less in the left eye, the threshold is well above the upper normal healthy age limit. This decreased chromatic sensitivity can be demonstrated even in the absence of obvious retinal changes linked to AMD .

YB, RG or both thresholds were found to be abnormal in every eye with AMD, when the thresholds were compared with the upper normal limits for the corresponding age. Colour vision depends on the normal functioning of cone photoreceptors and the normal processing

of these signals in the retina. Early changes in the retina that are not detected and labeled as structural changes using clinical fundus imaging techniques may cause the loss of chromatic sensitivity with high contrast visual acuity that is frequently spared. The latter is therefore a poor indicator of the earliest changes in the retina that must precede the loss of colour vision. In addition, the foveal cone mosaic and the corresponding visual acuity can remain normal even when the cone density decreases well below normal values at or near the fovea (Ratnam et al., 2013).

Although both rods and cones degenerate in AMD, rod loss precedes cone loss in 75% of early and intermediate AMD eyes (Curcio et al., 2000) as deficits in rod-mediated functions occur in AMD and RPD (Sivaprasad et al., 2016). In spite of these observations, changes in cone-mediated visual functions such as CV and rapid flicker sensitivity have been reported in early stage AMD. Cones may not therefore function normally or cone signals may not be processed efficiently in AMD despite unaltered foveal cone numbers, as evident on histopathological studies (Neelam et al., 2009).

The findings from this study demonstrate that YB loss starts earlier and tends to be greater than RG loss. This observation is consistent with observations made by Verriest and others who found YB loss to be the most common acquired CV deficiency in macular pathology (Verriest, 1963). It has been proposed that the much smaller number of S cones in the retina are more susceptible to damage in diseases of the retina (Boycott and Wassle, 1991). Alterations in the metabolic environment of the RPE –photoreceptor complex also appear to affect S more than L and M cones (Spraul et al., 1999). Eisner and her colleagues have demonstrated in more than one study that patients who exhibit lower S cone sensitivities were associated with higher risk of developing wet AMD (Eisner et al., 1991, Eisner et al., 1992).

There is alteration of various cone-mediated visual functions in addition to colour vision (temporal function and S-cone sensitivity) in patients with early stage AMD. This suggests that dysfunction of cone photoreceptors occurs in combination with rod dysfunction in early stages of AMD despite unaltered foveal cone numbers on histopathological studies. The widespread dysfunction of the cone photoreceptors in early stage AMD may reflect either the barrier effect of Bruch's membrane or dysfunction of the RPE. Although unlikely, the cone dysfunction may arise from the lower optical density or reduced quantum catch of the photopigment. VA is however preserved in such patients in spite of the colour loss.

Reliable upper threshold limits for YB and RG colour vision have been established (Barbur, 2015) as they are essential to detect the earliest signs of acquired loss of chromatic sensitivity, hence the presence of anatomical and physiological changes other than those attributable to normal aging. There is a rapid increase in sensitivity of RG/YB CAD thresholds during the first year of life and a more gradual increase continues into adolescence. The smallest (most sensitive) thresholds correspond to approximately 20 years of age followed by a gradual decline of approximately 1% per year for RG and 1.6% per year for YB over the remaining life span. Several factors that are not always the same may contribute to the normal aging of the RG and YB mechanisms. The almost linear loss of retinal ganglion cell (RGC) axons and cell bodies during the life span is arguably the most important factor and may account for the increased RG and YB thresholds observed in normal aging. The rapid loss of YB chromatic sensitivity involves other factors such as the greater reduction the contribution short wavelength light makes to retinal illumination with increasing age.

Colour thresholds remain relatively unaffected by small changes in refraction, pupil size and scattered light (Rodriguez-Carmona et al., 2012). Under optimum conditions of light adaptation colour appearance is also independent of optical density of the ocular media and surprisingly YB remain relatively independent of both macular pigment optical density and absorption of short wavelength by the lens (Rodriguez-Carmona, 2006) provided sufficient ambient light is available to avoid larger reductions in retinal illuminance for blue light. Significant retinal illumination and stimulus size can however cause large increases in colour thresholds (Barbur 2006 and 2015) .

A majority of colour vision tests were designed to detect congenital colour deficiency which results in RG loss. Many of these tests minimise detection of luminance contrast signals by employing spatial features that vary randomly in luminance contrast. Ishihara test plates employ YB chromatic noise to provide sensitive detection of RG deficiency (Rodriguez-Carmona et al., 2012). Lantern tests require the subject to name correctly the small colour signals presented against the dark background (Birch, 2008). These conditions do not favour chromatic mechanisms and many subjects with normal colour vision also fail, on various occasions subjects with mild congenital deficiency pass (Squire and Barbur, 2005). Other tests require the subject to differentiate spatially discrete stimuli on the basis of small colour differences or to arrange coloured samples according to hue changes. Farnsworth- Munsell 100 hue employs 85 samples and the smaller D15 uses 15 samples. Performance of the FM-100 hue may be affected by the subject's non -verbal IQ (Hurlbert and Leekam, 2011). In the Ishihara test the number of errors the subject makes is often taken as a measure of severity of loss, the total error scores correlate poorly to the subject's loss of chromatic sensitivity (Barbur et al., 2012)

An approach to isolate the use of colour signals as employed by the CAD tests has emerged from studies on camouflage which employ moving, colour-defined stimuli buried in dynamic luminance contract (LC) noise. The results show that when such stimuli are employed, the selective loss of colour signals makes the colour defined stimuli invisible for modulations along the corresponding colour confusion line, even for chromatic saturations limited only by the phosphors of the display (Rodriguez-Carmona, 2005). Exposing the retina to time-varying LC noise reveals the loss of chromatic sensitivity since the subjects cannot make use of luminance contrast signals to see the moving stimulus (Barbur, 2004). CAD testing also provides accurate assessment of the severity of both RG and YB loss. The latter can be used to compare and monitor the state of progress of the disease.

6.2: Chromatic sensitivity in age-related drusen categories:

Results of the study show an increased loss of chromatic sensitivity in drusen categories of reticular drusen and soft drusen when compared to normal healthy aging. The CAD thresholds were found to be largest for patients with reticular drusen.

In this section we have considered each entity in turn and discussed severity of ARM grading in relation to colour vision in the soft drusen group.

6.2.1 Reticular drusen:

Due to evolving imaging techniques and recent histological studies reticular drusen (RPD) have been identified as an additional phenotypic entity in AMD. In contrast to conventional drusen, RPD proved to be located internal to RPE. In a recent study (Pumariega et al., 2011) localisation of evolving RPD seems to be related to the presence and site of choroidal watershed zones, suggesting that choroidal hypoxia may play a role in RPD pathogenesis . In

addition decreased choridal thickness, choroidal volume and narrow sparse choroidal vessels have been reported in eyes with evolving RPD (Alten et al., 2013). All these observations maybe interpreted as either a cause or consequence of RPD and are presumed to be related to other factors (Mrejen and Spaide, 2014) . The major blood supply to the retina is from the choroid and the photoreceptors, as they are extremely metabolically active. The changes in the choroid in RPD may compromise the photoreceptors function, which in turn can affect colour vision. Choroidal hypoxia has been postulated in RPD. Barbur and Connolly (2011) showed a uniform loss of chromatic sensitivity for all colours in hypoxia under mesopic conditions.

Spaide (2013) recently presented data on the long term course of RPD with regression of lesions leading to outer retinal atrophy and loss of underlying choroidal thickness. A reduction of RPE function may lead to dysfunctional transport between RPE and Muller cells resulting in the accumulation of material in the outer retina. This material in turn impedes normal transport of outer segments towards RPE resulting in thinning of the outer retina and the overlying choroid. With attenuation of the photoreceptors metabolic activity, less oxygen is needed resulting in choroidal thinning. The term 'Outer Retinal Atrophy' has been suggested as a new entity in late stage AMD by Spaide (2013).

Marsiglia et al (2013) reported GA were areas previously affected by RPD, postulating that RPD represents an early manifestation of the process leading to GA. The fast progressing 'diffuse-trickling' GA subtype shows a striking higher incidence of RPD compared with GA subtypes additionally supporting this hypothesis (Fleckenstein, 2014). All studies consistently report a high degree of agreement, a preponderance of female sex and occurrence of RPD in

all AMD phenotypes such as GA, CNV and drusen maculopathy. The highest prevalence of RPD is however linked to multilobular GA (Alten and Eter, 2015).

Spaide (2013) investigated the long term course of eyes with RPD and evaluated that the photoreceptor length reduced to 74.4% and choridal thickness reduced to 81.4% of its initial value. This underlines the dynamic nature of RPD over time.

Using Adaptive Optics (AO) Mrejen et al (2014) investigated the cone photoreceptor mosaic in eyes with RPD and compared the cone density in eyes with soft drusen, interestingly they reported a dramatic reduction in cone density over the RPD lesions possibly due to change in their orientation, alteration in their cellular architecture or even absence of cones themselves. This suggests that eyes with RPD may experience decreased retinal function without the presence of CNV or GA.

Multifocal ERG (mfERG) does not show definite interference of electrophysiological activity in retinal areas affected exclusively by RPD. Decline in mfERG function over a year in subjects with progressive RPD has also been reported (Alten et al., 2013), yet functional decline could not be correlated to an individual's morphological parameters such as RPD number or size. Querques (2014) and colleagues reported a greater extent of reduced sensitivity on microperimetry in eyes with RPD than eyes with soft drusen. Ooto et al (2013) and Forte et al (2014) confirmed results of reduced sensitivity on microperimetry despite preserved visual acuity. Microperimetry was carried out after dark adaptation and investigated both rod and cone activity. Hogg et al (2006) found a nearly reduced visual acuity and impaired spatial vision under conditions of reduced contrast and luminance in RPD eyes, supporting the hypothesis by Curcio and co-workers (2013) that RPD is mainly derived from rod physiology.

The chromatic sensitivity in our study showed that the eyes with reticular drusen had abnormal thresholds in comparison to the age matched normative data and in comparison to the soft drusen group with differences that were highly statistically significant.

We identified RPD on OCT scans and IR imaging. We did not grade RPDs according to severity as preliminary grading (depending on its location in the fundus) failed to show any correlation to severity, also there is no standardised grading systems for RPD based on its location in fundus. However, Figure 6.2 shows an example where chromatic sensitivity deteriorates with severity of RPD. We included RPD eyes with or without soft drusen in our RPD group for comparison to eyes with only soft drusen.

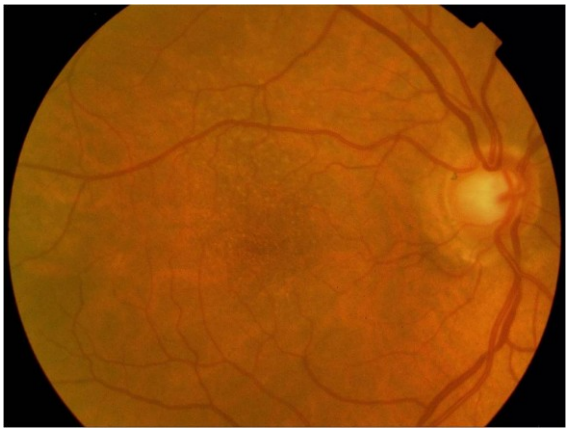

CAD thresholds: RG: 9.03
YB: 9.46
Moderate Chromatic loss

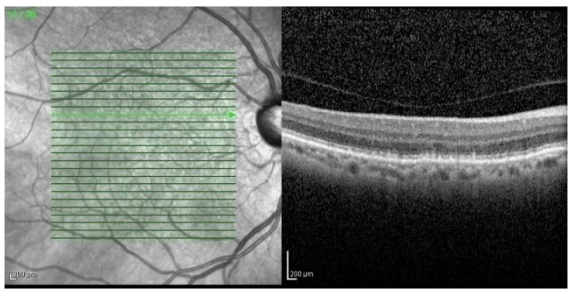

A)

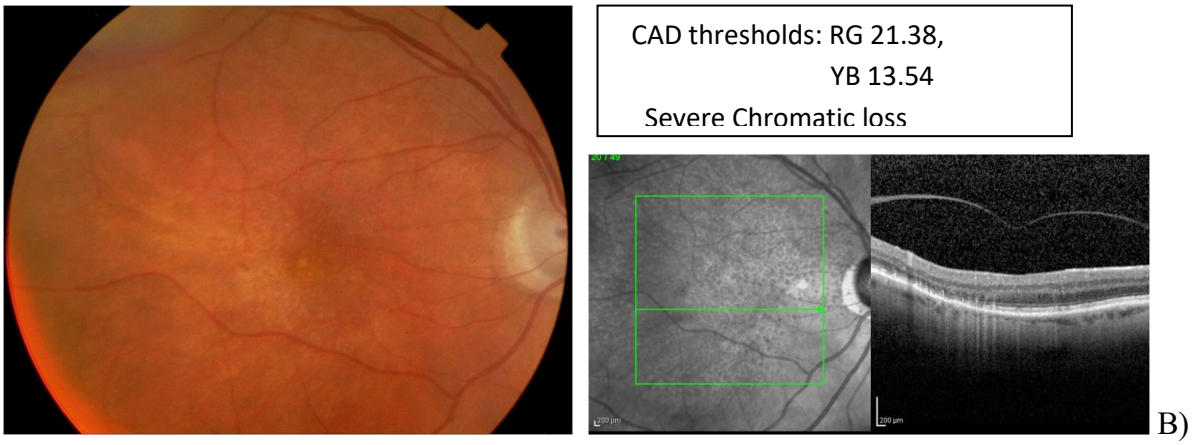

FIGURE 6.2: CAD Thresholds in Reticular drusen of different severity .Though we were unable to divide the eye according to severityof RD accurately and get any significant difference among different grades, these particular examples showed the CAD thresholds worsening with severity of RD. A) Subject with RD in superior fundus shows moderate chromatic sensitivity loss, B) Subject with RD in the inferior fundus shows severe to very severe chromatic sensitivity loss.

6.2.2 Soft Drusen:

The Age-Related Eye Disease Study (AREDS) is a multicentre prospective cohort study of the clinical course, prognosis and risk factors of AMD and cataract. Between 1992 and 1998, 11 retina clinics enrolled 4757 people aged 55 to 80 years in AREDS. In AREDS report 17 (Davis et al., 2005) they developed a severity scale for AMD based on fundus photographs which were graded for drusen characteristics (size, type and area) pigment abnormalities and neovascular AMD. Large drusen size, extensive drusen area, soft indistinct drusen and pigmentary abnormalities have all been recognised as risk factors for progression to advanced AMD both in people with bilateral AMD and people with one eye advanced AMD. AREDS grading was used to identify baseline risk categories, to track disease progression and perhaps as a surrogate outcome measure, mainly for research purposes. They developed a simplified severity scale to predict a 5 year risk of advanced AMD for clinical use. AREDS report 18 (Ferris et al., 2005) reported that the two features of AMD which are highly associated with

the development of advanced AMD are maximum drusen size and presence or absence of pigmentary abnormalities in one or both eyes. They recommended using these two features to predict the risk of advanced AMD in the clinical setting.

We adopted the International classification and grading system for ARM and AMD (Bird et al., 1995). This system includes drusen morphology, number, size, the extent of area covered by the drusen and main location of the drusen in the ETDRS grid. The grading produced enabled us to look for many characteristics of drusen which might affect chromatic sensitivity.

The CAD thresholds increased with the increase in drusen size in the ETDRS grid at the macula, the P value was highly statistically significant for RG ($p<0.0003$) and significant for YB ($p<0.02$). This was in accordance to the findings in the AREDS study. The other risk factor (pigmentary changes) found to be significant in AREDS has been assessed by our study in the clinical classification section. Subjects with pigmentary changes with or without drusen were grouped under intermediate/higher intermediate groups as this group had larger CAD thresholds than the early AMD groups, suggesting that pigmentation might be a significant risk factor for affecting loss of chromatic sensitivity.

The p value was highly significant ($p=0.02$) only for the RG thresholds of drusen morphology showing a good correlation of increase in RG CAD thresholds with increase in severity of drusen morphology grading.

Drusen characteristics of morphology (Figure 5.8), number (Figure 5.9) and area covered (Figure 5.11) showed an increase in mean CAD thresholds for increase in the severity grade for each category. R square of the mean CAD thresholds showed a significant linear trend

(0.9) with increase in severity grade for all the drusen characteristics (morphology, number and area covered), however the *p* was not significant because of the large variability in individual CAD thresholds. The significant linear trend of means showed that even with wide variation, the CAD values of the majority of the eyes increased with the severity of drusen grading of morphology, size, number and area covered.

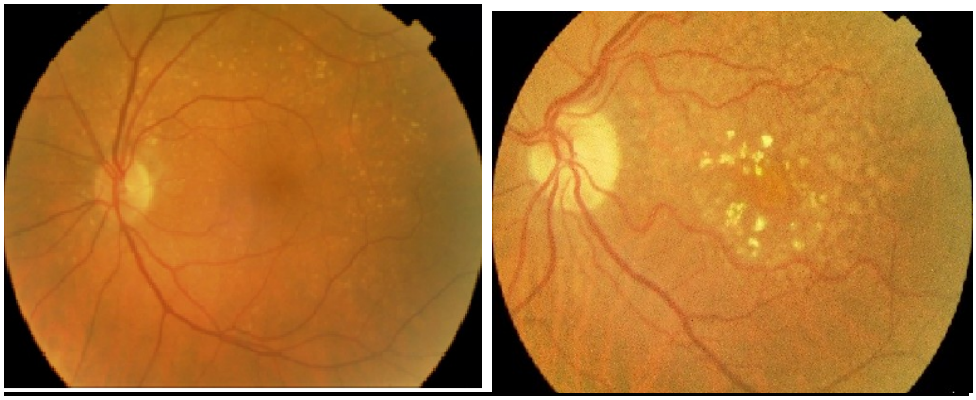

6.3a) RG 8.17
YB 6.76
Moderate chromatic loss

6.3b) RG 31.9
YB 18.0
Very Severe chromatic loss

Fig 6.3a) Mid peripheral drusen not involving centre; 6.3 b) Extensive soft/glistening drusen

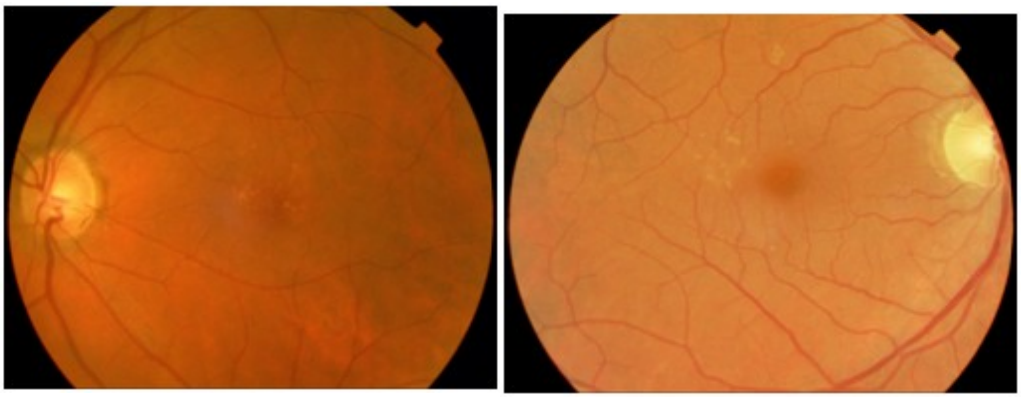

6.3c) RG 6.43
YB 8.71
Moderate chromatic loss

6.3d) RG 3.89
YB 4.91
Mild chromatic loss

6.3c) Drusen involving only the centre

6.3 d) Drusen involving only middle subfield

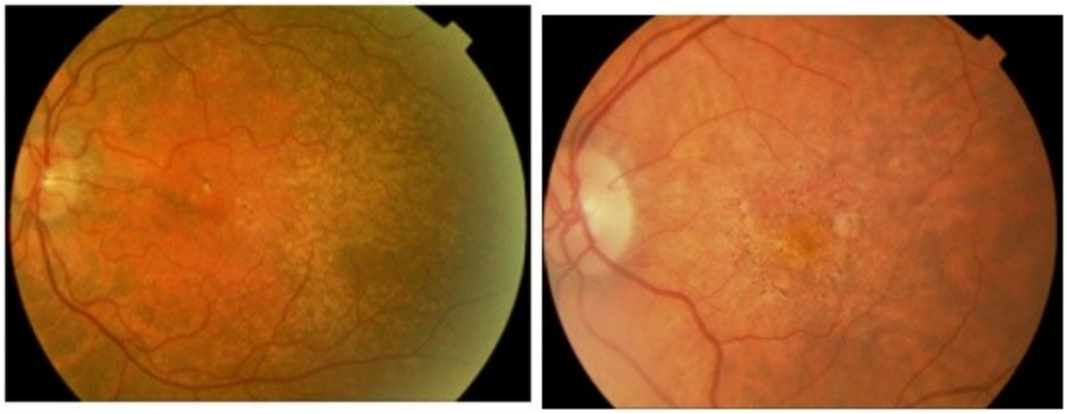

5.3e)

Drusen/pigment in mid periphery sparing fovea

6.3 f) Drusen/pigmentation involving Fovea

6.3e) RG 2.47 YB 3.14 Mild chromatic loss	6.3f) RG 14.82 YB 14.87 Severe chromatic loss

Figure 6.3: Examples of different location and grading of drusen and its effect on chromatic sensitivity. Variation of chromatic sensitivity is seen depending on the location of drusen, extend of drusen and the presence of pigmentation.

6.2.3 Normal Aging:

We had 2 eyes classified as normal aging as CAD thresholds were significantly smaller when compared to the CAD thresholds of eyes with Soft drusen and Reticular drusen. Study of disease showed that less than 50% of the AMD changes can be explained by aging (Bird, 2003). Various metabolic activities that might influence AMD are speed of outer segment renewal, RPE degrading activity, free radical, scavenging activity, RPE recycling ability, the efficiency of RPE cytoplasmic renewal, the speed of clearance of Bruch's membrane, and the response to age-change. The microenvironment in the retinal and the choroidal space in AMD might be undergoing changes which may not be visible on conventional imaging, whereas colour vision might be showing these early changes.

6.4 Drusen not related to AMD / Early onset Drusen (EOD):

The CAD thresholds of the eyes with EOD were significantly different than CAD thresholds of eyes with Soft drusen ($p=0.03$ RG and $p=0.01$YB) and Reticular drusen ($p<0.001$ for both RG and YB) showing that just the appearance of the drusen might not be the cause of chromatic loss, as the change of the microenvironment in AMD could be the cause of chromatic loss. This is an important finding since it confirms that the presence of drusen does not lead directly to loss of colour vision. The accumulations of drusen deposits in EOD may represent native lipoproteins in transit from RPE to choriocapillaries rather than accumulations /deposits as originally speculated (Curcio et al., 2013).

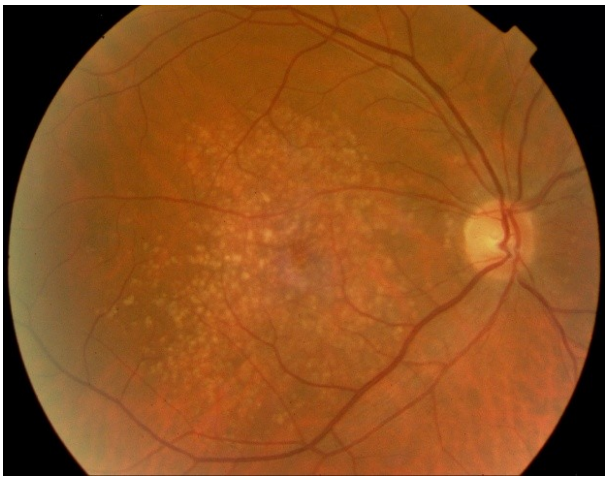

1) a

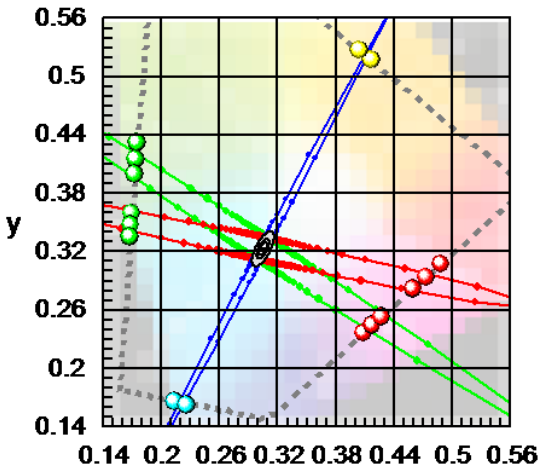

1)b

CAD thresholds: RG: 36.56
YB: 18.21
V. Severe Colour loss

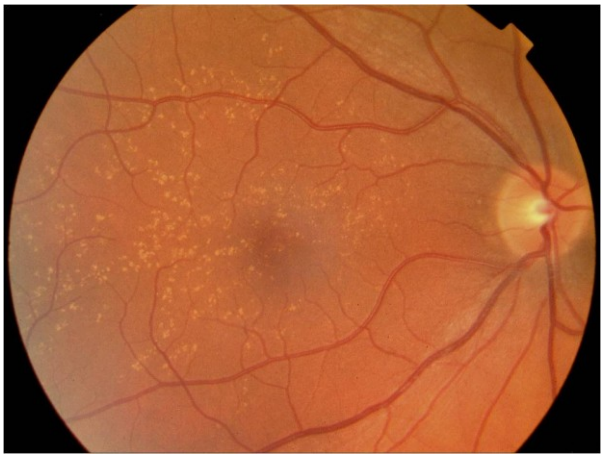

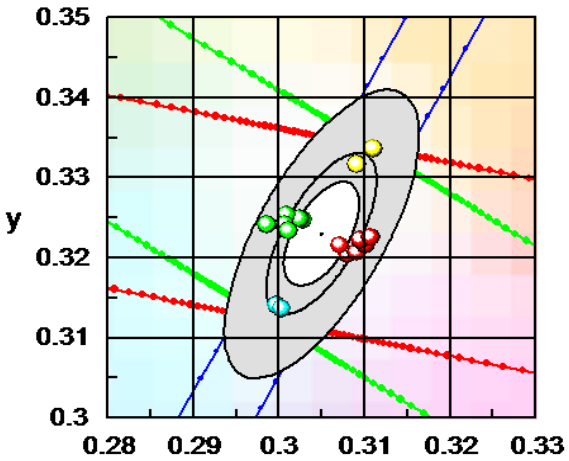

2)a

2)b

CAD thresholds: RG: 1.14
YB: 0.96
Normal colour vision

Figure 6.4: Comparison of chromatic sensitivity in AMD and EOD. Panel1 a) Fundus photograph of a subject with AMD showing extensive drusen b) CAD ellipsoidal graph showing severe colour loss. Panel 2 a) Fundus photograph showing EOD with extensive drusen b) CAD ellipsoidal graph showing normal colour vision.

6.5 Fundus Autofluorescence (FAF):

The underlying mechanisms of the pathophysiology of AMD are not completely understood as RPE is thought to play the key role in the disease process in both early and late forms of the disease. A hallmark of aging is the accumulation of lipofuscin (LF) granules in the cytoplasm. LF indicates by-products of the constant phagocytosis of shed photoreceptors outer segment disks (Weiter et al., 1986, Wing et al., 1978). Apparently once formed the LF granules are trapped. It has been suggested that the photo-oxidation of RPE lipofuscin could serve as a trigger for the complement system, predisposing the macula to pathological alterations, contributing to chronic inflammation over time.

Various alterations of normal FAF can be observed in patients with AMD. Areas of abnormal FAF are compared to the normal, homogenous background signal of the same image and are defined as either increased or decreased FAF. Assuming that LF encompasses the dominant flurophores of the fundus, variations in FAF signal intensities may derive from the actual alterations in density of LF granules in the RPE. Localised LF accumulations in RPE results in increased fluorescent properties and hence increases FAF signals from the site. In contrast, a decrease or absence of RPE LF will cause a decreased FAF signal. RPE atrophy typically appears as a dark patch in FAF images and can be clearly delineated. Decreased FAF intensities can also occur in association with hyperpigmented spots due to absorption by melanin or melanolipofuscin granules.

Sub-RPE deposits and Bruch's membrane exhibit strong autofluroscence at 488nm excitation in AMD eyes (Marmorstein et al., 2002), but the concomitant strong fluorescence of RPE LF appears to be roughly the same range or slightly less intense compared to the sub RPE deposits in AMD eyes. This could suggest it is difficult to resolve the issue between RPE LF and sub-RPE deposits using in vivo FAF, as opposed to post mortem cross-sectioning.

However reticular drusen are readily identified on FAF images and more easily detected than on fundoscopy or fundus photographs (Jorzik, 2000). These deposits show a unique FAF pattern of multiple small uniform areas of decreased FAF surrounded by normal FAF.

The in vivo FAF in AMD using cSLO has been described by several authors and has been reported that alterations of the FAF signals are not necessarily associated with corresponding fundoscopically or angiographically visible drusen or irregular pigmentations, which might indicate that FAF findings represent an independent measure of disease stage and activity.

Von Ruckmann and co-workers (1997) reported that eyes with early stage AMD may show focal areas of increased FAF in the neighbourhood of drusen, whereas FAF intensities over hard and soft drusen are within or below the range of the normal background signal in the eye itself as well as when compared with age-matched controls. Crystalline drusen are characterised by decreased FAF signals indicating the onset of atrophy (von Ruckmann et al., 1997) Focal areas of increased FAF next to drusen have been assigned to areas of pigment clumping adjacent to longstanding and mineralised drusen areas. Areas of confluent drusen were associated with focally, mildly increased FAF. Lois et al (2002) confirmed that of all drusen types, only the large foveal soft drusen (drusenoid PED detachments) topographically corresponds to focal changes of FAF.

Using image analysis software, which superimposed FAF images, and fundus photographs, Smith et al (2006) confirmed that large, soft drusen and hyperpigmentation with focal increased FAF maybe correlated topographically and the correlation was more in eyes with AMD (drusen /pigmentary abnormalities) than with GA.

The International FAF classification introduced 8 different FAF patterns in AMD. In a few patients, suffering from an early stage of AMD, a normal homogenous background FAF was noted even in the presence of soft or hard drusen. The presence was due to the masking effects of yellow macular pigments, if changes were limited to fovea or by image resolution and if the individual drusen deposits were < 63 μm. The study confirmed that drusen visible on fundus photography are not necessarily correlated with FAF changes. The observations suggested that FAF imaging on the RPE cell level may precede the occurrence of visible lesions as the disease progresses. A longitudinal analysis within the FAM study suggested

that the patchy pattern in early stage of AMD may represent a high risk marker for progression to exudative AMD.

Smith et al (2006) did not find FAF abnormalities in the fellow eyes of patients with unilateral CNV, however Spaide (2003) reported that patients with exudative AMD in one eye had FAF abnormalities in the other eye in comparison with patients with bilateral dry AMD.

Our study found the patchy pattern group to have the highest CAD thresholds (when compared with other FAF patterns). This is in agreement with the FAM study group suggesting that patchy FAF pattern is associated with high risk of AMD.

6.6 Central Macular thickness (CMT):

The Central Macular thickness (CMT) /Central subfield (CSF) macular thickness in normal eyes is 271.4 ± 19.6 (measured with Spectralis OCT) (Grover et al., 2010). CSF corresponds to the central 500 microns and to the central grid of the ETDRS grid. The thinning of CSF could indicate early GA and early loss of the photoreceptor function. Our study showed a good correlation with increasing CAD thresholds and thinning of CSF <200 microns.

The study selected patients with AMD and no signs of advanced disease. However 3 eyes had early GA on OCT as hyopigmentation on fundus were seen as signs of early GA. These 3 eyes showed a very severe loss of colour vision.

Example: CAD thresholds of a patient with GA

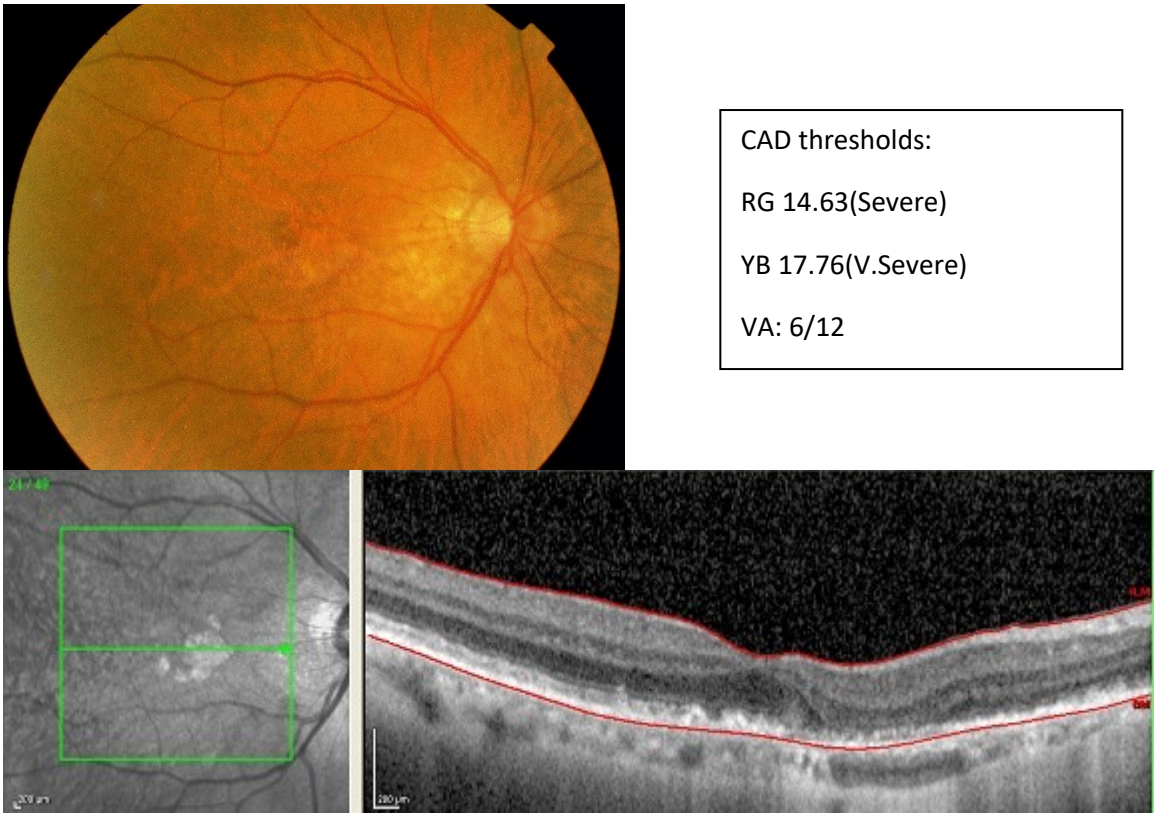

Figure 6.5: Subject with early GA: A *study subject showing hypopigmented change with thinning on OCT suggesting early GA. Severe to very severe loss of chromatic sensitivity was found.*

GA can cause significant compromise of visual functions when there is still good visual acuity (VA), because of parafoveal scotomas and foveal function abnormalities preceding visible atrophy. In a study by Sunness et al (1997) worsening of VA in decreased luminance and foveal dark adapted sensitivity showed severe abnormalities for the GA group. Contrast sensitivity was significantly reduced for the eyes with GA. Half the eyes with GA had maximum reading rates below 100 words per minute, which was very unlike the eyes with drusen. They concluded that the eyes with GA, even with normal VA, had a profound decrease in visual function, particularly when reading in dim lighting. We found in our study that chromatic sensitivity was affected in all the 3 eyes with GA.

6.7Clinical follow up of chromatic sensitivity changes in eyes converted to wet AMD:

Clinical follow up did not show a significant correlation of the CAD thresholds to the risk of converting to wet AMD. This suggests that chromatic sensitivity loss may be determined by other factors as it preceded the onset of wet AMD. Measuring colour threshold changes may not therefore be indicative of conversion to wet AMD especially in subjects who already experience a large loss of chromatic sensitivity. It remains to be established whether monitoring progression of colour vision loss is of advantage in predicting the conversion to wet AMD in subjects with less severe loss of chromatic sensitivity. Since other aspects of visual performance such as functional contrast sensitivity, dark adaptation and rapid flicker are also affected in AMD; the possibility remains that the combination of chromatic sensitivity with other tests may be more informative to predict the likelihood of conversion to wet AMD. Chromatic sensitivity as indicated by CAD thresholds remains, however, a very sensitive way of identifying early changes of GA as these affects directly cone photoreceptor functions.

6.8 Limitations of the study:

The study was limited in the number of eyes in early AMD and late AMD group while the majority of eyes belonged to intermediate AMD which meant useful comparisons between severity groups of AMD could not be made. The CAD test was performed as a one-off test and longitudinal analysis which could be predictive for wet AMD could not be achieved. Future studies recruiting subjects in all the severity groups of AMD can study the chromatic sensitivity in AMD with disease progression and may as well help to identify if disease

progression has correlation to the structural changes in AMD. Longitudinal follow up of AMD subjects with CAD tests can help identify if chromatic sensitivity can be a biomarker for advanced AMD.

7. Conclusions:

Patients with AMD can exhibit large losses of both RG and YB chromatic sensitivity. In some cases, such losses precede obvious clinical signs and may represent the earliest detectable functional changes. Patients with reticular pseudodrusen exhibited the greatest loss of chromatic sensitivity. Such losses may turn out to be sensitive and important indicators of early macular atrophy. In addition to loss of rod function which has been demonstrated in early phases of AMD, this study also reveals the significant loss of sensitivity to chromatic stimuli which indirectly implicates the normal functioning of cones and the subsequent processing of cone signals within the retina, particularly in patients with reticular pseudodrusen.

This study shows the loss of chromatic sensitivity in patients of age related macular degeneration (AMD) with clinically normal vision. This study addresses the need to recognise this functional loss in the elderly group who otherwise seem to have normal high contrast Snellen's acuity when measured in clinical settings. Health professionals need to be aware of the potential colour loss in these subjects and the impact it can have on the day to day life of these patients.

Curcio et al (2013) noted that the cone mosaic and the total number of cones at the fovea in AMD are similar to the age matched normals in contrast rods, as the macula decreases by 30% and the losses occur at the parafovea (3^o -10^o of fixation). Large, spatially distorted cones and very few rods remain at the parafoveal region. The mean scotopic loss is speculated to be in higher magnitude than the mean photopic sensitivity loss in AMD patients.

Patients with early stage AMD experience difficulty in changing light illumination which may be attributable to altered adaptation mechanisms in photoreceptor cells such as DA and glare recovery in early AMD, while difficulty in night driving may be related to reduced scotopic sensitivity due to dysfunction in the rod photoreceptors (Neelam et al., 2009)

Furthermore, various cone mediated visual functions such as colour vision, rapid flicker sensitivity and S-cone function can be seen in early AMD suggesting cone photoreceptor dysfunctions in combination with rod dysfunction in spite of unaltered foveal cone numbers in histopathological studies.

In this study, the YB thresholds are affected earlier than RG thresholds which are in agreement with findings from earlier studies (Verriest,1963). In general, RG thresholds are also outside the normal range and can vary from almost normal to complete absence of RG colour vision. The S cones mediating YB discrimination are more vulnerable to damage in AMD due to their territorial nature and limited response resulting in larger disease related changes, their susceptibility to alterations in metabolic environment of the RPE-photoreceptor complex than the other cone systems and relatively lower levels of MP at the parafovea where the S cones are in high density.

YB colour vision is mediated through S cone signals which are at a much-reduced density than the L and M cones that mediate RG colour vision. Normal YB thresholds are much larger in terms of cone contrast signals than RG thresholds. When expressed in SN CAD units the median thresholds correspond to one unit for both RG and YB discrimination. This accounts for the early saturation or smaller thresholds of the YB on the CAD test.

The risk factors assessed in AREDS's study for advanced AMD were drusen size and pigmentary changes; we also found both of these parameters to be associated with the deterioration of chromatic sensitivity. The increased drusen size correlates well with significant increase in both RG and YB thresholds. This observation may be taken to imply that colour vision might be affected in high risk eyes.

The other characteristics of drusen grading such as the drusen morphology, number, area involved, and location of the drusen did not show significant correlations to the severity of grading. The mean values that describe drusen morphology and numbers showed a linear trend suggesting that the majority of eyes had a tendency to have increased colour loss with increase in severity of the grading.

Eyes with reticular drusen (RPD) showed much higher loss of chromatic sensitivity than normal aging and soft drusen. This can be attributed to the histological changes in photoreceptors like OS shortening, inner segment deflection / absence and encroachment of SDD over photoreceptors as noted by Curcio et al (2013).

Some of the eyes examined failed to show noticeable/significant changes in fundus imaging, but showed wide variation in colour thresholds ranging from almost normal to complete absence of colour vision. This remains an intriguing observation suggesting that structures other than those present in conventional imaging such as selective loss of ganglion cells may cause the loss of colour vision.

The eyes which showed changes in fundus photographs, OCT scans and on FAF were examined as a separate group. The parameters describing the amount and size of drusen, the presence of reticular drusen, geographic atrophy, reduced CMT and type of FAF showed

some correlation with the severity of colour vision loss, but the results were not always predictable due to multiple less understood factors.

In general, the loss of chromatic sensitivity correlates with the severity of the ARM / AMD grading. The latter can be attributed to the histopathological changes occurring in aging and ARM such as decreased choroidal blood flow, increase in the oxidative stress, incomplete degradation of cells and the material accumulating between the RPE and Bruch's membrane in older adults and in ARM patients. Together, these processes are hypothesized to slow the transfer of fluids and essential nutrients across Bruch's membrane.

As standard VA is a poor indicator of the changes happening in the microenvironment of ARM, sensitive tests designed to assess specific aspects of visual processing like chromatic sensitivity or / and rapid flicker can be used to describe more accurately the extent of vision loss and to provide a clearer picture of the disease process and its overall effect on visual performance.

References:

ABADI, R. V. & PANTAZIDOU, M. 1996. Low contrast letter acuity in age-related maculopathy. *Ophthalmic Physiol Opt,* 16**,** 455-9.

AHNELT, P. K., KOLB, H. & PFLUG, R. 1987. Identification of a subtype of cone photoreceptor, likely to be blue sensitive, in the human retina. *J Comp Neurol,* 255**,** 18-34.

AHMAD, A. & SPEAR, P. D. 1993. Effects of aging on the size, density, and number of rhesus monkey lateral geniculate neurons. *J Comp Neurol,* 334**,** 631-43.

ALM, A. 1992. Ocular CIrculation. . *In: Hart, WM., editor. Adler's Physiology of the Eye..* Mosby-Year BookInc. St. Louis, MO: 1992.

ALM, A. & BILL, A. 1972. The oxygen supply to the retina. II. Effects of high intraocular pressure and of increased arterial carbon dioxide tension on uveal and retinal blood flow in cats. A study with radioactively labelled microspheres including flow determinations in brain and some other tissues. *Acta Physiol Scand,* 84**,** 306-19.

ALM, A. & BILL, A. 1973. Ocular and optic nerve blood flow at normal and increased intraocular pressures in monkeys (Macaca irus): a study with radioactively labelled microspheres including flow determinations in brain and some other tissues. *Exp Eye Res,* 15**,** 15-29.

ALPERN, M., MAASEIDVAAG, F. & OBA, N. 1971. The kinetics of cone visual pigments in man. *Vision Res,* 11**,** 539-49.

ALTEN, F., CLEMENS, C. R., HEIDUSCHKA, P. & ETER, N. 2013. Localized reticular pseudodrusen and their topographic relation to choroidal watershed zones and changes in choroidal volumes. *Invest Ophthalmol Vis Sci,* 54**,** 3250-7.

ALTEN, F. & ETER, N. 2015. Current knowledge on reticular pseudodrusen in age-related macular degeneration. *Br J Ophthalmol,* 99**,** 717-22.

ANDRADE, L. C., SOUZA, G. S., LACERDA, E. M., NAZIMA, M. T., RODRIGUES, A. R., OTERO, L. M., PENA, F. P., SILVEIRA, L. C. & CORTES, M. I. 2014. Influence of retinopathy on the achromatic and chromatic vision of patients with type 2 diabetes. *BMC Ophthalmol,* 14**,** 104.

ARDEN, G. B., SIDMAN, R. L., ARAP, W. & SCHLINGEMANN, R. O. 2005. Spare the rod and spoil the eye. *Br J Ophthalmol,* 89**,** 764-9.

ARDEN, G. B. & WOLF, J. E. 2004. Colour vision testing as an aid to diagnosis and management of age related maculopathy. *Br J Ophthalmol,* 88**,** 1180-5.

ARNOLD, J. J., SARKS, S. H., KILLINGSWORTH, M. C. & SARKS, J. P. 1995. Reticular pseudodrusen. A risk factor in age-related maculopathy. *Retina,* 15**,** 183-91.

ARNOLD, J. J., SARKS, J. P., KILLINGSWORTH, M. C., KETTLE, E. K. & SARKS, S. H. 2003. Adult vitelliform macular degeneration: a clinicopathological study. *Eye (Lond),* 17**,** 717-26.

AMOAKU, W.M., 2008. The Royal College of Ophthalmologists interim recommendations for the management of patients with age-related macular degeneration. *Eye (Lond),* 22**,** 864-868.

BARBUR, J. L. 2004. 'Double-blindsight' revealed through the processing of color and luminance contrast defined motion signals. *Prog Brain Res,* 144**,** 243-59.

APPLEGATE, R. A., ADAMS, A. J., CAVENDER, J. C. & ZISMAN, F. 1987. Early color vision changes in age-related maculopathy. *Appl Opt,* 26**,** 1458-62.

ATCHISON, D. A., LOVIE-KITCHIN, J. E. & SWANN, P. G. 1990. Investigation of central visual fields in patients with age-related macular changes. *Optom Vis Sci,* 67**,** 179-83.

BARBUR, J. L., RODRIGUEZ-CARMONA, M., AND HARLOW,A.J., 2006. “Establishing the statistical limits of “normal” chromatic sensitivity,”. *Commission Internationale de l’Eclairage,2006.* CIE x030:2006

REFERENCES

BARBUR, J. L., AND RODRIGUEZ-CARMONA, M. (2012)., VISION:, V. I. N. A. D. C., IN, C. F. O. E., J. BEST (ED.), C. D. P. & WOODHEAD., C. 2012. Variability in normal and defective colour vision: consequences for occupational environments. *In:* BEST, J. (ed.) *Colour Design* Cambridge: Woodhead.

BARBUR, J. L., RODRIGUEZ-CARMONA,M., 2015. *Colour vision changes in normal aging;* Cambridge university press.

BARBUR, J. L., RODRIGUEZ-CARMONA, M., HARLOW, J.A., MANCUSO, K., NEITZ, J., & NEITZ, M. 2008. A study of unusual Rayleigh matches in deutan deficiency. *Vis.Neurosci., 25, (3) 507-516*.

BARBUR, J. L., CONNOLLY, D.M. 2011. Effects of hypoxia on color vision with emphasis on the mesopic range. *Expert Rev. Ophthalmol.,* 6(4).

BARBUR, J. L., RODRIGUEZ-CARMONA, M., HICKEY, J., EVANS, S. CHORLEY,A 2016. Analysis of European colour vision certification requirements for air traffic control officers CAP 1429.

BELCHER, S. J., GREENSHIELDS, K. W. & WRIGHT, W. D. 1958. Colour vision survey using the Ishihara, Dvorine, Bostrom and Kugelberg, Bostrom, and American-Optical Hardy-Rand-Rittler tests. *Br J Ophthalmol,* 42**,** 355-9.

BEN-SHABAT, S., PARISH, C. A., HASHIMOTO, M., LIU, J., NAKANISHI, K. & SPARROW, J. R. 2001. Fluorescent pigments of the retinal pigment epithelium and age-related macular degeneration. *Bioorg Med Chem Lett,* 11**,** 1533-40.

BILL, A. 1962. Intraocular pressure and blood flow through the uvea. *Arch Ophthalmol,* 67**,** 336-48.

BIRCH, J. 2008. Performance of colour-deficient people on the Holmes–Wright lantern (type A):consistency of occupational colour vision standards in aviation. *Ophthalmic and Physiological Optics,,* 28**,** 253-8.

BIRD, A. C. 2003. The Bowman lecture. Towards an understanding of age-related macular disease. *Eye (Lond),* 17**,** 457-66.

BIRD, A. C. 2010. Therapeutic targets in age-related macular disease. *J Clin Invest,* 120**,** 3033-41.

BIRD, A. C., BRESSLER, N. M., BRESSLER, S. B., CHISHOLM, I. H., COSCAS, G., DAVIS, M. D., DE JONG, P. T., KLAVER, C. C., KLEIN, B. E., KLEIN, R. & ET AL. 1995. An international classification and grading system for age-related maculopathy and age-related macular degeneration. The International ARM Epidemiological Study Group. *Surv Ophthalmol,* 39**,** 367-74.

BIRD, A. C. & MARSHALL, J. 1986. Retinal pigment epithelial detachments in the elderly. *Trans Ophthalmol Soc U K,* 105 (Pt 6)**,** 674-82.

BLAIR, C. J. 1975. Geographic atrophy of the retinal pigment epithelium. A manifestation of senile macular degeneration. *Arch Ophthalmol,* 93**,** 19-25.

BODDU, S., LEE, M. D., MARSIGLIA, M., MARMOR, M., FREUND, K. B. & SMITH, R. T. 2014. Risk factors associated with reticular pseudodrusen versus large soft drusen. *Am J Ophthalmol,* 157**,** 985-993 e2.

BOOIJ, J. C., BAAS, D. C., BEISEKEEVA, J., GORGELS, T. G. & BERGEN, A. A. 2010. The dynamic nature of Bruch's membrane. *Prog Retin Eye Res,* 29**,** 1-18.

BOULTON, M. & DAYHAW-BARKER, P. 2001. The role of the retinal pigment epithelium: topographical variation and ageing changes. *Eye (Lond),* 15**,** 384-9.

BOULTON M. 1991. Ageing of the retinal pigment epithelium*, Progress in Retinal research,* New York: Pergamon,125-151.

BOWMAN, K. J. 1978. The effect of illuminance on colour discrimination in senile macular degeneration. *Mod Probl Ophthalmol,* 19**,** 71-6.

BOYCOTT, B. B. & WASSLE, H. 1991. Morphological Classification of Bipolar Cells of the Primate Retina. *Eur J Neurosci,* 3**,** 1069-1088.

BRESSLER, N. M., SILVA, J. C., BRESSLER, S. B., FINE, S. L. & GREEN, W. R. 1994. Clinicopathologic correlation of drusen and retinal pigment epithelial abnormalities in age-related macular degeneration. *Retina,* 14**,** 130-42.

BRESSLER, S. B., MAGUIRE, M. G., BRESSLER, N. M. & FINE, S. L. 1990. Relationship of drusen and abnormalities of the retinal pigment epithelium to the prognosis of neovascular macular degeneration. The Macular Photocoagulation Study Group. *Arch Ophthalmol,* 108**,** 1442-7.

BRETON ME, D. B. 1989. The Glaucomas. *In:* RITCH R, S. M., KRUPIN T, (ed.). St.Louis: CV Mosby Co.

BROWN, B. & GARNER, L. F. 1983. Effects of luminance on contrast sensitivity in senile macular degeneration. *Am J Optom Physiol Opt,* 60**,** 788-93.

BROWN, B. & LOVIE-KITCHIN, J. E. 1989. Temporal summation in age-related maculopathy. *Optom Vis Sci,* 66**,** 426-9.

CARROLL, J., NEITZ, J., & NEITZ, M. 2002. Estimates of L:M cone ratio from ERG flicker photometry and genetics. *J.Vis* 8**,** 531-542.

CHAKRAVARTHY, U., WONG, T. Y., FLETCHER, A., PIAULT, E., EVANS, C., ZLATEVA, G., BUGGAGE, R., PLEIL, A. & MITCHELL, P. 2010. Clinical risk factors for age-related macular degeneration: a systematic review and meta-analysis. *BMC Ophthalmol,* 10**,** 31.

CHEN, J. S. & ADELMAN, R. A. 2016. Hyperacuity Exam Screens for Choroidal Neovascularization in Age-Related Macular Degeneration on a Mobile Device. *Ophthalmic Surg Lasers Imaging Retina,* 47**,** 708-15.

CHENG, A. S. & VINGRYS, A. J. 1993. Visual losses in early age-related maculopathy. *Optom Vis Sci,* 70**,** 89-96.

COHEN, S. Y., DUBOIS, L., TADAYONI, R., DELAHAYE-MAZZA, C., DEBIBIE, C. & QUENTEL, G. 2007. Prevalence of reticular pseudodrusen in age-related macular degeneration with newly diagnosed choroidal neovascularisation. *Br J Ophthalmol,* 91**,** 354-9.

COHEN, S. Y., MEUNIER, I., SOUBRANE, G., GLACET-BERNARD, A. & COSCAS, G. J. 1994. Visual function and course of basal laminar drusen combined with vitelliform macular detachment. *Br J Ophthalmol,* 78**,** 437-40.

COLLINS, M., BROWN, B., 1989. Glare recovery and its relation to other clinicalfindings in age-related maculopathy. *Clin Vision Sci,* 4**,** 155-163.

COUSINS, S. W., ESPINOSA-HEIDMANN, D. G. & CSAKY, K. G. 2004. Monocyte activation in patients with age-related macular degeneration: a biomarker of risk for choroidal neovascularization? *Arch Ophthalmol,* 122**,** 1013-8.

CRISH SD, S. R., INMAN DM, HORNER PJ, CALKINS DJ. 2010. Distal axonopathy with structural persistence in glaucomatous neurodegeneration. *Proc Natl Acad Sci U SA.* 107:5196–5201.

CROSSLAND, M. & RUBIN, G. 2007. The Amsler chart: absence of evidence is not evidence of absence. *Br J Ophthalmol,* 91**,** 391-3.

CURCIO, C. A. & ALLEN, K. A. 1990. Topography of ganglion cells in human retina. *J Comp Neurol,* 300**,** 5-25.

CURCIO, C. A., JOHNSON, M., RUDOLF, M. & HUANG, J. D. 2011. The oil spill in ageing Bruch membrane. *Br J Ophthalmol,* 95**,** 1638-45.

CURCIO, C. A., JOHNSON, M. 2012. Structure, function, and pathology of Bruch's membrane. *In:* S.J. RYAN, A. P. S., C.P. WILKINSON, D.R. HINTON, S. SADDA, P. WIEDEMANN. (ed.) *Retina.* London, Elsevier

CURCIO, C. A., MILLICAN, C. L., ALLEN, K. A. & KALINA, R. E. 1993. Aging of the human photoreceptor mosaic: evidence for selective vulnerability of rods in central retina. *Invest Ophthalmol Vis Sci,* 34**,** 3278-96.

CURCIO, C. A., MEDEIROS, N. E. & MILLICAN, C. L. 1996. Photoreceptor loss in age-related macular degeneration. *Invest Ophthalmol Vis Sci,* 37**,** 1236-49.

CURCIO, C. A., OWSLEY, C. & JACKSON, G. R. 2000. Spare the rods, save the cones in aging and age-related maculopathy. *Invest Ophthalmol Vis Sci,* 41**,** 2015-8.

CURCIO, C. A., PRESLEY, J. B., MALEK, G., MEDEIROS, N. E., AVERY, D. V. & KRUTH, H. S. 2005. Esterified and unesterified cholesterol in drusen and basal deposits of eyes with age-related maculopathy. *Exp Eye Res,* 81**,** 731-41.

CURCIO, C. A., SLOAN, K. R., JR., PACKER, O., HENDRICKSON, A. E. & KALINA, R. E. 1987. Distribution of cones in human and monkey retina: individual variability and radial asymmetry. *Science,* 236**,** 579-82.

DAVIS, M. D., GANGNON, R. E., LEE, L. Y., HUBBARD, L. D., KLEIN, B. E., KLEIN, R., FERRIS, F. L., BRESSLER, S. B. & MILTON, R. C. 2005. The Age-Related Eye Disease Study severity scale for age-related macular degeneration: AREDS Report No. 17. *Arch Ophthalmol,* 123**,** 1484-98.

DE JONG, P. T. 2006. Age-related macular degeneration. *N Engl J Med,* 355**,** 1474-85.

DE VALOIS, R. L., DE VALOIS, K.K., 1988. *Spatial Vision.,* New York,Oxford University Press.

DELORI, F. C., FLECKNER, M. R., GOGER, D. G., WEITER, J. J. & DOREY, C. K. 2000. Autofluorescence distribution associated with drusen in age-related macular degeneration. *Invest Ophthalmol Vis Sci,* 41**,** 496-504.

DIAZ F, V. A., GONZALEZ P, REQUENA V, RIUS F, PEREZ DEVARGAS I. 1999. Stereological age-related changes in neurons of the ratdorsal lateral geniculate nucleus. *Anat Rec***,** 255:396–400.

DOBELLE WH, M. W., MACNICHOL EF JR. 1969. Visual pigment density in single primate foveal cones. *Science.166(3912):*1508-10.

DOREY, C. K., STAURENGHI, G., DELORI, F.C., 1993. Lipofuscin in aged and AMD eyes. *In:* IN HOLYFIELD JG ET AL, E. (ed.) *Retinal Degeneration.* New York: Plenum Press.

DREXLER, W., MORGNER, U., KARTNER, F. X., PITRIS, C., BOPPART, S. A., LI, X. D., IPPEN, E. P. & FUJIMOTO, J. G. 1999. In vivo ultrahigh-resolution optical coherence tomography. *Opt Lett,* 24**,** 1221-3.

DUKE-ELDER, S., COOK, C. 1963. Normal and abnormal development. *Part 1. Embryology. InDuke-Elder, S. (ed.) System of Ophthalmology, .* Henry Kimpton,LondonEINBOCK, W., MOESSNER, A., SCHNURRBUSCH, U. E., HOLZ, F. G. & WOLF, S. 2005. Changes in fundus autofluorescence in patients with age-related maculopathy. Correlation to visual function: a prospective study. *Graefes Arch Clin Exp Ophthalmol,* 243**,** 300-5.EISNER, A. 1994. Nonmonotonic effects of test illuminance on flicker detection: a study of foveal light adaptation with annular surrounds. *J Opt Soc Am A Opt Image Sci Vis,* 11**,** 33-47.

EISNER, A., KLEIN, M. L., ZILIS, J. D. & WATKINS, M. D. 1992. Visual function and the subsequent development of exudative age-related macular degeneration. *Invest Ophthalmol Vis Sci,* 33**,** 3091-102.

EISNER, A., STOUMBOS, V. D., KLEIN, M. L. & FLEMING, S. A. 1991. Relations between fundus appearance and function. Eyes whose fellow eye has exudative age-related macular degeneration. *Invest Ophthalmol Vis Sci,* 32**,** 8-20.

ELLIOTT, S. L., WERNER, J. S. & WEBSTER, M. A. 2012. Individual and age-related variation in chromatic contrast adaptation. *J Vis,* 12**,** 11

ENOCH JM, W. J., HAEGERSTROM-PORTNOY G, LAKSHMINARAYANANV, RYNDERS M. 1999. Forever young: visual functions not affected or minimally affected by aging: a review.*J Gerontol ABiol Sci Med Sci,* 54**,** B336–B351.

ERIKSSON, U., ALM, A. & LARSSON, E. 2012. Is quantitative spectral-domain superior to time-domain optical coherence tomography (OCT) in eyes with age-related macular degeneration? *Acta Ophthalmol,* 90**,** 620-7.

FAES, L., BODMER, N. S., BACHMANN, L. M., THIEL, M. A. & SCHMID, M. K. 2014. Diagnostic accuracy of the Amsler grid and the preferential hyperacuity perimetry in the screening of patients with age-related macular degeneration: systematic review and meta-analysis. *Eye (Lond),* 28**,** 788-96.

FEIGL, B., BROWN, B., LOVIE-KITCHIN, J. & SWANN, P. 2005. Monitoring retinal function in early age-related maculopathy: visual performance after 1 year. *Eye (Lond),* 19**,** 1169-77.

FERRIS, F. L., 3RD, FINE, S. L. & HYMAN, L. 1984. Age-related macular degeneration and blindness due to neovascular maculopathy. *Arch Ophthalmol,* 102**,** 1640-2.

FERRIS, F. L., 3RD, WILKINSON, C. P., BIRD, A., CHAKRAVARTHY, U., CHEW, E., CSAKY, K. & SADDA, S. R. 2013. Clinical classification of age-related macular degeneration. *Ophthalmology,* 120**,** 844-51.

FERRIS, F. L., DAVIS, M. D., CLEMONS, T. E., LEE, L. Y., CHEW, E. Y., LINDBLAD, A. S., MILTON, R. C., BRESSLER, S. B. & KLEIN, R. 2005. A simplified severity scale for age-related macular degeneration: AREDS Report No. 18. *Arch Ophthalmol,* 123**,** 1570-4.

FLAMENDORF, J., AGRON, E., WONG, W. T., THOMPSON, D., WILEY, H. E., DOSS, E. L., AL-HOLOU, S., FERRIS, F. L., 3RD, CHEW, E. Y. & CUKRAS, C. 2015. Impairments in Dark Adaptation Are Associated with Age-Related Macular Degeneration Severity and Reticular Pseudodrusen. *Ophthalmology,* 122**,** 2053-62.

FONG, D. S., BARTON, F. B. & BRESNICK, G. H. 1999. Impaired color vision associated with diabetic retinopathy: Early Treatment Diabetic Retinopathy Study Report No. 15. *Am J Ophthalmol,* 128**,** 612-7.

FORRESTER 2002. *The Eye: Basic Sciences in Practice©*, Elsevier.

FORTE, R., CENNAMO, G., DE CRECCHIO, G. & CENNAMO, G. 2014. Microperimetry of subretinal drusenoid deposits. *Ophthalmic Res,* 51**,** 32-6.

FRENNESSON, C., NILSSON, U. L. & NILSSON, S. E. 1995. Colour contrast sensitivity in patients with soft drusen, an early stage of ARM. *Doc Ophthalmol,* 90**,** 377-86.

FRIEDMAN, E. 2000. The role of the atherosclerotic process in the pathogenesis of age-related macular degeneration. *Am J Ophthalmol,* 130**,** 658-63.

GAO, H. & HOLLYFIELD, J. G. 1992. Aging of the human retina. Differential loss of neurons and retinal pigment epithelial cells. *Invest Ophthalmol Vis Sci,* 33**,** 1-17.

GASS 1967. Pathogenesis of disciform detachment of neuroepithelium III. Senile disciform macular degeneration. *Am J Ophthalmol,* 63**,** 617-644.

GASS, J. D., JALLOW, S. & DAVIS, B. 1985. Adult vitelliform macular detachment occurring in patients with basal laminar drusen. *Am J Ophthalmol,* 99**,** 445-59.

GREEN, S. N., YARIAN, D. 1983. Acute tear of the retinal pigment epithelium. *Retina.*

GROH, M. J., MICHELSON, G., LANGHANS, M. J. & HARAZNY, J. 1996. Influence of age on retinal and optic nerve head blood circulation. *Ophthalmology,* 103**,** 529-34.

GROSSNIKLAUS, H. E. & GREEN, W. R. 2004. Choroidal neovascularization. *Am J Ophthalmol,* 137**,** 496-503.

GROVER, S., MURTHY, R. K., BRAR, V. S. & CHALAM, K. V. 2010. Comparison of retinal thickness in normal eyes using Stratus and Spectralis optical coherence tomography. *Invest Ophthalmol Vis Sci,* 51**,** 2644-7.

GRUNWALD, J. E., HARIPRASAD, S. M., DUPONT, J., MAGUIRE, M. G., FINE, S. L., BRUCKER, A. J., MAGUIRE, A. M. & HO, A. C. 1998. Foveolar choroidal blood flow in age-related macular degeneration. *Invest Ophthalmol Vis Sci,* 39**,** 385-90.

GUIGUI, B., LEVEZIEL, N., MARTINET, V., MASSAMBA, N., STERKERS, M., COSCAS, G. & SOUIED, E. H. 2011. Angiography features of early onset drusen. *Br J Ophthalmol,* 95**,** 238-44.

GUPTA, B., JYOTHI, S. & SIVAPRASAD, S. 2010. Current treatment options for retinal angiomatous proliferans (RAP). *Br J Ophthalmol,* 94**,** 672-7.

HAEGERSTROM-PORTNOY, G. 1988. Short-wavelength-sensitive-cone sensitivity loss with aging: a protective role for macular pigment? *J Opt Soc Am A,* 5**,** 2140-4.

HAGEMAN, G. S., LUTHERT, P. J., VICTOR CHONG, N. H., JOHNSON, L. V., ANDERSON, D. H. MULLINS, R. F. 2001. An integrated hypothesis that considers drusen as biomarkers of immune-mediated processes at the RPE-Bruch's membrane interface in aging and age-related macular degeneration. *Prog Retin Eye Res,* 20**,** 705-32.

HAMMOND, B. R., JR. & WOOTEN, B. R. 2005. CFF thresholds: relation to macular pigment optical density. *Ophthalmic Physiol Opt,* 25**,** 315-9.

HAMMOND, B. R., JR., WOOTEN, B. R. & SNODDERLY, D. M. 1998. Preservation of visual sensitivity of older subjects: association with macular pigment density. *Invest Ophthalmol Vis Sci,* 39**,** 397-406.

HARWERTH, R. S., WHEAT, J. L. & RANGASWAMY, N. V. 2008. Age-related losses of retinal ganglion cells and axons. *Invest Ophthalmol Vis Sci,* 49**,** 4437-43.

HENDRICKSON, A. E. 1993. Morphological development of the primate retina. . *In:* SIMONS, K. E. (ed.) *Early Visual Development, Normal and Abnormal.* Oxford University, New York, Oxford (1993)

HERING, E. 1964. Outlines of a theory of the light sense (translated by Leo M Huvich and Dorothea Jameson),. Cambridge (MA): Harvard University Press.

HOGG, R., CURRY, E., MULDREW, A., WINDER, J., STEVENSON, M., MCCLURE, M. & CHAKRAVARTHY, U. 2003. Identification of lesion components that influence visual function in age related macular degeneration. *Br J Ophthalmol,* 87**,** 609-14.

HOGG, R. E. & CHAKRAVARTHY, U. 2006. Visual function and dysfunction in early and late age-related maculopathy. *Prog Retin Eye Res,* 25**,** 249-76.

HOLZ, F. G., GROSS-JENDROSKA, M., ECKSTEIN, A., HOGG, C. R., ARDEN, G. B. & BIRD, A. C. 1995. Colour contrast sensitivity in patients with age-related Bruch's membrane changes. *Ger J Ophthalmol,* 4**,** 336-41.

HOOD, D. C., BENIMOFF, N. I. & GREENSTEIN, V. C. 1984. The response range of the blue-cone pathways: a source of vulnerability to disease. *Invest Ophthalmol Vis Sci,* 25**,** 864-7.

HUANG, D., SWANSON, E. A., LIN, C. P., SCHUMAN, J. S., STINSON, W. G., CHANG, W., HEE, M. R., FLOTTE, T., GREGORY, K., PULIAFITO, C. A. & ET AL. 1991. Optical coherence tomography. *Science,* 254**,** 1178-81.

HUGHES, A. E., ORR, N., PATTERSON, C., ESFANDIARY, H., HOGG, R., MCCONNELL, V., SILVESTRI, G. & CHAKRAVARTHY, U. 2007. Neovascular age-related macular degeneration risk based on CFH, LOC387715/HTRA1, and smoking. *PLoS Med,* 4**,** e355.

HURLBERT, A., LOVERIDGE, C., LING, Y., KOURKOULOU, A., & LEEKAM, S. 2011. Color discrimination and preference in autism spectrum disorder. *Journal of Vision, ,* 11**,** 429.

HUSSAIN, A. A., STARITA, C., HODGETTS, A. & MARSHALL, J. 2010. Macromolecular diffusion characteristics of ageing human Bruch's membrane: implications for age-related macular degeneration (AMD). *Exp Eye Res,* 90**,** 703-10.

IBRAHIM, Y. W., BOTS, M. L., MULDER, P. G., GROBBEE, D. E., HOFMAN, A. & DE JONG, P. T. 1998. Number of perifoveal vessels in aging, hypertension, and atherosclerosis: the Rotterdam Study. *Invest Ophthalmol Vis Sci,* 39**,** 1049-53.

ISASHIKI, Y., TABATA, Y., KAMIMURA, K. & OHBA, N. 1999. Sorsby's fundus dystrophy in two Japanese families with unusual clinical features. *Jpn J Ophthalmol,* 43**,** 472-80.

JACKSON, G. R., OWSLEY, C. & CURCIO, C. A. 2002. Photoreceptor degeneration and dysfunction in aging and age-related maculopathy. *Ageing Res Rev,* 1**,** 381-96.

JOHNSON, C. A., ADAMS, A. J., TWELKER, J. D. & QUIGG, J. M. 1988. Age-related changes in the central visual field for short-wavelength-sensitive pathways. *J Opt Soc Am A,* 5**,** 2131-9.

JOHNSON, M., DABHOLKAR, A., HUANG, J. D., PRESLEY, J. B., CHIMENTO, M. F. & CURCIO, C. A. 2007. Comparison of morphology of human macular and peripheral Bruch's membrane in older eyes. *Curr Eye Res,* 32**,** 791-9.

JONAS, J. B., SCHMIDT, A. M., MULLER-BERGH, J. A., SCHLOTZER-SCHREHARDT, U. M. & NAUMANN, G. O. 1992. Human optic nerve fiber count and optic disc size. *Invest Ophthalmol Vis Sci,* 33**,** 2012-8.

JORZIK 2000. *ARVO.* Invest Ophthalmol.2000;43:B2517/B514 [ARVO-abstract]).

KALLONIATIS, M., LUU C. 2005 May 1 [Updated 2007 Jun 5]. *Temporal Resolution; Visual acuity,* [Online]. Webvision: The Organization of the Retina and Visual System. Available: https://www.ncbi.nlm.nih.gov/books/NBK11559/ [Accessed 1/07/2015]. KARLSSON, J. O., INOMATA, M. & KAWASHIMA, S. 1992. Slow axonal transport of soluble proteins and calpain in retinal ganglion cells of aged rabbits. *Neurosci Lett,* 141**,** 127-9.

KHANIFAR, A. A., KOREISHI, A. F., IZATT, J. A. & TOTH, C. A. 2008. Drusen ultrastructure imaging with spectral domain optical coherence tomography in age-related macular degeneration. *Ophthalmology,* 115**,** 1883-90.

KINCAID, M. C., GREEN, W.R 1991. Anatomy of the vitrous, retina and choroid. *In:* REGILLO, C. D., BROWN, G.C., FLYNN, H.W (ed.) *Vitreoretinal Disease.* Thieme, New York,Stuttgart (1999) Springer-Verlag; New York.

KIRYU, J., ASRANI, S., SHAHIDI, M., MORI, M. & ZEIMER, R. 1995. Local response of the primate retinal microcirculation to increased metabolic demand induced by flicker. *Invest Ophthalmol Vis Sci,* 36**,** 1240-6.

KLEIN, M. L., FERRIS, F. L., 3RD, ARMSTRONG, J., HWANG, T. S., CHEW, E. Y., BRESSLER, S. B. & CHANDRA, S. R. 2008a. Retinal precursors and the development of geographic atrophy in age-related macular degeneration. *Ophthalmology,* 115**,** 1026-31.

KLEIN, M. L., FERRIS, F. L., 3RD, ARMSTRONG, J., HWANG, T. S., CHEW, E. Y., BRESSLER, S. B. & CHANDRA, S. R. 2008b. Retinal precursors and the development of geographic atrophy in age-related macular degeneration. *Ophthalmology,* 115**,** 1026-31.

KLEIN, R., DAVIS, M. D., MAGLI, Y. L., SEGAL, P., KLEIN, B. E. & HUBBARD, L. 1991. The Wisconsin age-related maculopathy grading system. *Ophthalmology,* 98**,** 1128-34.

KLEIN, R., CRUICKSHANKS, K. J., NASH, S. D., KRANTZ, E. M., NIETO, F. J., HUANG, G. H., PANKOW, J. S. & KLEIN, B. E. 2010. The prevalence of age-related macular degeneration and associated risk factors. *Arch Ophthalmol,* 128**,** 750-8.

KLEIN, R., KLEIN, B. E., KNUDTSON, M. D., MEUER, S. M., SWIFT, M. & GANGNON, R. E. 2007. Fifteen-year cumulative incidence of age-related macular degeneration: the Beaver Dam Eye Study. *Ophthalmology,* 114**,** 253-62.

KLEIN, R., KLEIN, B. E. & LINTON, K. L. 1992. Prevalence of age-related maculopathy. The Beaver Dam Eye Study. *Ophthalmology,* 99**,** 933-43.

KLEIN, R., KLEIN, B. E., TOMANY, S. C., MEUER, S. M. & HUANG, G. H. 2002. Ten-year incidence and progression of age-related maculopathy: The Beaver Dam eye study. *Ophthalmology,* 109**,** 1767-79.

KLEIN, R., MEUER, S. M., KNUDTSON, M. D., IYENGAR, S. K. & KLEIN, B. E. 2008. The epidemiology of retinal reticular drusen. *Am J Ophthalmol,* 145**,** 317-326.

KLEINER, R. C., ENGER, C., ALEXANDER, M. F. & FINE, S. L. 1988. Contrast sensitivity in age-related macular degeneration. *Arch Ophthalmol,* 106**,** 55-7.

KOLAR, P. 2013. Age-related Maccular Degeneration - Etiology, Diagnosis and Management - A Glance at the Future,. *In:* GIUSEPPE LO GUIDICE (ed.). Intech,.

Kolb H. Photoreceptors. 2005 May 1 [Updated 2012 Feb 28]. In: Kolb H, Fernandez E, Nelson R, (ed). Webvision: *The Organization of the Retina and Visual System [Internet].* Salt Lake City (UT): University of Utah Health Sciences Center; 1995-. Available from: https://www.ncbi.nlm.nih.gov/books/NBK11522/

KOLB H, L. L. I. G. P. E. 1991. *The anatomical basis for colour vision in the vertebrate retina. Vision and Visual Dysfunction,*.

KONSTANTAKOPOULOU, E. 2012. *Fundamental studies and clinical significance.* PhD, City University.

KREBS, W. K., I. 1991. Primate Retina and Choroid: Atlas of Fine Structure in Man and Monkey.

REMINGTON, L. A. 2005. Clinical Anatomy of the Visual System. 2nd Ed. Elsevier; 2005.

LAATIKAINEN, L. & LARINKARI, J. 1977. Capillary-free area of the fovea with advancing age. *Invest Ophthalmol Vis Sci,* 16**,** 1154-7.

LAMB, T. D. & PUGH, E. N., JR. 2004. Dark adaptation and the retinoid cycle of vision. *Prog Retin Eye Res,* 23**,** 307-80.

LAUDE, A., CACKETT, P. D., VITHANA, E. N., YEO, I. Y., WONG, D., KOH, A. H., WONG, T. Y. & AUNG, T. 2010. Polypoidal choroidal vasculopathy and neovascular age-related macular degeneration: same or different disease? *Prog Retin Eye Res,* 29**,** 19-29.

LEYS, A., VANRENTERGHEM, Y., VAN DAMME, B., SNYERS, B., PIRSON, Y. & LEYS, M. 1991. Fundus changes in membranoproliferative glomerulonephritis type II. A fluorescein angiographic study of 23 patients. *Graefes Arch Clin Exp Ophthalmol,* 229**,** 406-10.

LIM, L. S., MITCHELL, P., SEDDON, J. M., HOLZ, F. G. & WONG, T. Y. 2012. Age-related macular degeneration. *Lancet,* 379**,** 1728-38.

LI, M., HE, H. G., SHI, W., LI, J., LV, B., WANG, C. H., MIAO, Q. W., WANG, Z. C., WANG, N. L., WALTER, M. & SABEL, B. A. 2012. Quantification of the human lateral geniculate nucleus in vivo using MR imaging based on morphometry: volume loss with age. *AJNR Am J Neuroradiol,* 33**,** 915-21.

LINSENMEIER, R. A. & BRAUN, R. D. 1992. Oxygen distribution and consumption in the cat retina during normoxia and hypoxemia. *J Gen Physiol,* 99**,** 177-97.

LINSENMEIER, R. A., GOLDSTICK, T. K., BLUM, R. S. & ENROTH-CUGELL, C. 1981. Estimation of retinal oxygen transients from measurements made in the vitreous humor. *Exp Eye Res,* 32**,** 369-79.

LOANE, E., NOLAN, J. M., O'DONOVAN, O., BHOSALE, P., BERNSTEIN, P. S. & BEATTY, S. 2008. Transport and retinal capture of lutein and zeaxanthin with reference to age-related macular degeneration. *Surv Ophthalmol,* 53**,** 68-81.

LOIS, N.,OWENS,S.L.,COCO,R.,HOPKINS, J., FITZKE, F. W. & BIRD, A. C. 2002. Fundus autofluorescence in patients with age-related macular degeneration and high risk of visual loss. *Am J Ophthalmol,* 133**,** 341-9.

LOVIE-KITCHIN, J. & FEIGL, B. 2005. Assessment of age-related maculopathy using subjective vision tests. *Clin Exp Optom,* 88**,** 292-303.

LYNN, J. R., FELLMAN, R.L., STARITA, R.J., 1980. *The Glaucomas: Basic Sciences.* .

MADDOX, D. A. & BRENNER, B. M. 1977. Glomerular filtration of fluid and macromolecules: the renal response to injury. *Annu Rev Med,* 28**,** 91-102.

MAGUIRE, P. & VINE, A. K. 1986. Geographic atrophy of the retinal pigment epithelium. *Am J Ophthalmol,* 102**,** 621-5.

MARMOR, M. F., ABDUL-RAHIM, A. S. & COHEN, D. S. 1980. The effect of metabolic inhibitors on retinal adhesion and subretinal fluid resorption. *Invest Ophthalmol Vis Sci,* 19**,** 893-903.

MARMORSTEIN, A. D., MARMORSTEIN, L. Y., SAKAGUCHI, H. & HOLLYFIELD, J. G. 2002. Spectral profiling of autofluorescence associated with lipofuscin, Bruch's Membrane, and sub-RPE deposits in normal and AMD eyes. *Invest Ophthalmol Vis Sci,* 43**,** 2435-41.

MARMORSTEIN, L. Y., MCLAUGHLIN, P. J., PEACHEY, N. S., SASAKI, T. & MARMORSTEIN, A. D. 2007. Formation and progression of sub-retinal pigment epithelium deposits in Efemp1 mutation knock-in mice: a model for the early pathogenic course of macular degeneration. *Hum Mol Genet,* 16**,** 2423-32.

MARSHALL J, H. A., STARITA C, ET AL., EDITORS. 1998. The retinal pigment epithelium:Function and disease.: New York: Oxford University Press;.

MARSIGLIA, M., BODDU, S., BEARELLY, S., XU, L., BREAUX, B. E., JR., FREUND, K. B., YANNUZZI, L. A. & SMITH, R. T. 2013. Association between geographic atrophy progression and reticular pseudodrusen in eyes with dry age-related macular degeneration. *Invest Ophthalmol Vis Sci,* 54**,** 7362-9.

MAYNARD, M. L., ZELE, A. J. & FEIGL, B. 2016. Mesopic Pelli-Robson contrast sensitivity and MP-1 microperimetry in healthy ageing and age-related macular degeneration. *Acta Ophthalmol,* 94**,** e772-e778.

MCLEOD, D. S., GREBE, R., BHUTTO, I., MERGES, C., BABA, T. & LUTTY, G. A. 2009. Relationship between RPE and choriocapillaris in age-related macular degeneration. *Invest Ophthalmol Vis Sci,* 50**,** 4982-91.

MICELI, M. V., LILES, M. R. & NEWSOME, D. A. 1994. Evaluation of oxidative processes in human pigment epithelial cells associated with retinal outer segment phagocytosis. *Exp Cell Res,* 214**,** 242-9.

MIDENA, E., DEGLI ANGELI, C., BLARZINO, M. C., VALENTI, M. & SEGATO, T. 1997. Macular function impairment in eyes with early age-related macular degeneration. *Invest Ophthalmol Vis Sci,* 38**,** 469-77.

MIDENA, E. & PILOTTO, E. 2017. Microperimetry in age: related macular degeneration. *Eye (Lond)*.

MIDENA, E., VUJOSEVIC, S., CONVENTO, E., MANFRE, A., CAVARZERAN, F. & PILOTTO, E. 2007. Microperimetry and fundus autofluorescence in patients with early age-related macular degeneration. *Br J Ophthalmol,* 91**,** 1499-503.

MILLER, J. W. 2013. Age-related macular degeneration revisited--piecing the puzzle: the LXIX Edward Jackson memorial lecture. *Am J Ophthalmol,* 155**,** 1-35.e13.

MIKELBERG, F. S., DRANCE, S. M., SCHULZER, M., YIDEGILIGNE, H. M. & WEIS, M. M. 1989. The normal human optic nerve. Axon count and axon diameter distribution. *Ophthalmology,* 96**,** 1325-8.

MIMOUN, G., SOUBRANE, G. & COSCAS, G. 1990. [Macular drusen]. *J Fr Ophtalmol,* 13**,** 511-30.

MONHART, M. 2007. What are the options of psychophysical approaches in glaucoma? *Surv Ophthalmol,* 52 Suppl 2**,** S127-33.

MOON, B. G., JOE, S. G., HWANG, J. U., KIM, H. K., CHOE, J. & YOON, Y. H. 2012. Prevalence and risk factors of early-stage age-related macular degeneration in patients examined at a health promotion center in Korea. *J Korean Med Sci,* 27**,** 537-41.

MOORE, D. J. & CLOVER, G. M. 2001. The effect of age on the macromolecular permeability of human Bruch's membrane. *Invest Ophthalmol Vis Sci,* 42**,** 2970-5.

MORA, B. N., CARMAN, G. J. & ALLMAN, J. M. 1989. In vivo functional localization of the human visual cortex using positron emission tomography and magnetic resonance imaging. *Trends Neurosci,* 12**,** 282-4.

MORRISON, J. C., CORK, L. C., DUNKELBERGER, G. R., BROWN, A. & QUIGLEY, H. A. 1990. Aging changes of the rhesus monkey optic nerve. *Invest Ophthalmol Vis Sci,* 31**,** 1623-7.

MREJEN, S., SATO, T., CURCIO, C. A. & SPAIDE, R. F. 2014. Assessing the cone photoreceptor mosaic in eyes with pseudodrusen and soft Drusen in vivo using adaptive optics imaging. *Ophthalmology,* 121**,** 545-51.

MREJEN, S. & SPAIDE, R. F. 2014. The relationship between pseudodrusen and choroidal thickness. *Retina,* 34**,** 1560-6.

MULLINS, R. F., RUSSELL, S. R., ANDERSON, D. H. & HAGEMAN, G. S. 2000. Drusen associated with aging and age-related macular degeneration contain proteins common to extracellular deposits associated with atherosclerosis, elastosis, amyloidosis, and dense deposit disease. *FASEB J,* 14**,** 835-46.

NASSIF, N., CENSE, B., PARK, B., PIERCE, M., YUN, S., BOUMA, B., TEARNEY, G., CHEN, T. & DE BOER, J. 2004. In vivo high-resolution video-rate spectral-domain optical coherence tomography of the human retina and optic nerve. *Opt Express,* 12**,** 367-76.

NATIONAL RESEARCH COUNCIL-NATIONAL ACADEMY OF SCIENCES 1981 Procedures for testing color vision. *Report of working group 41.* National Academy Press, Washington, DC.

NEELAM, K., NOLAN, J., CHAKRAVARTHY, U. & BEATTY, S. 2009. Psychophysical function in age-related maculopathy. *Surv Ophthalmol,* 54**,** 167-210.

NICKLA, D. L. & WALLMAN, J. 2010. The multifunctional choroid. *Prog Retin Eye Res,* 29**,** 144-68.

NIVEN, J. E. & LAUGHLIN, S. B. 2008. Energy limitation as a selective pressure on the evolution of sensory systems. *J Exp Biol,* 211**,** 1792-804.

NOBLE, J. & CHAUDHARY, V. 2010. Age-related macular degeneration. *Cmaj,* 182**,** 1759.

NORREN, D. V. & VOS, J. J. 1974. Spectral transmission of the human ocular media. *Vision Res,* 14**,** 1237-44.

O'NEILL-BIBA, M., SIVAPRASAD, S., RODRIGUEZ-CARMONA, M., WOLF, J. E. & BARBUR, J. L. 2010. Loss of chromatic sensitivity in AMD and diabetes: a comparative study. *Ophthalmic Physiol Opt,* 30**,** 705-16.

OLAF, S. R. 2005. The Retinal Pigment Epithelium in Visual Function. *Physiol Rev.* doi:10.1152/physrev.00021.2004.

OOTO, S., ELLABBAN, A. A., UEDA-ARAKAWA, N., OISHI, A., TAMURA, H., YAMASHIRO, K., TSUJIKAWA, A. & YOSHIMURA, N. 2013. Reduction of retinal sensitivity in eyes with reticular pseudodrusen. *Am J Ophthalmol,* 156**,** 1184-1191.e2.

OWSLEY, C. & SLOANE, M. E. 1987. Contrast sensitivity, acuity, and the perception of 'real-world' targets. *Br J Ophthalmol,* 71**,** 791-6.

OWSLEY, C. 2003. Contrast sensitivity. *Ophthalmol Clin North Am,* 16**,** 171-7.

OWSLEY C, S. M., SKALKAHW, ET AL. 1990. A comparison of the Regan Low-Contrast Letter Charts and contrast sensitivity testing in older patients. . *Clin Vision Sci. 1990;5:325--34,* 5**,** 325--34. OYSTER, C. E. 1999. Retinal III: regional variation and spatial organization (Chapter 15). . *The Human Eye – Structure and Function.* Sinauer Associates, Sunderland, Massachusetts

PAULEIKHOFF, D., BARONDES, M. J., MINASSIAN, D., CHISHOLM, I. H. & BIRD, A. C. 1990. Drusen as risk factors in age-related macular disease. *Am J Ophthalmol,* 109**,** 38-43. PENFOLD, P. L., MADIGAN, M. C., GILLIES, M. C. & PROVIS, J. M. 2001. Immunological and aetiological aspects of macular degeneration. *Prog Retin Eye Res,* 20**,** 385-414.

PHIPPS, J. A., DANG, T. M., VINGRYS, A. J. & GUYMER, R. H. 2004. Flicker perimetry losses in age-related macular degeneration. *Invest Ophthalmol Vis Sci,* 45**,** 3355-60.

PIGUET, B., HAIMOVICI, R. & BIRD, A. C. 1995. Dominantly inherited drusen represent more than one disorder: a historical review. *Eye (Lond),* 9 (Pt 1)**,** 34-41.

Pokorny, J., Smith, V.C., Verriest, G. & Pinckers, A.J.L.G. (1979). *Congenital and acquired colour vision defects*. New York: Grune and Stratton.

POLKINGHORNE, P. J., CAPON, M. R., BERNINGER, T., LYNESS, A. L., SEHMI, K. & BIRD, A. C. 1989. Sorsby's fundus dystrophy. A clinical study. *Ophthalmology,* 96**,** 1763-8.

PUCHE, N., BLANCO-GARAVITO, R., RICHARD, F., LEVEZIEL, N., ZERBIB, J., TILLEUL, J., MIMOUN, G., QUERQUES, G., COHEN, S. Y. & SOUIED, E. H. 2013. Genetic and environmental factors

associated with reticular pseudodrusen in age-related macular degeneration. *Retina,* 33**,** 998-1004.

PUMARIEGA, N. M., SMITH, R. T., SOHRAB, M. A., LETIEN, V. & SOUIED, E. H. 2011. A prospective study of reticular macular disease. *Ophthalmology,* 118**,** 1619-25.

PURVES, D., AUGUSTINE, G.J., FITZPATRICK, D., ET AL. 2001. Functional Specialization of the Rod and Cone Systems. *Neuroscience.* 2nd Edition ed.: Sunderland (MA): Sinauer Associates.

QUERQUES, G., MASSAMBA, N., SROUR, M., BOULANGER, E., GEORGES, A. & SOUIED, E. H. 2014. Impact of reticular pseudodrusen on macular function. *Retina,* 34**,** 321-9.

RAMRATTAN, R. S., VAN DER SCHAFT, T. L., MOOY, C. M., DE BRUIJN, W. C., MULDER, P. G. & DE JONG, P. T. 1994. Morphometric analysis of Bruch's membrane, the choriocapillaris, and the choroid in aging. *Invest Ophthalmol Vis Sci,* 35**,** 2857-64.

RATNAM, K., CARROLL, J., PORCO, T. C., DUNCAN, J. L. & ROORDA, A. 2013. Relationship between foveal cone structure and clinical measures of visual function in patients with inherited retinal degenerations. *Invest Ophthalmol Vis Sci,* 54**,** 5836-47.

RENNIE, C. A., STINGE, A., KING, E. A., SOTHIRACHAGAN, S., OSMOND, C. & LOTERY, A. J. 2012. Can genetic risk information for age-related macular degeneration influence motivation to stop smoking? A pilot study. *Eye (Lond),* 26**,** 109-18.

REGAN,D., 1988. Low-contrast letter charts and sinewave grating tests in ophthalmological and neurological disorders. . *ClinVision Sci. ,* 2**,** 235--50.

RODRIGUEZ-CARMONA, M. 2006. *"Variability of chromatic sensitivity: fundamental studies and clinical applications,".* PhD, City University, London.

RODRIGUEZ-CARMONA M, O. N.-B. M., BARBUR JL 2012. Assessing the Severity of Color Vision Loss with Implications for Aviation and Other Occupational Environments. *Aviat Space Environ Med,* 83**,** 19-29.

ROHALY, A. M. & OWSLEY, C. 1993. Modeling the contrast-sensitivity functions of older adults. *J Opt Soc Am A,* 10**,** 1591-9.

RUDOLF, M., CLARK, M. E., CHIMENTO, M. F., LI, C. M., MEDEIROS, N. E. & CURCIO, C. A. 2008. Prevalence and morphology of druse types in the macula and periphery of eyes with age-related maculopathy. *Invest Ophthalmol Vis Sci,* 49**,** 1200-9.

SAMPLE, P. A., WEINREB, R. N. & BOYNTON, R. M. 1986. Acquired dyschromatopsia in glaucoma. *Surv Ophthalmol,* 31**,** 54-64.

SANDBERG, M. A. & GAUDIO, A. R. 1995. Slow photostress recovery and disease severity in age-related macular degeneration. *Retina,* 15**,** 407-12.

SANDBERG, M. A., WEINER, A., MILLER, S. & GAUDIO, A. R. 1998. High-risk characteristics of fellow eyes of patients with unilateral neovascular age-related macular degeneration. *Ophthalmology,* 105**,** 441-7.

SARKS, J. P., SARKS, S. H. & KILLINGSWORTH, M. C. 1988. Evolution of geographic atrophy of the retinal pigment epithelium. *Eye (Lond),* 2 (Pt 5)**,** 552-77.

SARKS, S., CHEREPANOFF, S., KILLINGSWORTH, M. & SARKS, J. 2007. Relationship of Basal laminar deposit and membranous debris to the clinical presentation of early age-related macular degeneration. *Invest Ophthalmol Vis Sci,* 48**,** 968-77.

SARKS, S. H. 1976. Ageing and degeneration in the macular region: a clinico-pathological study. *Br J Ophthalmol,* 60**,** 324-41.

SAKAGUCHI H, M. M., SHADRACH KG, RAYBORN ME, CRABB & JW, A. H. J. 2002. Clusterin is present in drusen in age related macular degeneration. *Exp Eye Res,Neuroscience.* 2nd ed.

SCHATZ, H. & MCDONALD, H. R. 1989. Atrophic macular degeneration. Rate of spread of geographic atrophy and visual loss. *Ophthalmology,* 96**,** 1541-51.

SCHMITZ-VALCKENBERG, S., FLECKENSTEIN, M., SCHOLL, H. P. & HOLZ, F. G. 2009. Fundus autofluorescence and progression of age-related macular degeneration. *Surv Ophthalmol,* 54**,** 96-117.

SCHMITZ-VALCKENBERG, S., STEINBERG, J. S., FLECKENSTEIN, M., VISVALINGAM, S., BRINKMANN, C. K. & HOLZ, F. G. 2010. Combined confocal scanning laser ophthalmoscopy and spectral-domain optical coherence tomography imaging of reticular drusen associated with age-related macular degeneration. *Ophthalmology,* 117**,** 1169-76.

SCHNECK, M. E., HAEGERSTROM-PORTNOY, G., LOTT, L. A. & BRABYN, J. A. 2014. Comparison of panel D-15 tests in a large older population. *Optom Vis Sci,* 91**,** 284-90.

SEDDON, J. M., SHARMA, S. & ADELMAN, R. A. 2006. Evaluation of the clinical age-related maculopathy staging system. *Ophthalmology,* 113**,** 260-6.

SEDDON, J. M., WILLETT, W. C., SPEIZER, F. E. & HANKINSON, S. E. 1996. A prospective study of cigarette smoking and age-related macular degeneration in women. *Jama,* 276**,** 1141-6.

SELEMON, L. D. & BEGOVIC, A. 2007. Stereologic analysis of the lateral geniculate nucleus of the thalamus in normal and schizophrenic subjects. *Psychiatry Res,* 151**,** 1-10.

SEVERIN, S. L., HARPER, J. Y., JR. & CULVER, J. F. 1963. PHOTOSTRESS TEST FOR THE EVALUATION OF MACULAR FUNCTION. *Arch Ophthalmol,* 70**,** 593-7.

SHARMA, R. K., EHINGER, B.E.J 2003. Development and structure of the retina. *Kaufman, P.L., Alm, A. (eds.) Adler's Physiology of the Eye.* Mosby, St Louis

SHERMAN,J.AND EPSHTEIN,D. 2012. *The ABCs of OCT ;Take a guided tour of this innovative technology to better understand its relevance to your practice.*[Online]. Review of Optometry. Available: https://www.reviewofoptometry.com/article/the-abcs-of-oct.

SIMUNOVIC, M. P. 2012. On seeing yellow: the case for, and against, short-wavelength light-absorbing intraocular lenses. *Arch Ophthalmol,* 130**,** 919-26.

SIMUNOVIC, M. P. 2016. Acquired color vision deficiency. *Surv Ophthalmol,* 61**,** 132-55.

SIVAPRASAD, S., BIRD, A., NITIAHPAPAND, R., NICHOLSON, L., HYKIN, P. & CHATZIRALLI, I. 2016. Perspectives on reticular pseudodrusen in age-related macular degeneration. *Surv Ophthalmol,* 61**,** 521-37.

SMITH, R. T., CHAN, J. K., BUSUOIC, M., SIVAGNANAVEL, V., BIRD, A. C. & CHONG, N. V. 2006. Autofluorescence characteristics of early, atrophic, and high-risk fellow eyes in age-related macular degeneration. *Invest Ophthalmol Vis Sci,* 47**,** 5495-504.

SMITH, R. T., SOHRAB, M. A., BUSUIOC, M. & BARILE, G. 2009. Reticular macular disease. *Am J Ophthalmol,* 148**,** 733-743 e2.

SMITH, V. C., POKORNY, J. & DIDDIE, K. R. 1988. Color matching and the Stiles-Crawford effect in observers with early age-related macular changes. *J Opt Soc Am A,* 5**,** 2113-21.

SMITH, W., ASSINK, J., KLEIN, R., MITCHELL, P., KLAVER, C. C., KLEIN, B. E., HOFMAN, A., JENSEN, S., WANG, J. J. & DE JONG, P. T. 2001. Risk factors for age-related macular degeneration: Pooled findings from three continents. *Ophthalmology,* 108**,** 697-704.

SOHRAB, M. A., SMITH, R. T., SALEHI-HAD, H., SADDA, S. R. & FAWZI, A. A. 2011. Image registration and multimodal imaging of reticular pseudodrusen. *Invest Ophthalmol Vis Sci,* 52**,** 5743-8.

SORSBY, A. & MASON, M. E. 1949. A fundus dystrophy with unusual features. *Br J Ophthalmol,* 33**,** 67-97.

SPAIDE, R. F. 2003. Fundus autofluorescence and age-related macular degeneration. *Ophthalmology,* 110**,** 392-9.

SPAIDE, R. F. 2013. Outer retinal atrophy after regression of subretinal drusenoid deposits as a newly recognized form of late age-related macular degeneration. *Retina,* 33**,** 1800-8.

SPAIDE, R. F. & CURCIO, C. A. 2010. Drusen characterization with multimodal imaging. *Retina,* 30**,** 1441-54.

REFERENCES

SPAIDE , R. F. 2007. Autofluorescence Imaging with the fundus camera. *Atlas of Autofluorescence Imaging.* Berlin Heidelberg, Springer; 2007.

SPECTRALIS CATALOGUE. 2007. *Spectralis hardware operating instructions.* [Online]. Version 001,August 2007 © Heidelberg Engineering GmbH 2007 Art.No. 19963 [Accessed 1/7/2017].

SPRAUL, C. W., LANG, G. E., GROSSNIKLAUS, H. E. & LANG, G. K. 1999. Histologic and morphometric analysis of the choroid, Bruch's membrane, and retinal pigment epithelium in postmortem eyes with age-related macular degeneration and histologic examination of surgically excised choroidal neovascular membranes. *Surv Ophthalmol,* 44 Suppl 1**,** S10-32.

SQUIRE, T. J., RODRIGUEZ-CARMONA, M., EVANS, A. D., & BARBUR, J. L. 2005. Color vision tests for aviation: comparison of the anomaloscope and three lantern types. *Aviation, Space and Environmental Medicine, ,* 76**,** 421–9.

STANGOS, N., VOUTAS, S., TOPOUZIS, F. & KARAMPATAKIS, V. 1995. Contrast sensitivity evaluation in eyes predisposed to age-related macular degeneration and presenting normal visual acuity. *Ophthalmologica,* 209**,** 194-8.

STEINMETZ, R. L., HAIMOVICI, R., JUBB, C., FITZKE, F. W. & BIRD, A. C. 1993. Symptomatic abnormalities of dark adaptation in patients with age-related Bruch's membrane change. *Br J Ophthalmol,* 77**,** 549-54.

STEINMETZ, R. L., POLKINGHORNE, P. C., FITZKE, F. W., KEMP, C. M. & BIRD, A. C. 1992. Abnormal dark adaptation and rhodopsin kinetics in Sorsby's fundus dystrophy. *Invest Ophthalmol Vis Sci,* 33**,** 1633-6.

STONE, E. M., LOTERY, A. J., MUNIER, F. L., HEON, E., PIGUET, B., GUYMER, R. H., VANDENBURGH, K., COUSIN, P., NISHIMURA, D., SWIDERSKI, R. E., SILVESTRI, G., MACKEY, D. A., HAGEMAN, G. S., BIRD, A. C., SHEFFIELD, V. C. & SCHORDERET, D. F. 1999. A single EFEMP1 mutation associated with both Malattia Leventinese and Doyne honeycomb retinal dystrophy. *Nat Genet,* 22**,** 199-202.

STREILEIN, J. W., MA, N., WENKEL, H., NG, T. F. & ZAMIRI, P. 2002. Immunobiology and privilege of neuronal retina and pigment epithelium transplants. *Vision Res,* 42**,** 487-95.

SUNNESS, J. S., GONZALEZ-BARON, J., APPLEGATE, C. A., BRESSLER, N. M., TIAN, Y., HAWKINS, B., BARRON, Y. & BERGMAN, A. 1999. Enlargement of atrophy and visual acuity loss in the geographic atrophy form of age-related macular degeneration. *Ophthalmology,* 106**,** 1768-79.

SUNNESS, J. S., RUBIN, G. S., APPLEGATE, C. A., BRESSLER, N. M., MARSH, M. J., HAWKINS, B. S. & HASELWOOD, D. 1997. Visual function abnormalities and prognosis in eyes with age-related geographic atrophy of the macula and good visual acuity. *Ophthalmology,* 104**,** 1677-91.

SUZUKI, M., SATO, T. & SPAIDE, R. F. 2014. Pseudodrusen subtypes as delineated by multimodal imaging of the fundus. *Am J Ophthalmol,* 157**,** 1005-12.

SWANSON, W. H. & COHEN, J. M. 2003. Color vision. *Ophthalmol Clin North Am,* 16**,** 179-203.

TAMAKOSHI, A., YUZAWA, M., MATSUI, M., UYAMA, M., FUJIWARA, N. K. & OHNO, Y. 1997. Smoking and neovascular form of age related macular degeneration in late middle aged males: findings from a case-control study in Japan. Research Committee on Chorioretinal Degenerations. *Br J Ophthalmol,* 81**,** 901-4.

THORNDYKE PW., T. 1977. Cognitive structures in comprehension and memory of narrative discourse. *Cognitive Psychol. 1977;9:77*

TSERENTSOODOL, N., GORDIYENKO, N. V., PASCUAL, I., LEE, J. W., FLIESLER, S. J. & RODRIGUEZ, I. R. 2006. Intraretinal lipid transport is dependent on high density lipoprotein-like particles and class B scavenger receptors. *Mol Vis,* 12**,** 1319-33.

UEDA-ARAKAWA, N., OOTO, S., TSUJIKAWA, A., YAMASHIRO, K., OISHI, A. & YOSHIMURA, N. 2013. Sensitivity and specificity of detecting reticular pseudodrusen in multimodal imaging in Japanese patients. *Retina,* 33**,** 490-7.

VAN DE KRAATS, J. & VAN NORREN, D. 2007. Sharp cutoff filters in intraocular lenses optimize the balance between light reception and light protection. *J Cataract Refract Surg,* 33**,** 879-87.

VAN LEEUWEN, R., KLAVER, C. C., VINGERLING, J. R., HOFMAN, A. & DE JONG, P. T. 2003. The risk and natural course of age-related maculopathy: follow-up at 6 1/2 years in the Rotterdam study. *Arch Ophthalmol,* 121**,** 519-26.

VELILLA, S., GARCIA-MEDINA, J. J., GARCIA-LAYANA, A., DOLZ-MARCO, R., PONS-VAZQUEZ, S., PINAZO-DURAN, M. D., GOMEZ-ULLA, F., AREVALO, J. F., DIAZ-LLOPIS, M. & GALLEGO-PINAZO, R. 2013. Smoking and age-related macular degeneration: review and update. *J Ophthalmol,* 2013**,** 895147.

VERRIEST, G. 1963. Further studies on acquired deficiency of color discrimination. *J Opt Soc Am,* 53**,** 185-95.

VON RUCKMANN, A., FITZKE, F. W. & BIRD, A. C. 1997. Fundus autofluorescence in age-related macular disease imaged with a laser scanning ophthalmoscope. *Invest Ophthalmol Vis Sci,* 38**,** 478-86.

VUJOSEVIC, S., PUCCI, P., CASCIANO, M., LONGHIN, E., CONVENTO, E., BINI, S. & MIDENA, E. 2016. Long-term longitudinal modifications in mesopic microperimetry in early and intermediate age-related macular degeneration. *Graefes Arch Clin Exp Ophthalmol*.

WAJER, S. D., TAOMOTO, M., MCLEOD, D. S., MCCALLY, R. L., NISHIWAKI, H., FABRY, M. E., NAGEL, R. L. & LUTTY, G. A. 2000. Velocity measurements of normal and sickle red blood cells in the rat retinal and choroidal vasculatures. *Microvasc Res,* 60**,** 281-93.

WANG, A. L., YUAN, M. & NEUFELD, A. H. 2007. Age-related changes in neuronal susceptibility to damage: comparison of the retinal ganglion cells of young and old mice before and after optic nerve crush. *Ann N Y Acad Sci,* 1097**,** 64-6.

WANG, J. J., FORAN, S., SMITH, W. & MITCHELL, P. 2003. Risk of age-related macular degeneration in eyes with macular drusen or hyperpigmentation: the Blue Mountains Eye Study cohort. *Arch Ophthalmol,* 121**,** 658-63.

WANG, Y. Z., WILSON, E., LOCKE, K. G. & EDWARDS, A. O. 2002. Shape discrimination in age-related macular degeneration. *Invest Ophthalmol Vis Sci,* 43**,** 2055-62.

WANGSA-WIRAWAN, N. D. & LINSENMEIER, R. A. 2003. Retinal oxygen: fundamental and clinical aspects. *Arch Ophthalmol,* 121**,** 547-57.

WEBB, R. H., HUGHES, G. W. & DELORI, F. C. 1987. Confocal scanning laser ophthalmoscope. *Appl Opt,* 26**,** 1492-9.

WEINER, D. E., TIGHIOUART, H., REYNOLDS, R. & SEDDON, J. M. 2011. Kidney function, albuminuria and age-related macular degeneration in NHANES III. *Nephrol Dial Transplant,* 26**,** 3159-65.

WEINREB, R. N., AUNG, T. & MEDEIROS, F. A. 2014. The pathophysiology and treatment of glaucoma: a review. *JAMA,* 311**,** 1901-11.

WEITER, J. J., DELORI, F. C., WING, G. L. & FITCH, K. A. 1986. Retinal pigment epithelial lipofuscin and melanin and choroidal melanin in human eyes. *Invest Ophthalmol Vis Sci,* 27**,** 145-52.

WHITTAKER,S.G.,Lovie-kitchin, J.E., 1994. *Low Vision—Research and New Development in Rehabilitation.Amsterdam,* , Amsterdam, IOS Press.

WILLIAMS, D. R. & COLETTA, N. J. 1987. Cone spacing and the visual resolution limit. *J Opt Soc Am A,* 4**,** 1514-23.

WING, G. L., BLANCHARD, G. C. & WEITER, J. J. 1978. The topography and age relationship of lipofuscin concentration in the retinal pigment epithelium. *Invest Ophthalmol Vis Sci,* 17**,** 601-7.

WOJTKOWSKI, M., SRINIVASAN, V., KO, T., FUJIMOTO, J., KOWALCZYK, A. & DUKER, J. 2004. Ultrahigh-resolution, high-speed, Fourier domain optical coherence tomography and methods for dispersion compensation. *Opt Express,* 12**,** 2404-22.

WOLLSTEIN, G., PAUNESCU, L. A., KO, T. H., FUJIMOTO, J. G., KOWALEVICZ, A., HARTL, I., BEATON, S., ISHIKAWA, H., MATTOX, C., SINGH, O., DUKER, J., DREXLER, W. & SCHUMAN, J. S. 2005. Ultrahigh-resolution optical coherence tomography in glaucoma. *Ophthalmology,* 112**,** 229-37.

WONG, W. L., SU, X., LI, X., CHEUNG, C. M., KLEIN, R., CHENG, C. Y. & WONG, T. Y. 2014. Global prevalence of age-related macular degeneration and disease burden projection for 2020 and 2040: a systematic review and meta-analysis. *Lancet Glob Health,* 2**,** e106-16.

WOODS, R. L. & WOOD, J. M. 1995. The role of contrast sensitivity charts and contrast letter charts in clinical practice. *Clinical and experimental optometry,* 78**,** 43-57.

WU, Z., AYTON, L. N., LUU, C. D. & GUYMER, R. H. 2014. Relationship between retinal microstructures on optical coherence tomography and microperimetry in age-related macular degeneration. *Ophthalmology,* 121**,** 1445-52.

XU, H., CHEN, M., MANIVANNAN, A., LOIS, N. & FORRESTER, J. V. 2008. Age-dependent accumulation of lipofuscin in perivascular and subretinal microglia in experimental mice. *Aging Cell,* 7**,** 58-68.

YAMADA, Y., ISHIBASHI, K., ISHIBASHI, K., BHUTTO, I. A., TIAN, J., LUTTY, G. A. & HANDA, J. T. 2006. The expression of advanced glycation endproduct receptors in rpe cells associated with basal deposits in human maculas. *Exp Eye Res,* 82**,** 840-8.

YANNUZZI, L. A., NEGRAO, S., IIDA, T., CARVALHO, C., RODRIGUEZ-COLEMAN, H., SLAKTER, J., FREUND, K. B., SORENSON, J., ORLOCK, D. & BORODOKER, N. 2001. Retinal angiomatous proliferation in age-related macular degeneration. *Retina,* 21**,** 416-34.

YEHOSHUA, Z., GREGORI, G., SADDA, S. R., PENHA, F. M., GOLDHARDT, R., NITTALA, M. G., KONDURU, R. K., FEUER, W. J., GUPTA, P., LI, Y. & ROSENFELD, P. J. 2013. Comparison of drusen area detected by spectral domain optical coherence tomography and color fundus imaging. *Invest Ophthalmol Vis Sci,* 54**,** 2429-34.

YI, K., MUJAT, M., PARK, B. H., SUN, W., MILLER, J. W., SEDDON, J. M., YOUNG, L. H., DE BOER, J. F. & CHEN, T. C. 2009. Spectral domain optical coherence tomography for quantitative evaluation of drusen and associated structural changes in non-neovascular age-related macular degeneration. *Br J Ophthalmol,* 93**,** 176-81.

YOUNG, R. W. 1971. The renewal of rod and cone outer segments in the rhesus monkey. *J Cell Biol,* 49**,** 303-18.

YU, Y., BHANGALE, T. R., FAGERNESS, J., RIPKE, S., THORLEIFSSON, G., TAN, P. L., SOUIED, E. H., 2011. Common variants near FRK/COL10A1 and VEGFA are associated with advanced age-related macular degeneration. *Hum Mol Genet,* 20**,** 3699-709.

ZARBIN, M. A. 2004. Current concepts in the pathogenesis of age-related macular degeneration. *Arch Ophthalmol,* 122**,** 598-614.

ZWEIFEL, S. A., SPAIDE, R. F., CURCIO, C. A., MALEK, G. & IMAMURA, Y. 2010. Reticular pseudodrusen are subretinal drusenoid deposits. *Ophthalmology,* 117**,** 303-12.e1.